N.M. Patrikalakis
C. Chryssostomidis

Theoretical and Experimental Prediction of the Response of a Marine Riser Model Subjected to Sinusoid Excitation of its Top End with Amplitude of Two Diameters Orthogonal to a Uniform Stream of Speed Equal to 120 mm/s

MIT Sea Grant Program

Massachusetts Institute of Technology
Cambridge
Massachusetts 02139

Report Number
MITSG 83-5
March 1983

MASSACHUSETTS INSTITUTE OF TECHNOLOGY
Sea Grant Program

Addendum to MITSG 83-5, THEORETICAL AND EXPERIMENTAL PREDICTION OF THE RESPONSE OF A MARINE RISER MODEL SUBJECTED TO SINUSOID EXCITATION OF ITS TOP END WITH AMPLITUDE OF TWO DIAMETERS ORTHOGONAL TO A UNIFORM STREAM OF SPEED EQUAL TO 120 mm/s

N.M. Patrikalakis, C. Chryssostomidis

Grant No. R/O-8
Project No. NA81AA-D-00069

Room E38-366 77 Massachusetts Avenue Cambridge, Massachusetts 02139 617/253-7041

THEORETICAL AND EXPERIMENTAL PREDICTION OF THE RESPONSE OF A MARINE RISER MODEL SUBJECTED TO SINUSOID EXCITATION OF ITS TOP END WITH AMPLITUDE OF TWO DIAMETERS ORTHOGONAL TO A UNIFORM STREAM OF SPEED EQUAL TO 120 mm/s

by
N. M. PATRIKALAKIS
C. CHRYSSOSTOMIDIS

MIT SEA GRANT REPORT NO. 83-5

MARCH, 1983

ABSTRACT

The objective of this report is to provide:

1. An analysis of the experimental results obtained from a 3 m flexible riser model with its top end oscillated harmonically with an amplitude of two diameters orthogonal to a uniform stream which is constant with depth and of speed equal to 120 mm/s.

2. A comparison of the experimental results from the flexible model with theoretical predictions of the response based on rigid cylinder experimental results.

ACKNOWLEDGEMENTS

Funding for this research was obtained from the MIT Sea Grant College Program, Conoco, Inc. and Gulf Oil Company. All experiments were performed at the Laboratory for Hydrodynamics of the National Technical University of Athens, Greece. The typed manuscript was prepared by M. Staruch.

RELATED SEA GRANT REPORTS

"Theoretical and Experimental Prediction of the Response of a Marine Riser Model Subjected to Sinusoid Excitation of its Top End with Amplitude Equal to Two Diameters," C. Chryssostomidis, N. M. Patrikalakis, and E. Vrakas, MIT Sea Grant Report No. 83-2, March 1983.

"Theoretical and Experimental Prediction of the Response of a Marine Riser Model Subjected to Sinusoid Excitation of its Top End with Amplitude of Two Diameters Parallel to a Uniform Stream of Speed Equal to 120 mm/s," C. Chryssostomidis and N. M. Patrikalakis, MIT Sea Grant Report No. 83-3, March, 1983

"Prediction of the Response of a Marine Riser Model Subjected to Sinusoid Excitation of its Top End with Amplitude of Two Diameters Parallel to a Uniform Stream of Speed Equal to 240 mm/s," C. Chryssostomidis and N. M. Patrikalakis, MIT Sea Grant Report No. 83-4, March, 1983.

"Theoretical and Experimental Prediction of the Response of a Marine Riser Model Subjected to Sinusoid Excitation of its Top End with Amplitude of Two Diameters Orthogonal to a Uniform Stream of Speed Equal to 240 mm/s," N. M. Patrikalakis and C. Chryssostomidis, MIT Sea Grant Report No. 83-6, March, 1983.

TABLE OF CONTENTS

	Page
Abstract	1
Acknowledgements	2
Table of Contents	3
List of Tables	4
List of Figures	5
1. A Description of the Riser Model	6
2. Presentation of Experimental and Theoretical Results	9
Experiment 52	14
Experiment 59	27
Experiment 71	40
Experiment 80	53
Experiment 89	66
References	78
Appendix A	79

LIST OF TABLES

Table 2-I: Description of experiments and information for the theoretical prediction of the response in planes A and B. 10

LIST OF FIGURES

Page

EXPERIMENT 52:

-Spectra 14
-Theoretical predictions and maxima 23
-T-Figures. 25

EXPERIMENT 59:

-Spectra 27
-Theoretical predictions and maxima 36
-T-Figures. 38

EXPERIMENT 71:

-Spectra 40
-Theoretical predictions and maxima 49
-T-Figures. 51

EXPERIMENT 80:

-Spectra 53
-Theoretical predictions and maxima 62
-T-Figures. 64

EXPERIMENT 89:

-Spectra 66
-Theoretical predictions and maxima 75
-T-Figures. 77

Figures A1, A2 and A3:

-Rigid cylinder results. 80

Figure A4:

-Spring Mounted Rigid cylinder results. 83

1. A DESCRIPTION OF THE RISER MODEL

Preliminary data describing the riser model can be found in Chryssostomidis and Patrikalakis (1982) and MITSG Report 83-2, and more refined estimates in Patrikalakis (1983). A description of the model based on the information given in Patrikalakis (1983) is included here for the reader's convenience.

The model is made up of an aluminum tube covered externally with a sealing material. The overall model characteristics are:

- Length between ball joints (L) = 3.000m
- Aluminum tube I.D. (D_i) = 10.92 mm
- Aluminum tube O.D. (D_o) = 12.61 mm
- External sealing diameter (D_e) = 15.3 mm
- Average mass per unit length (M) = 0.327 kg/m
- Average effective weight per unit length (We)= 1.378 N/m
- Effective overpull at the lower ball joint (Pe(0)) = 1.72 N
- Bending stiffness of a cross section (EI) = 37.6 Nm^2

The inside of an aluminum tube is filled with a glycerin solution in water of density approximately equal to 900 kg/m^3. At the ends of the model there are ball joints which minimize the end bending moments. Above the upper ball joint there is a slip joint, which is designed to minimize tension variations due to flexural motions. The riser model is also designed so it can be tensioned to the desired tension. The first two "natural frequencies" of the model in water are approximately equal to 1.57 and 6.06 Hz, respectively. These have been determined theoretically using c_m=1 and have been verified from a decay test in quiescent

water, where the initial amplitude of the response was of the order of 1/10 of the effective diameter.

The model is instrumented at ten equidistant locations, 1-10, each with two strain gage full bridges installed on the outer surface of the aluminum tube, designed to isolate bending from tension and to measure bending strains on two orthogonal directions A and B. In the vertical static equilibrium condition, planes A and B are parallel and orthogonal to the centerline of the towing tank, respectively. The actual location of each branch of the bending bridges is at approximately 9.80 degrees from planes A and B. The numbering of the bridges begins at the upper end, while their elevation is measured from the axis of the lower ball joint. The first and last bending bridges are L/11 from the axes of the top and bottom ball joints, respectively, and the separation between bending bridges is L/11. For example, bridge A6 measures bending strains created by deflections in plane A at elevation Z=5L/11 from the axis of the lower ball joint. In addition, the model is instrumented at two extra positions T1 and T2, 101 mm from the axes of each ball joint, with specially designed full bridges isolating tension from bending. Tension bridge T2 is at the lower end of the model. Finally, the model is instrumented at an additional location, Q1, 1773 mm from the upper ball joint, with a full torsion bridge. The mass per unit length of a single wire is 0.198 grams/m, while the total mass of all wires for all 23 full bridges is approximately 2.73% of the total model mass. Their total volume is approximately equal to 5.32 cm^3. The four wires of each bridge are braided to avoid interference and are sent internally to the lower end of the model.

The oscillation of the top end of the model is created by a DC motor driven by a signal generator and controlled by a tachometer measuring angular velocities and a linear variable differential transducer, LVDT, measuring displacements. The rotational motion of the motor is converted to linear motion via a specially designed rack anti-backlash pinion system. During the experiments, measurements

from a number of strain bridges and the LVDT were made simultaneously and were recorded digitally. Using the torque bridge, it was observed that the structural torsion was negligible, see Chapter III of Patrikalakis (1983). It was estimated analytically, and also confirmed by the tension bridge measurements, that the tension variation during the experiments was small, approximately 5% of the effective tension. Therefore, even for the lowest excited mode, the ratio of the change of restoring force due to tension variation to the overall restoring force is very small (0.3%). This implies that the assumption of constant effective tension with time is an acceptable approximation for theoretical estimates of the response.

From calibration experiments in air, it was estimated that the structural damping ratio ς was approximately equal to 0.016 and 0.010 for the first and second flexural modes, respectively. Therefore, typical fluid drag forces are much larger than our estimates of the structural damping forces. Our experiments in air also revealed that when the upper end of the model was oscillated in air in a certain plane, some flexural response orthogonal to this plane existed. This happens because our model was not rotationally uniform. It was estimated that the flexural response orthogonal to the direction of excitation was not larger than approximately 12% of the response in the plane of applied oscillation. It was felt that such an imperfection would not substantially affect the experimental results in water.

2. PRESENTATION OF EXPERIMENTAL AND THEORETICAL RESULTS

The experiments presented in this report involve harmonic excitation of the top end of the riser model orthogonal to plane A at an amplitude approximately equal to two effective diameters and orthogonal to a uniform stream which is constant with depth and of speed V_c equal to 120 mm/s for the conditions shown in Table 2-1. Bending strains in plane A at Z=3L/11, 5L/11 and 8L/11, and in plane B at Z=3L/11, 5L/11, 6L/11 and 8L/11 were recorded. The Reynolds number and water temperature for all experiments analyzed in this report are 1568 and 14.1 degrees C, respectively. Reynolds number is defined by $Re = V_c D_e/\nu$ where ν is the kinematic viscosity of fresh water. A partial preliminary analysis of the experiments presented in this report has been given earlier in Chryssostomidis and Patrikalakis (1982).

The experimental and theoretical results reported here include plots of:

1. The root mean square of the measured motion of the top end as a function of frequency.

2. The root mean square measured dynamic bending strains as a function of the response frequency and the measured static bending strains.

3. The measured and theoretical predictions of the bending strains parallel and orthogonal to the oscillation of the top end.

4. The measured maximum bending strains parallel and orthogonal to the oscillation of the top end and independent of direction.

5. Indicative partial synchronous time traces of the motion of the top end and measured bending strains from three bridges.

The root mean square responses have been calculated using standard FFT codes from the International Mathematical and Statistical Library (IMSL) on an IBM 370/168 computer. The root mean square response is the square root of the

Table 2-1: Description of experiments and information for the theoretical prediction of the response in planes A and B

Experiment Number	52	59	71	80	89
Frequency of Excitation f_e in Hz	0.5	0.775	1.5	1.95	2.925
Measured A/D_e	1.89	1.90	1.91	1.93	1.94
Reduced Velocity U*	15.69	10.12	5.23	4.02	2.68
Reduced Frequency β	100	155	300	390	585
Measurement Record Length in Seconds	51.15	51.15	34.1	34.1	34.1
Added Mass Coefficient $\hat{c}_m$ Used in Theoretical Prediction	-0.28	-0.27	0.10	0.42	1.03
Drag Coefficient $\hat{c}_d$ Used in Theoretical Prediction	1.03	1.02	0.72	0.95	1.02
Maximum Calculated Dynamic Displacement Ratio y/D_e	1.89	1.90	2.61	2.15	1.94
Mean Calculated Dynamic Displacement Ratio y/D_e	1.02	1.11	1.94	1.49	0.77
Average Drag Coefficient $\hat{c}_D$ Used in Theoretical Prediction	1.18	1.29	2.35	1.66	1.62

product of the power spectral density of the response times the effective bandwidth B_e employed in the Fourier analysis of the results. The root mean square rather than the magnitude of the power spectral density was selected for presentation because, in most cases, the experimental response was practically periodic. The logarithmic representation of the power spectral density was not selected because it tends to visually exaggerate the significance of smaller components, which are not important in this problem. For each major peak of the root mean square plots, the root mean square value of the response is shown. This is computed as the square root of the sum of the squares of the rms response strains at discrete frequencies, B_e Hz apart, in the neighborhood of each peak. In addition, the overall dynamic root mean square value of the response is shown together with the static bending strain response. The Fourier and maxima calculations were performed using the record length shown in Table 2-1.

The nomenclature used in the Figures and Table 2-1 is defined below:

The experiment number corresponds to the numbering system employed during the performance of the experiments. BE is the effective bandwidth B_e employed in the Fourier analysis in Hz. THETA is the angle of oscillation of the top end with respect to the longer side of the towing tank in degrees. VC is the current speed V_c in mm/s. FE is the nominal frequency of excitation f_e of the top end in Hz. A/DE is the ratio of the measured amplitude A of the excitation of the top end divided by the effective diameter D_e. U* is the reduced velocity defined by $U^*=V_c/f_eD_e$ and β is the frequency parameter defined by $\beta=f_eD_e^2/\nu$.

The Figures of the root mean square motion of the top end are referred to by the experiment number and the letters LVDT. The Figures of root mean square measured bending strains are referred to by the experiment identification number and the bridge name. The Figures showing the measured and theoretical predictions and maxima are referred to by the experiment identification number

and the plane name. Figures showing the time traces are referred to by the experiment identification number and the letter T (trace).

Table 2-1 includes information about the theoretical prediction of the response at $f=f_e$ in plane B and the static response in plane A. These predictions have been performed as described in Section IV.4.3 and Appendix B, and Section V.4.3 of Patrikalakis (1983),respectively. The rigid cylinder derived hydrodynamic coefficients c_d, c_m and c_D employed in the determination of $\hat{c}_d$, $\hat{c}_m$ and $\hat{c}_D$ of Table 2-1 are shown in Figures A-1, A-2 and A-3, taken from Mercier (1973). The Reynolds number in Mercier's experiments was, for the most part, equal to 8000. The amplitude to diameter ratio of the imposed motion was less than 1.3 for c_d and c_m and less than 1.5 for c_D. In the computation of $\hat{c}_d$, $\hat{c}_m$ and $\hat{c}_D$ no Reynolds number correction was included and linear extrapolation was used for amplitude to diameter ratios outside the domain of existing data.

The lift response frequency due to vortex shedding, f_r, for a spring mounted rigid cylinder is shown in Figure A-4. When the frequency of oscillation of the top end, f_e, is sufficiently smaller than f_r then the response in plane B is primarily at f_e and f_r. On the other hand, when the frequency of oscillation of the top end is close to f_r then the response in plane B is primarily at f_e and is nearly monochromatic. In addition, in all cases of excitation some response in plane B is also present at very low frequencies. This is associated with slow variation of the spanwise correlation of the lift force, see Mercier (1973).

A summary of the results for the response in plane B is shown in Figures 52B, 59B, 71B, 80B and 89B. These include the theoretical and measured dynamic response strain at f_e and the maximum measured dynamic response strain in plane B. Our present theoretical estimate of the maximum response in plane B is the same as our estimate of the dynamic response at f_e in plane B. This is expected to give realistic results for the maximum in plane B when the response orthogonal to

the current is practically monochromatic. When the frequency of imposed oscillation is much lower than the first "natural frequency" of the cylinder and the lift response frequency due to vortex shedding, f_r, the procedure suggested in Section IV.4.3 of Patrikalakis (1983), may be employed to estimate the response at f_r. This procedure does not supply any phase information between the response at f_e and the lift response at f_r. In addition, it assumes that there are no appreciable interactions between force components at f_e and f_r.

The dynamic response in plane A is significant when compared to the dynamic response in plane B. When the lift response frequency due to vortex shedding, f_r, is not synchronized with the frequency of oscillation, dynamic response in plane A occurs at f_e, f_r and $f_r \pm f_e$. When the lift response frequency due to vortex shedding, f_r, is synchronized with the frequency of oscillation, dynamic response in plane A occurs at nf_e, where n is a small integer, and is magnified when nf_e is close to a "natural frequency" of the model. Some low frequency response in plane A is also encountered and as before it is associated with slow variation of the spanwise correlation of the dynamic force parallel to the current, see Mercier (1973).

A summary of the results for the response in plane A is shown in Figures 52A, 59A, 71A, 80A and 89A. These include the theoretical and measured static response strain; the maximum measured dynamic response strain; the maximum dynamic response strain independent of plane; and our present theoretical estimate of the maximum response strain independent of plane. The latter is computed as the square root of the sum of the squares of the static strain and of the maximum dynamic response strain in plane B.

EXPERIMENT 52

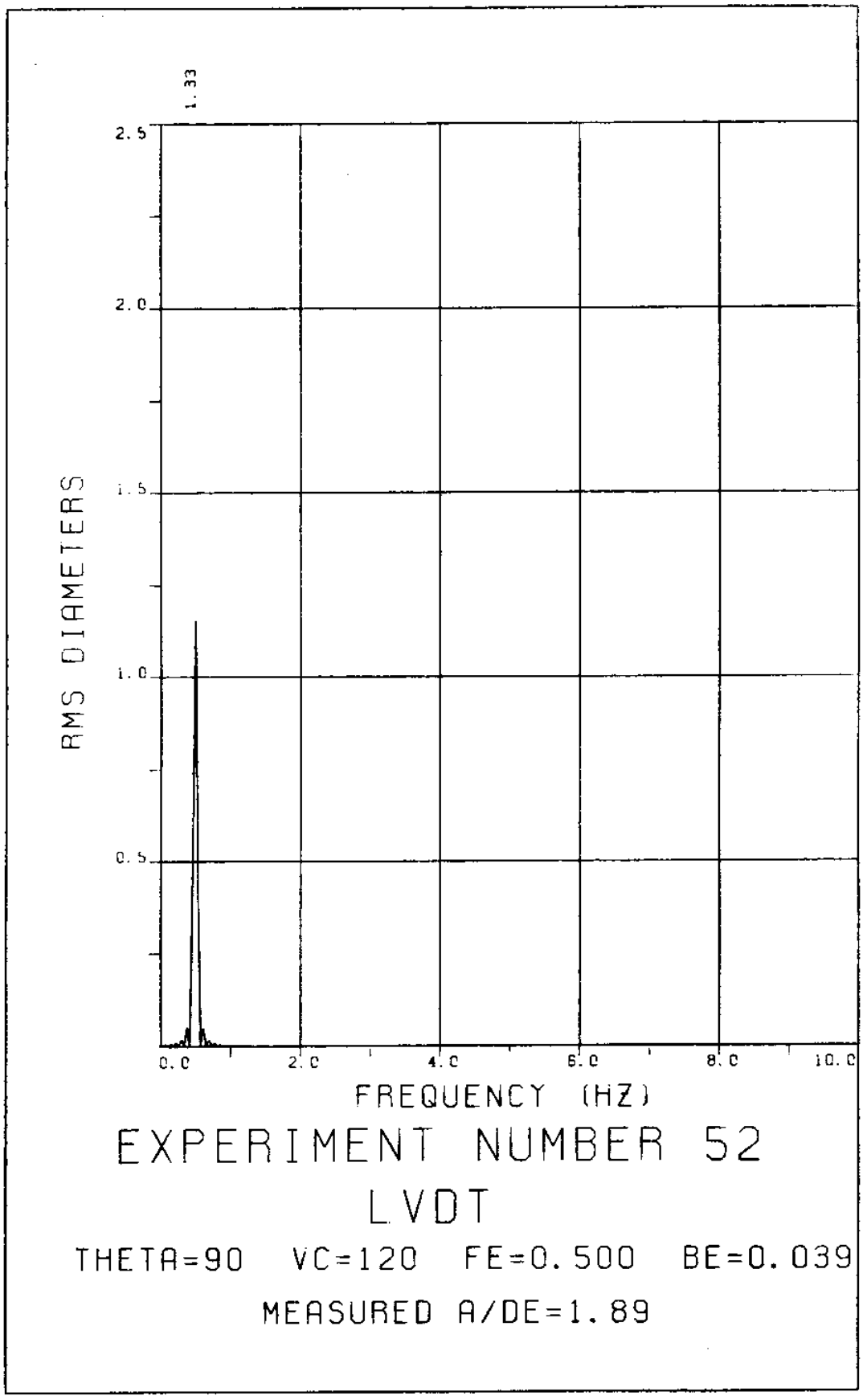
1.33
2.5
2.0
1.5
1.0
0.5
RMS DIAMETERS
0.0
2.0
4.0
6.0
8.0
10.0
FREQUENCY (HZ)
EXPERIMENT NUMBER 52
LVDT
THETA=90 VC=120 FE=0.500 BE=0.039
MEASURED A/DE=1.89

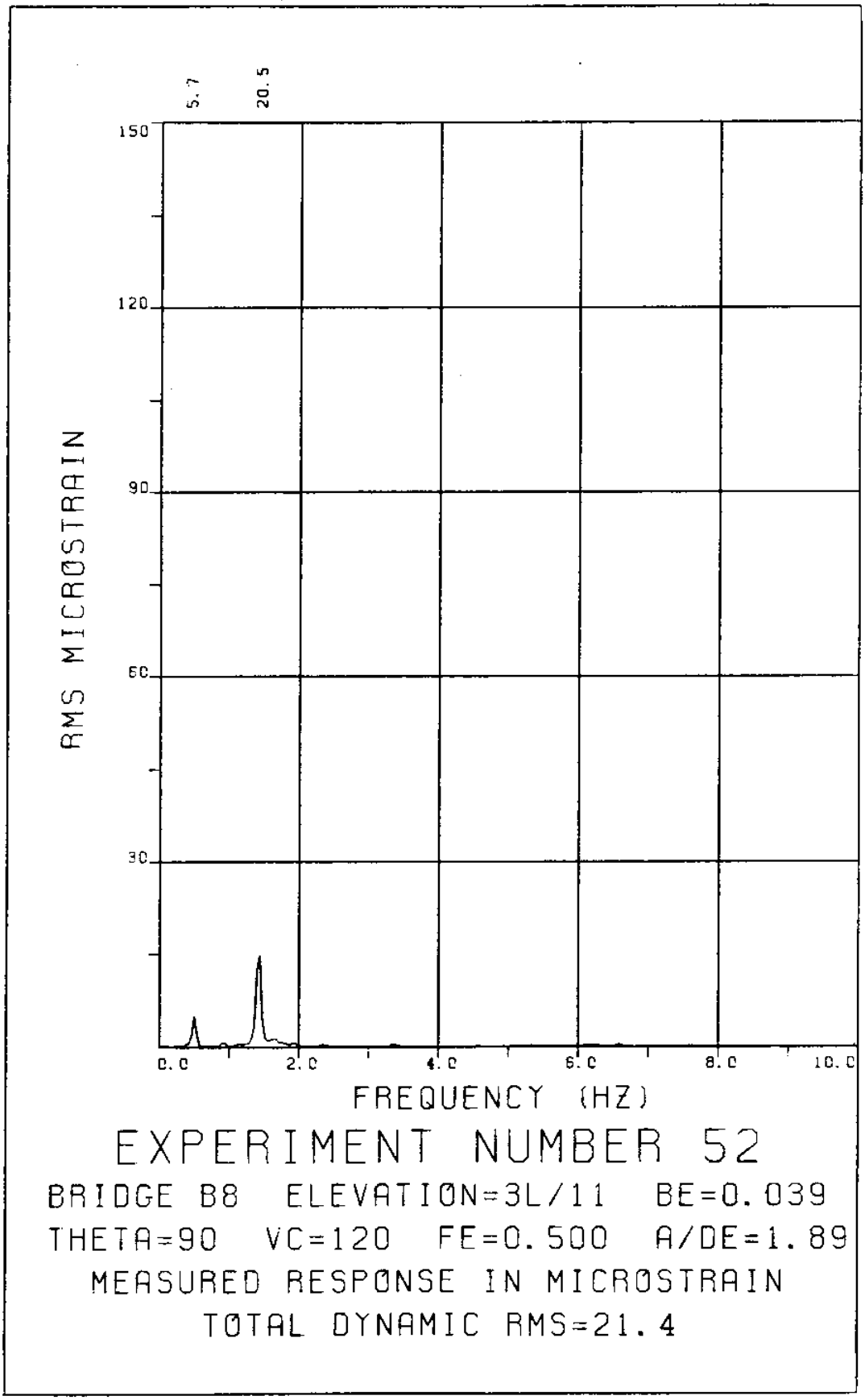
5.7
20.5
150
120
90
60
30
RMS MICROSTRAIN
0.0
2.0
4.0
6.0
8.0
10.0
FREQUENCY (HZ)
EXPERIMENT NUMBER 52
BRIDGE B8 ELEVATION=3L/11 BE=0.039
THETA=90 VC=120 FE=0.500 A/DE=1.89
MEASURED RESPONSE IN MICROSTRAIN
TOTAL DYNAMIC RMS=21.4

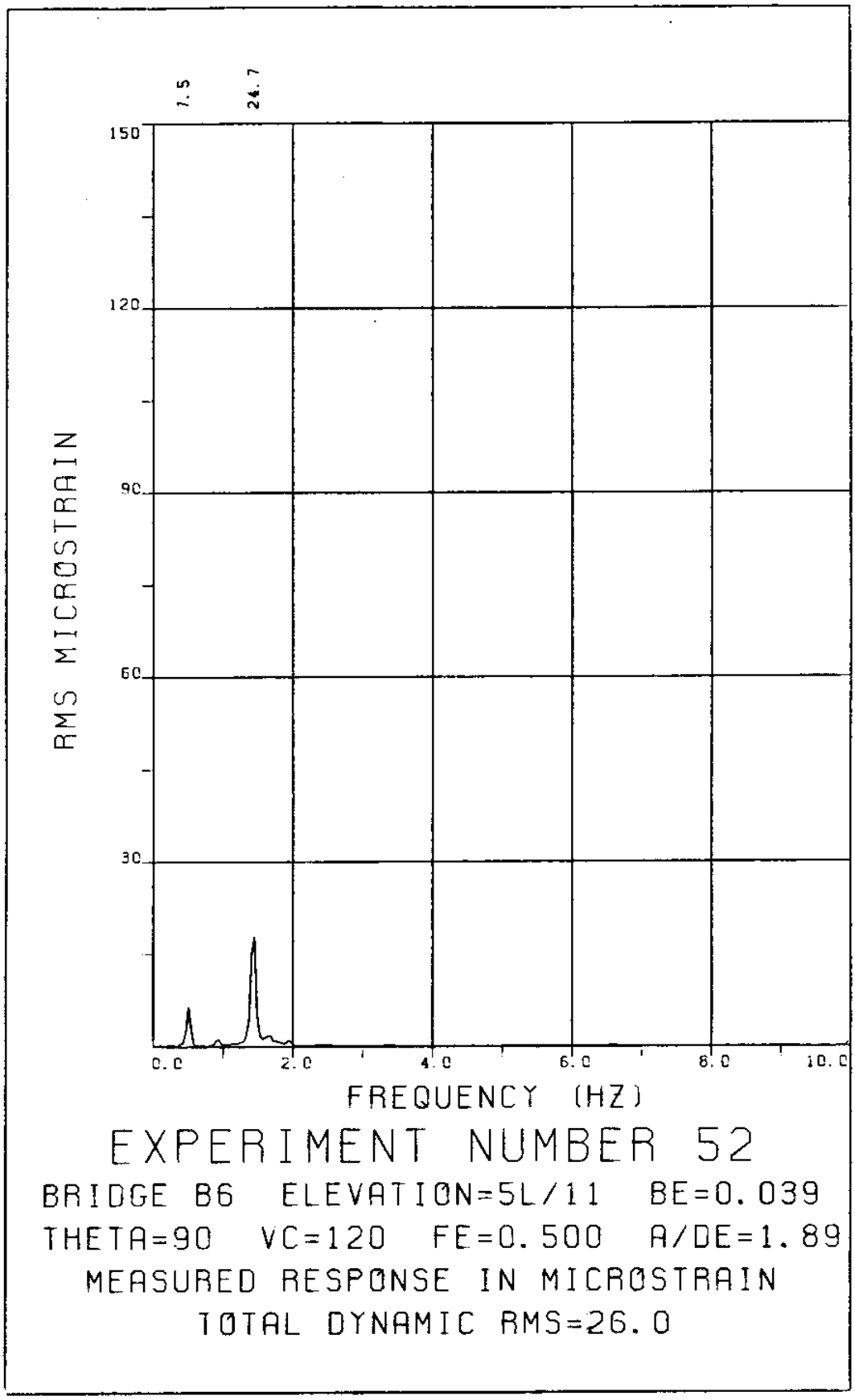
1.5
24.7
150
120
90
60
30
RMS MICROSTRAIN
0.0
2.0
4.0
6.0
8.0
10.0
FREQUENCY (HZ)
EXPERIMENT NUMBER 52
BRIDGE B6 ELEVATION=5L/11 BE=0.039
THETA=90 VC=120 FE=0.500 A/DE=1.89
MEASURED RESPONSE IN MICROSTRAIN
TOTAL DYNAMIC RMS=26.0

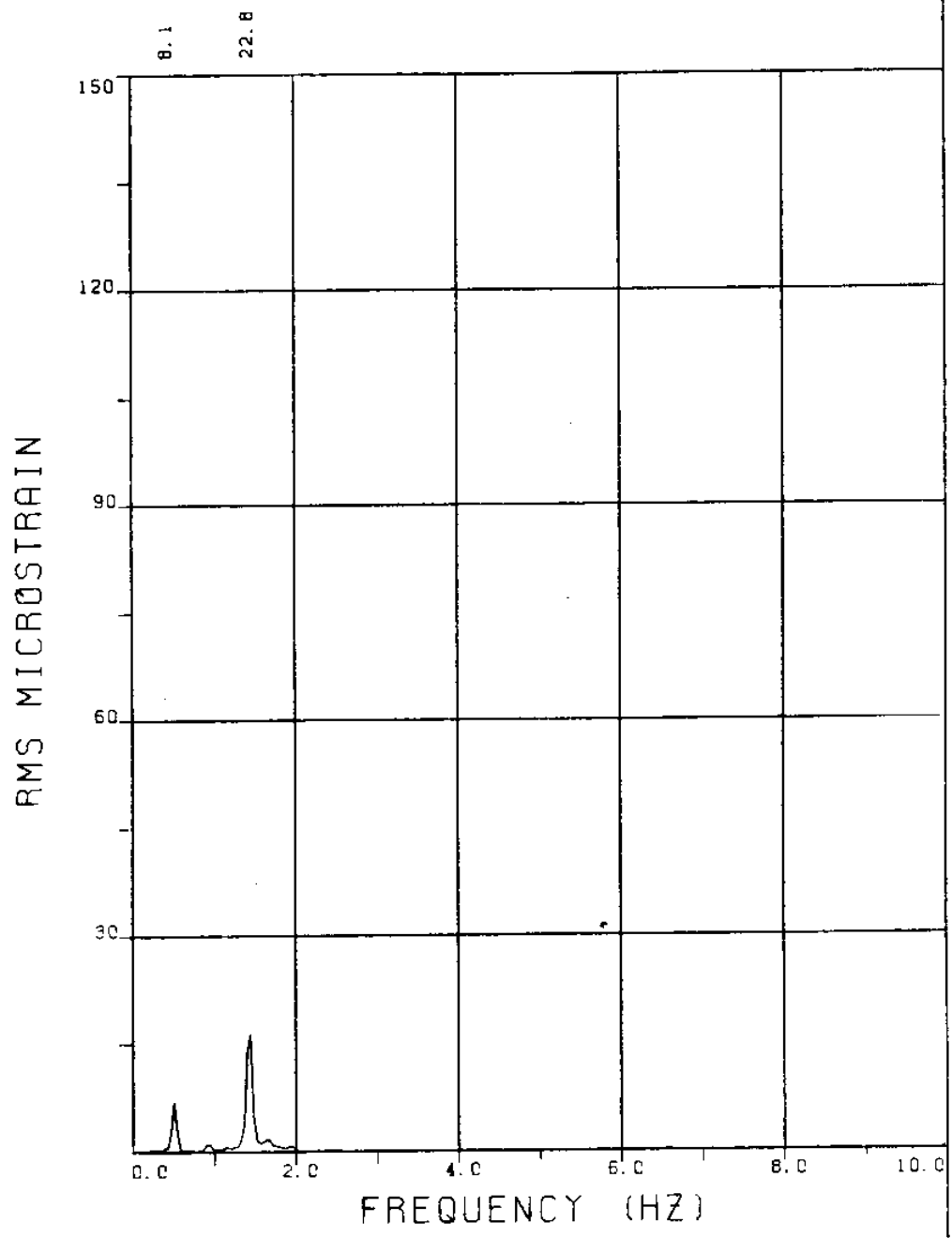

EXPERIMENT NUMBER 52

BRIDGE B5 ELEVATION=6L/11 BE=0.039

THETA=90 VC=120 FE=0.500 A/DE=1.89

MEASURED RESPONSE IN MICROSTRAIN

TOTAL DYNAMIC RMS=24.3

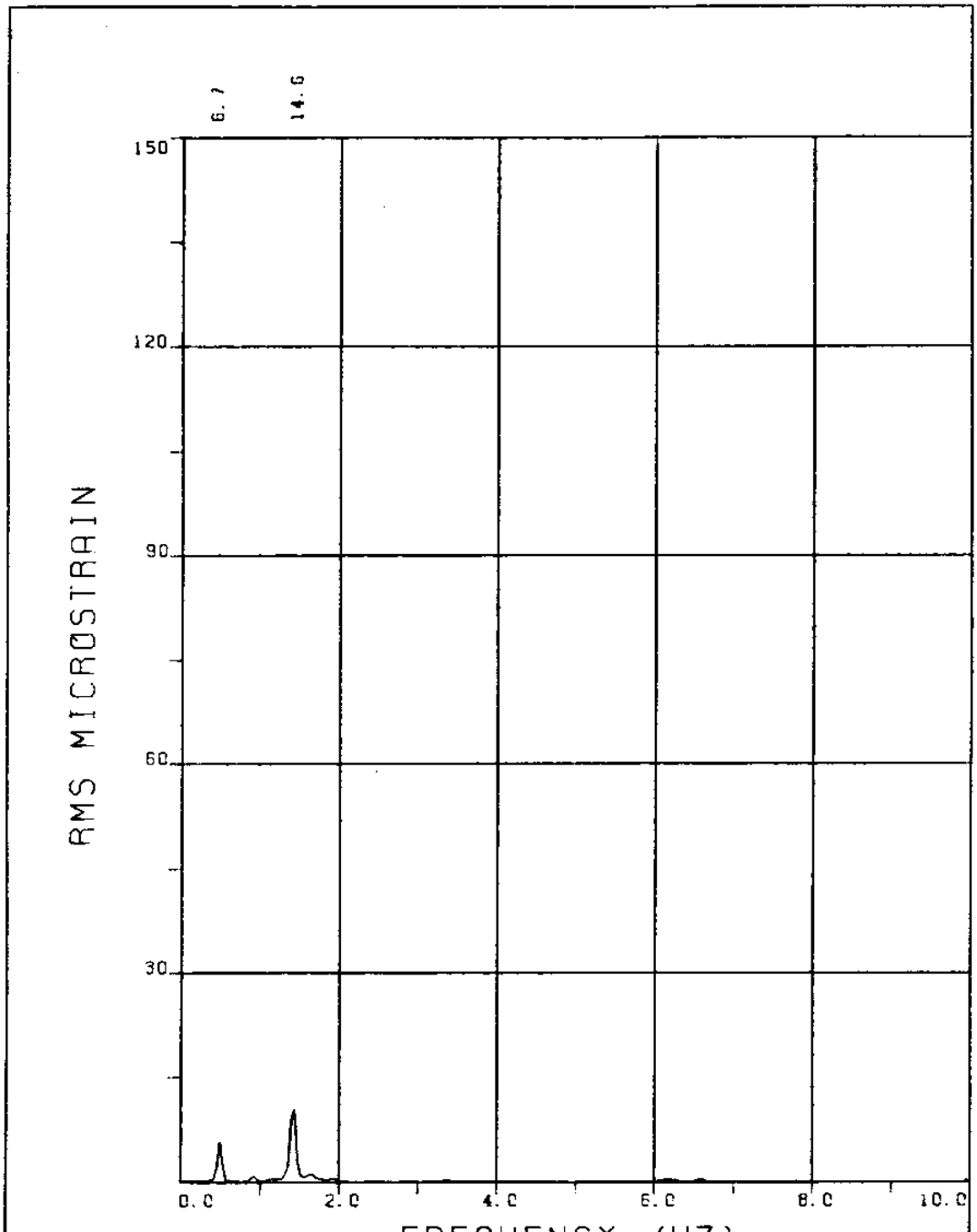

EXPERIMENT NUMBER 52

BRIDGE B3 ELEVATION=8L/11 BE=0.039

THETA=90 VC=120 FE=0.500 A/DE=1.89

MEASURED RESPONSE IN MICROSTRAIN

TOTAL DYNAMIC RMS=16.2

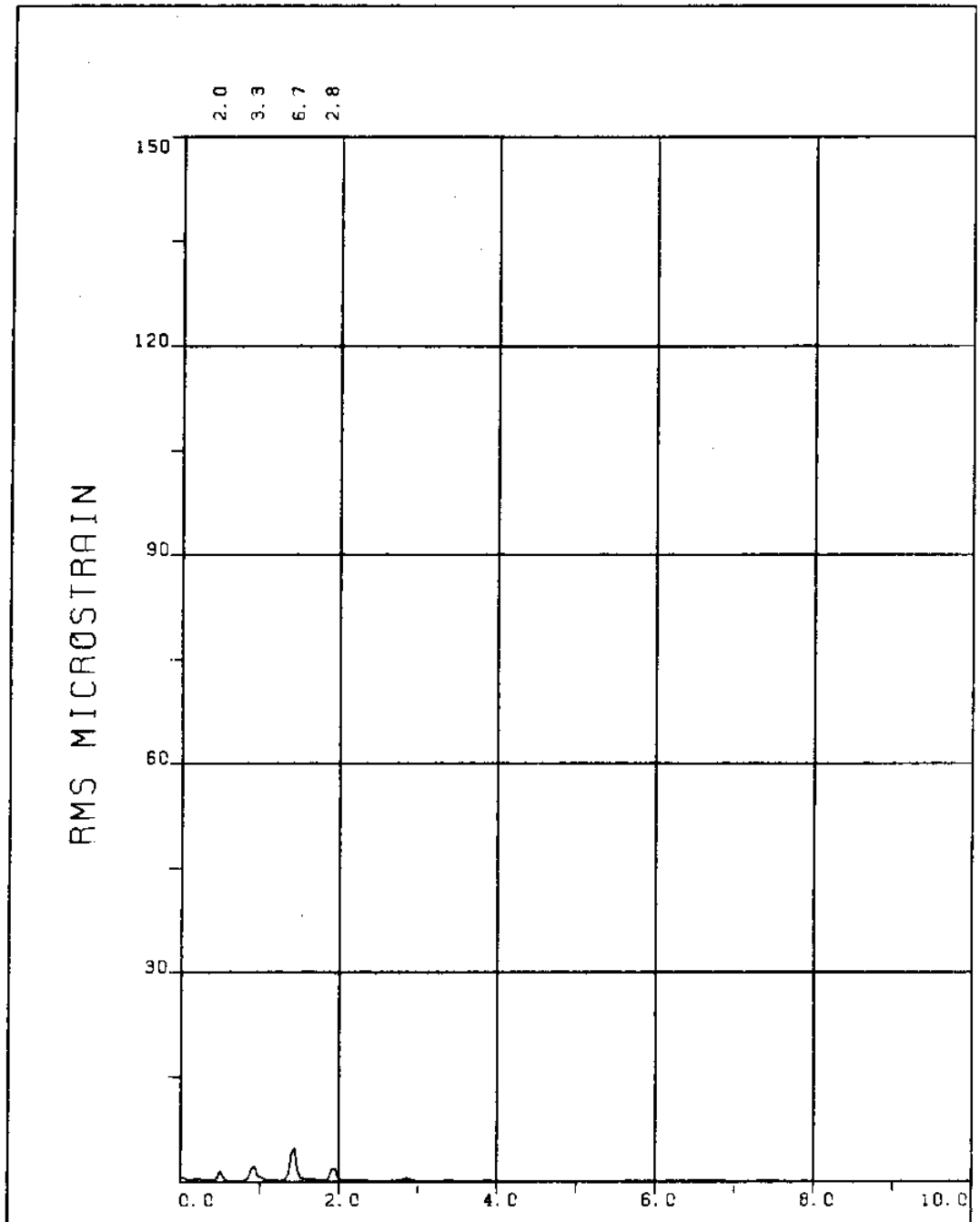

EXPERIMENT NUMBER 52

BRIDGE A8 ELEVATION=3L/11 BE=0.039

THETA=90 VC=120 FE=0.500 A/DE=1.89

MEASURED RESPONSE IN MICROSTRAIN

MEAN=24.3

TOTAL DYNAMIC RMS=8.4

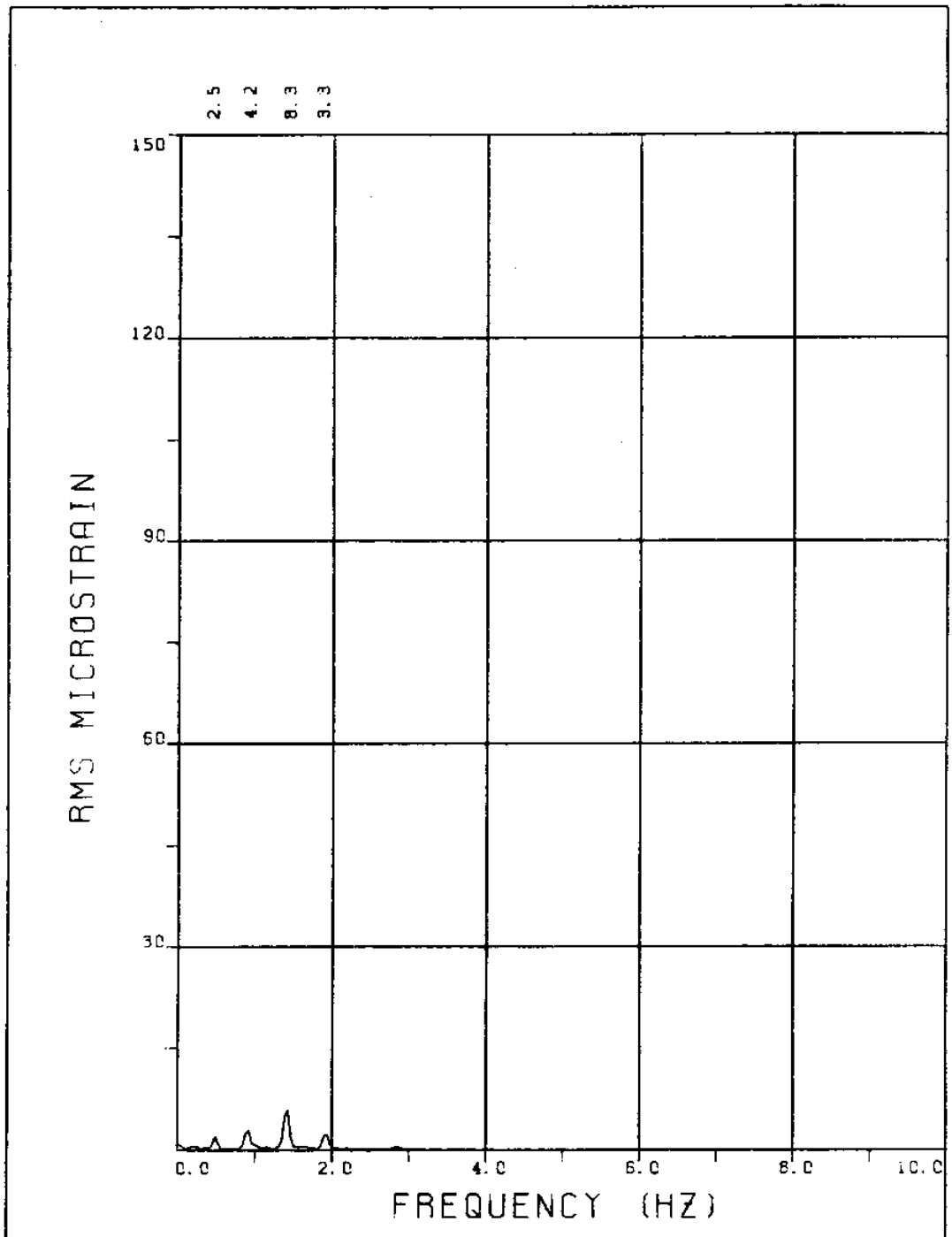

EXPERIMENT NUMBER 52

BRIDGE A6 ELEVATION=5L/11 BE=0.039

THETA=90 VC=120 FE=0.500 A/DE=1.89

MEASURED RESPONSE IN MICROSTRAIN

MEAN=29.0

TOTAL DYNAMIC RMS=10.3

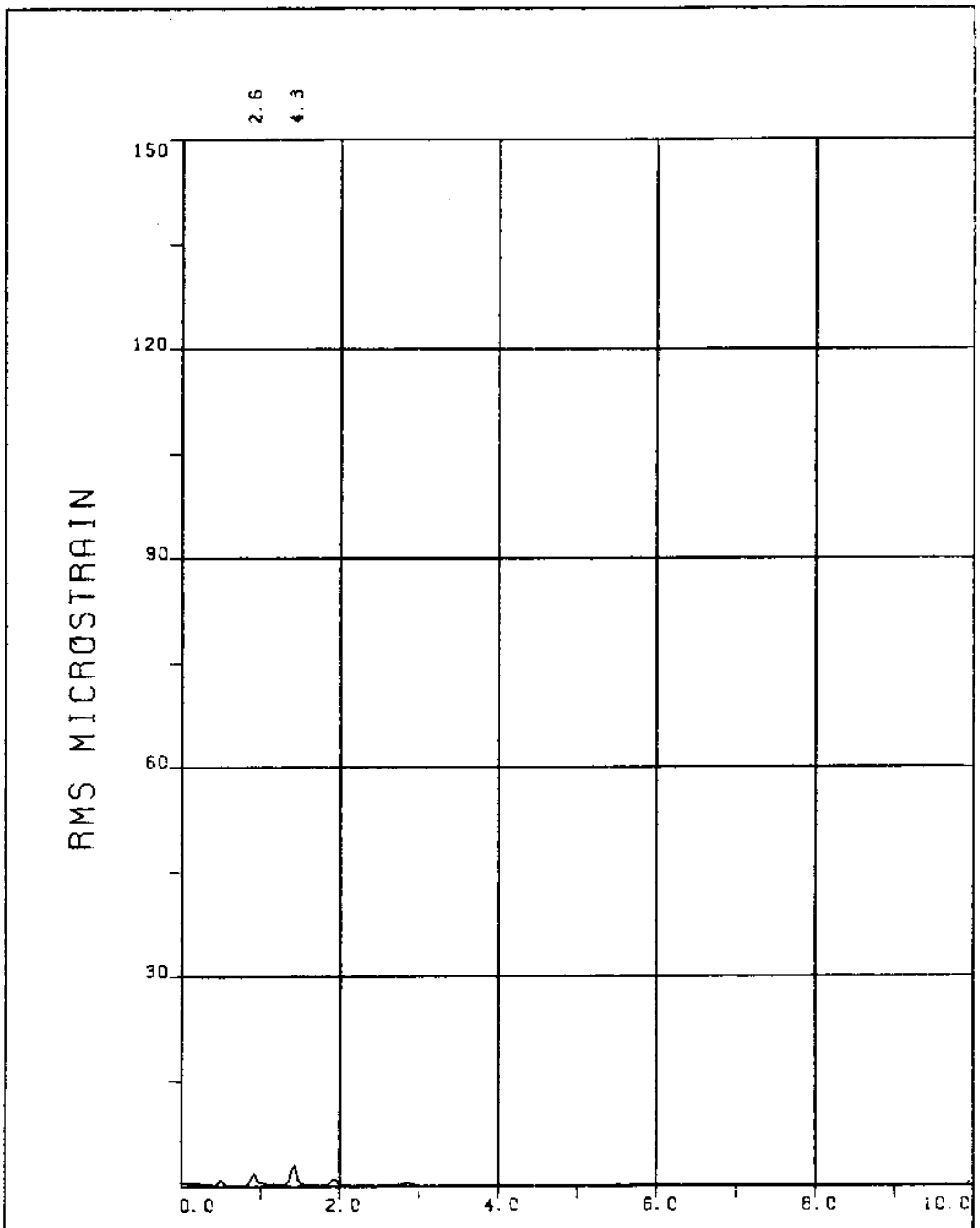

EXPERIMENT NUMBER 52

BRIDGE A3 ELEVATION=8L/11 BE=0.039

THETA=90 VC=120 FE=0.500 A/DE=1.89

MEASURED RESPONSE IN MICROSTRAIN

MEAN=19.6

TOTAL DYNAMIC RMS=5.8

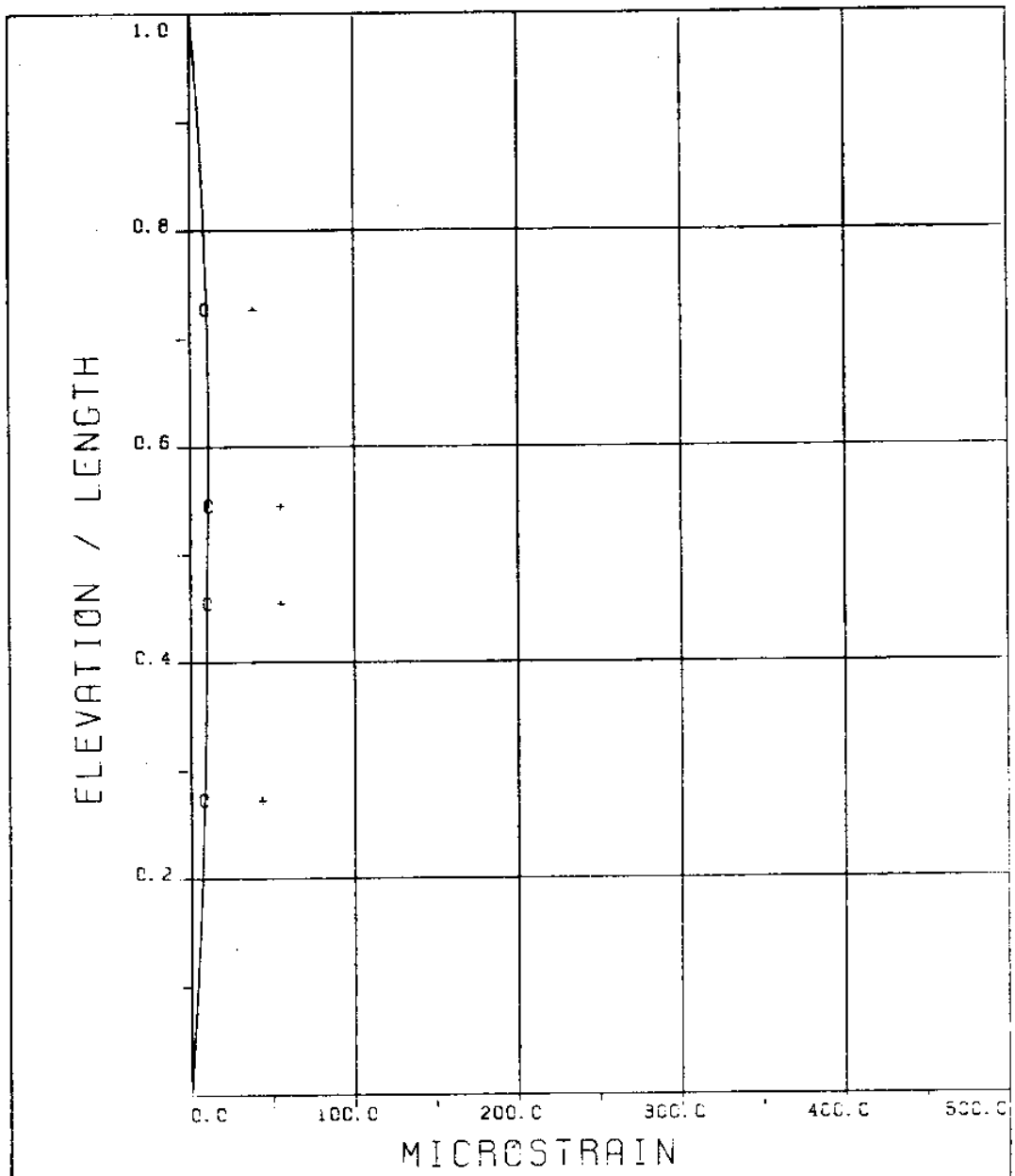

EXPERIMENT NUMBER 52

THETA=90 VC=120 FE=0.500 A/DE=1.89

DYNAMIC RESPONSE AT F=FE IN PLANE B

——— THEORY o o o EXPERIMENT

MAXIMUM DYNAMIC RESPONSE IN PLANE B

——— THEORY + + + EXPERIMENT

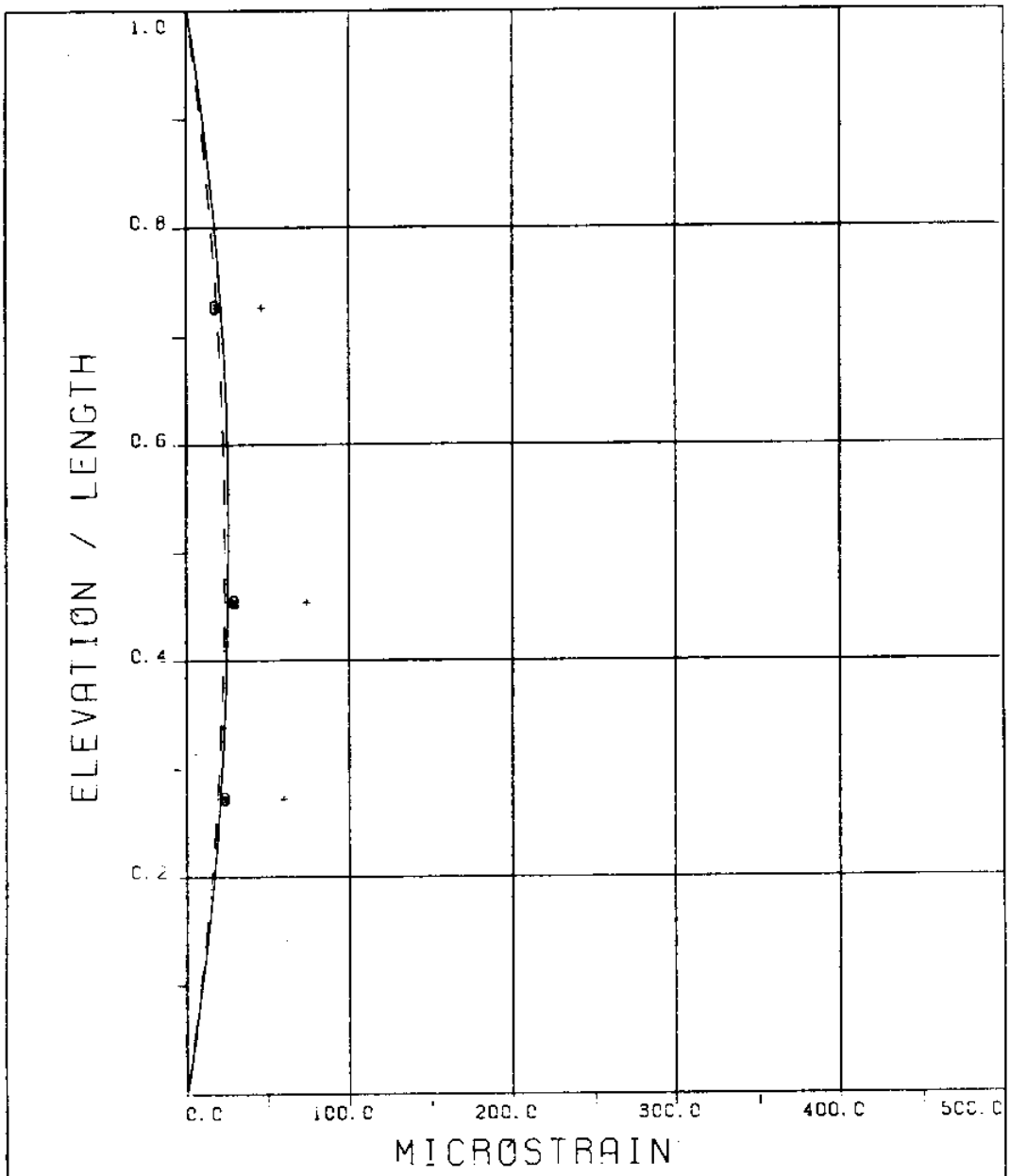

EXPERIMENT NUMBER 52

THETA=90 VC=120 FE=0.500 A/DE=1.89

STATIC RESPONSE IN PLANE A

----- THEORY * * * EXPERIMENT

MAXIMUM DYNAMIC RESPONSE IN PLANE A

o o o EXPERIMENT

MAXIMUM RESPONSE

_____ THEORY + + + EXPERIMENT

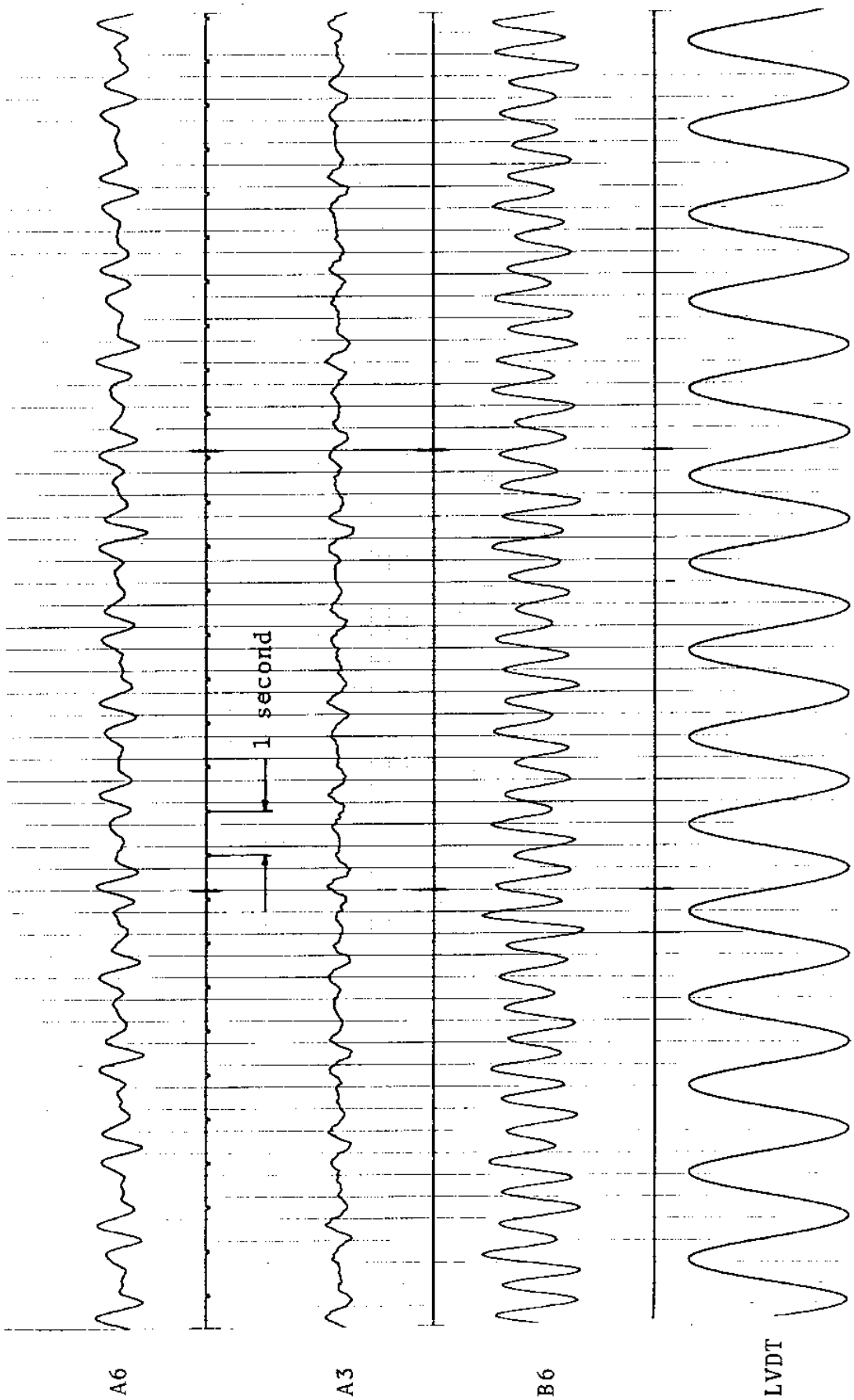

FIGURE 52Ta: LVDT: 0.087 D_e/DIVISION; STRAINS: 3.82 MICROSTRAIN/DIVISION

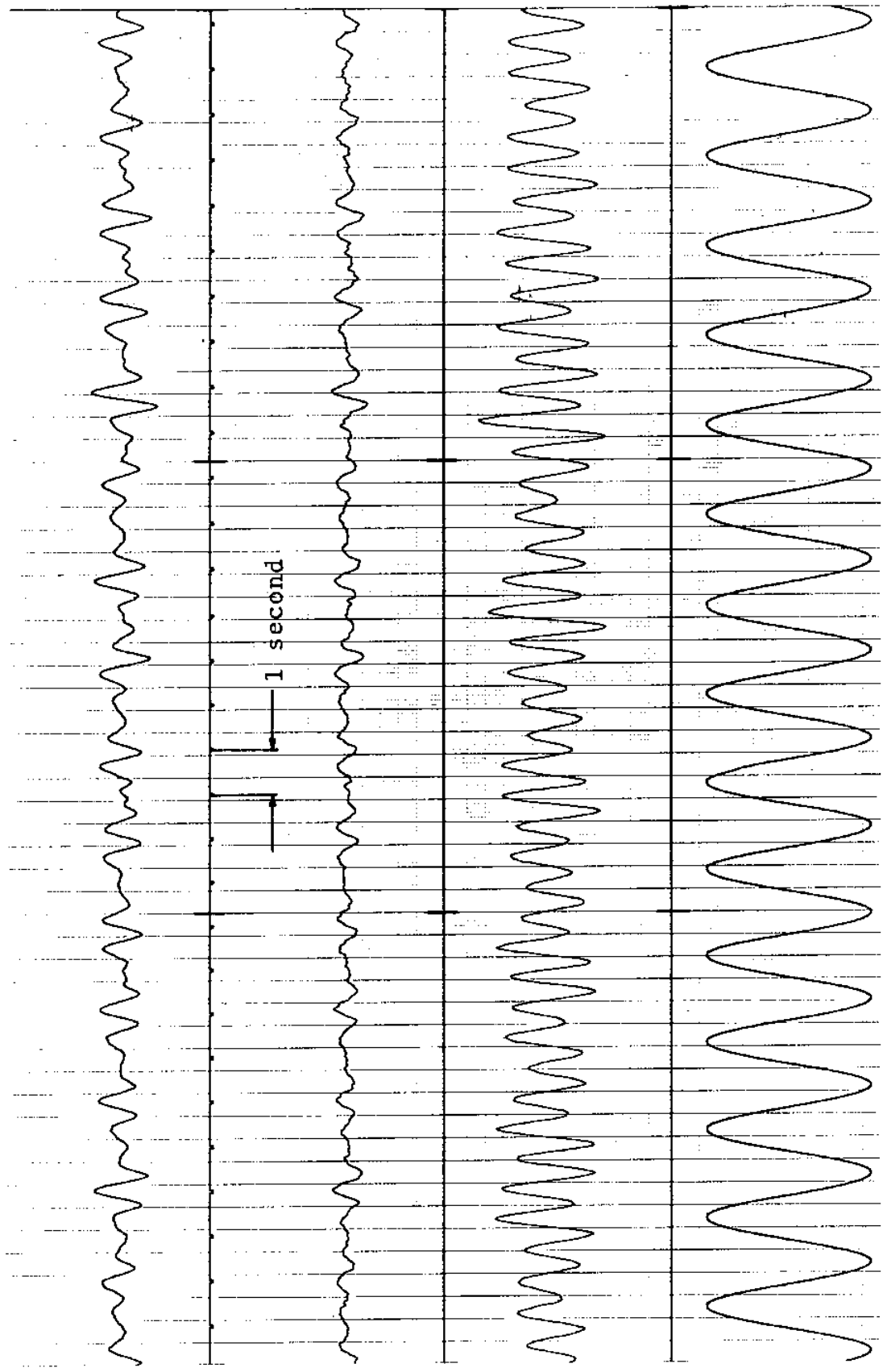

FIGURE 52Tb: LVDT: 0.087 D_e/DIVISION; STRAINS: 3.82 MICROSTRAIN/DIVISION

EXPERIMENT 59

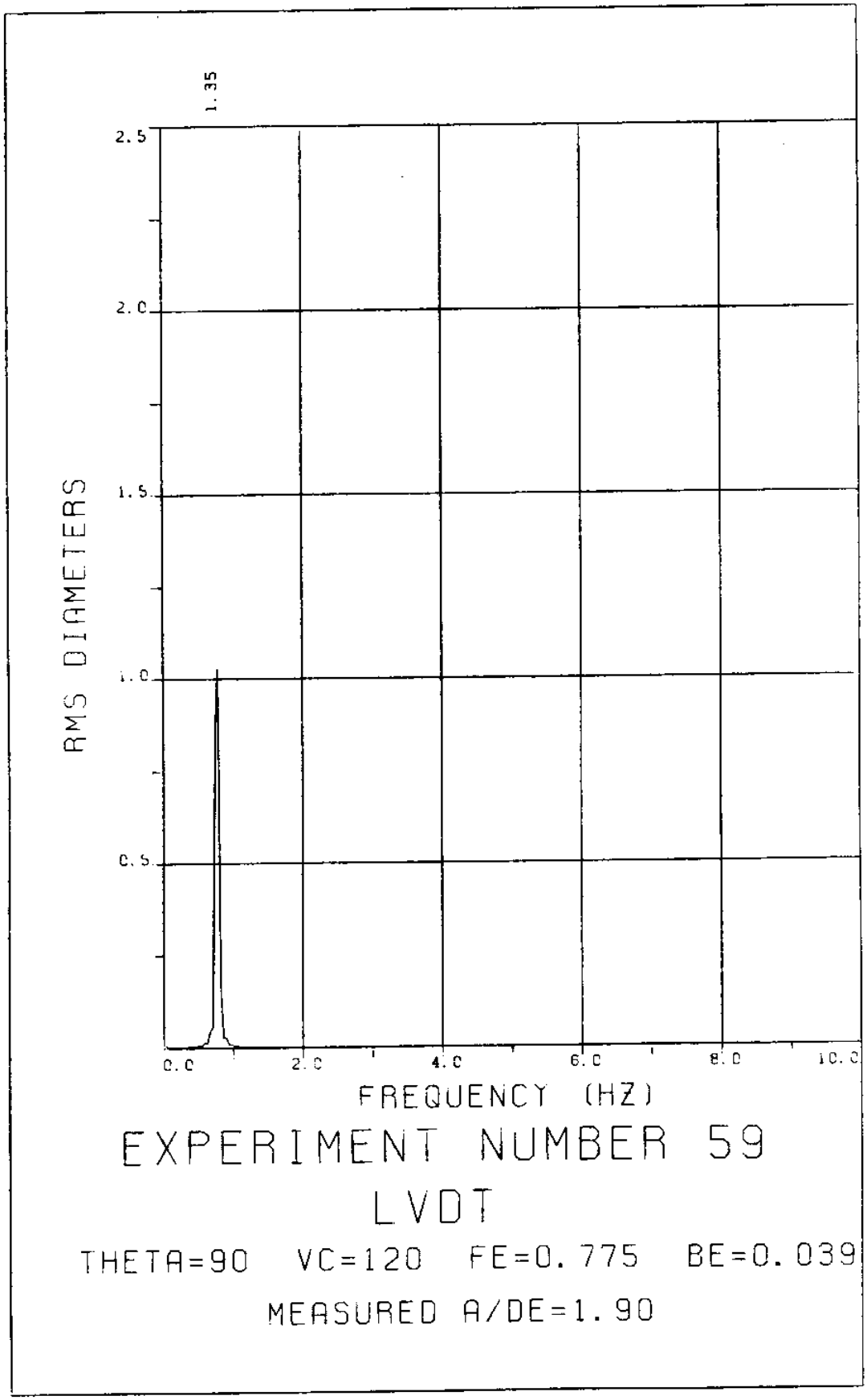

EXPERIMENT NUMBER 59

LVDT

THETA=90 VC=120 FE=0.775 BE=0.039

MEASURED A/DE=1.90

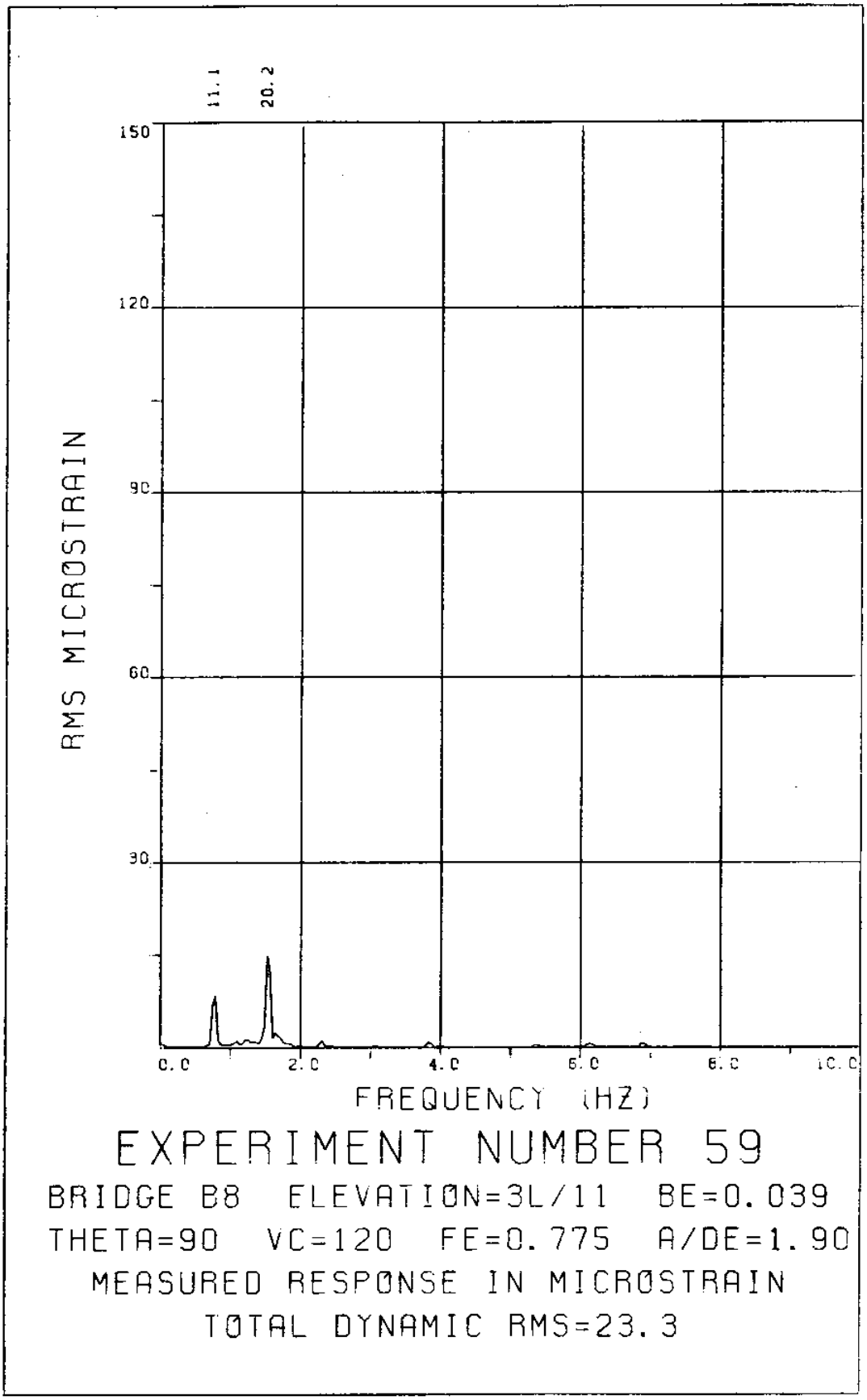
11.1
20.2
150
120
90
60
30
RMS MICROSTRAIN
0.0
2.0
4.0
6.0
8.0
10.0
FREQUENCY (HZ)
EXPERIMENT NUMBER 59
BRIDGE B8 ELEVATION=3L/11 BE=0.039
THETA=90 VC=120 FE=0.775 A/DE=1.90
MEASURED RESPONSE IN MICROSTRAIN
TOTAL DYNAMIC RMS=23.3

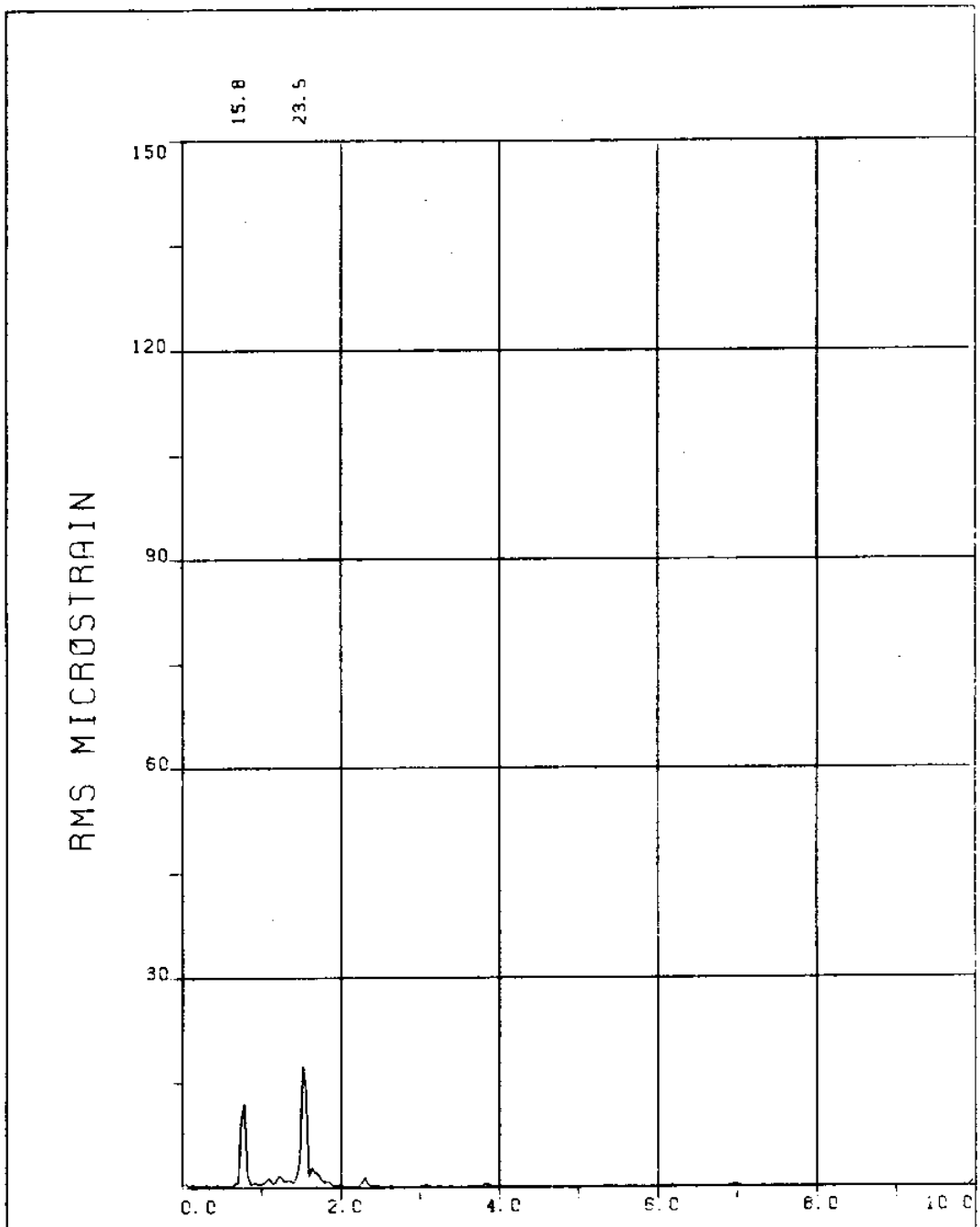

EXPERIMENT NUMBER 59

BRIDGE B6 ELEVATION=5L/11 BE=0.039

THETA=90 VC=120 FE=0.775 A/DE=1.90

MEASURED RESPONSE IN MICROSTRAIN

TOTAL DYNAMIC RMS=28.4

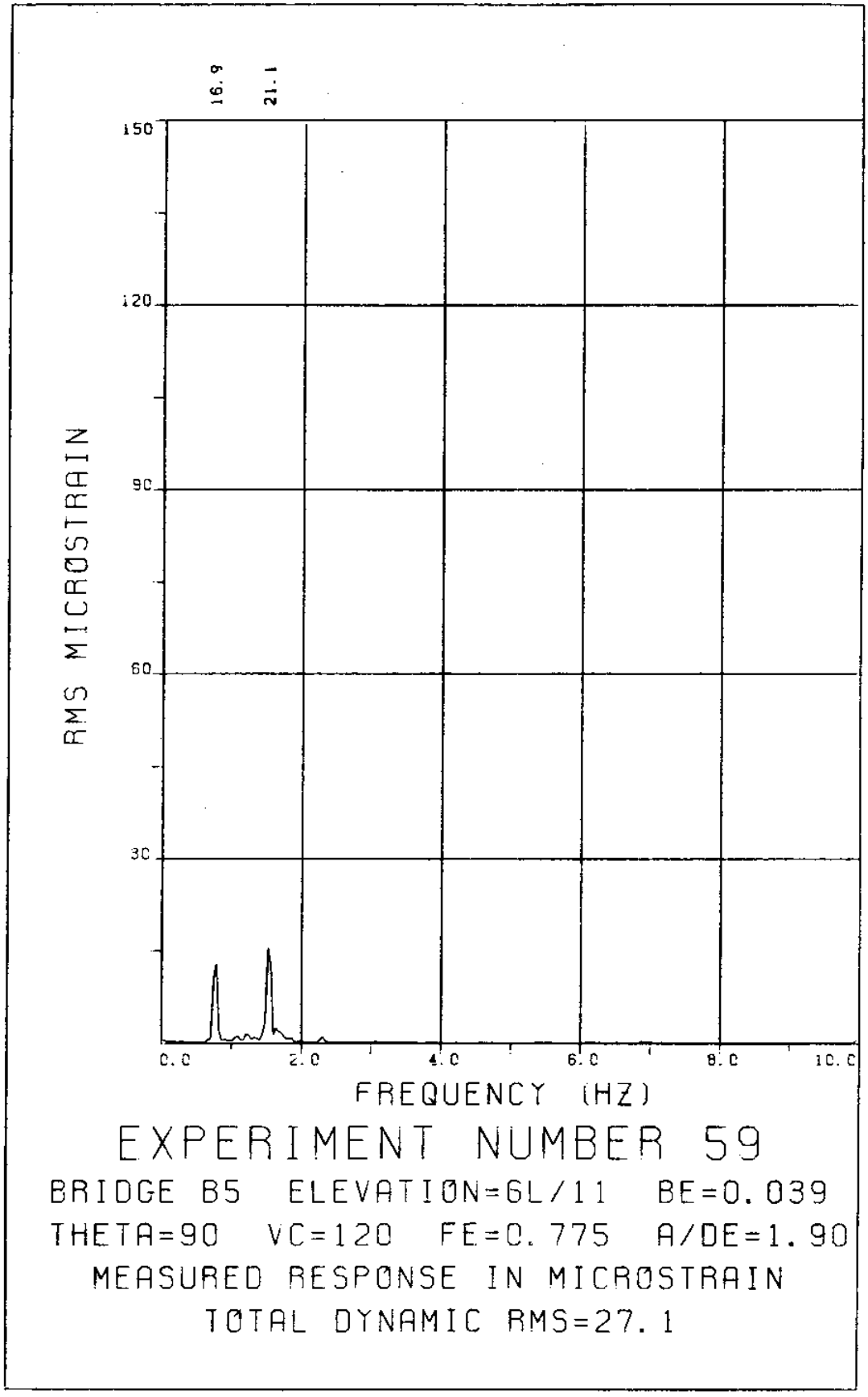
16.9
21.1
150
120
90
60
30
RMS MICROSTRAIN
0.0
2.0
4.0
6.0
8.0
10.0
FREQUENCY (HZ)
EXPERIMENT NUMBER 59
BRIDGE B5 ELEVATION=6L/11 BE=0.039
THETA=90 VC=120 FE=0.775 A/DE=1.90
MEASURED RESPONSE IN MICROSTRAIN
TOTAL DYNAMIC RMS=27.1

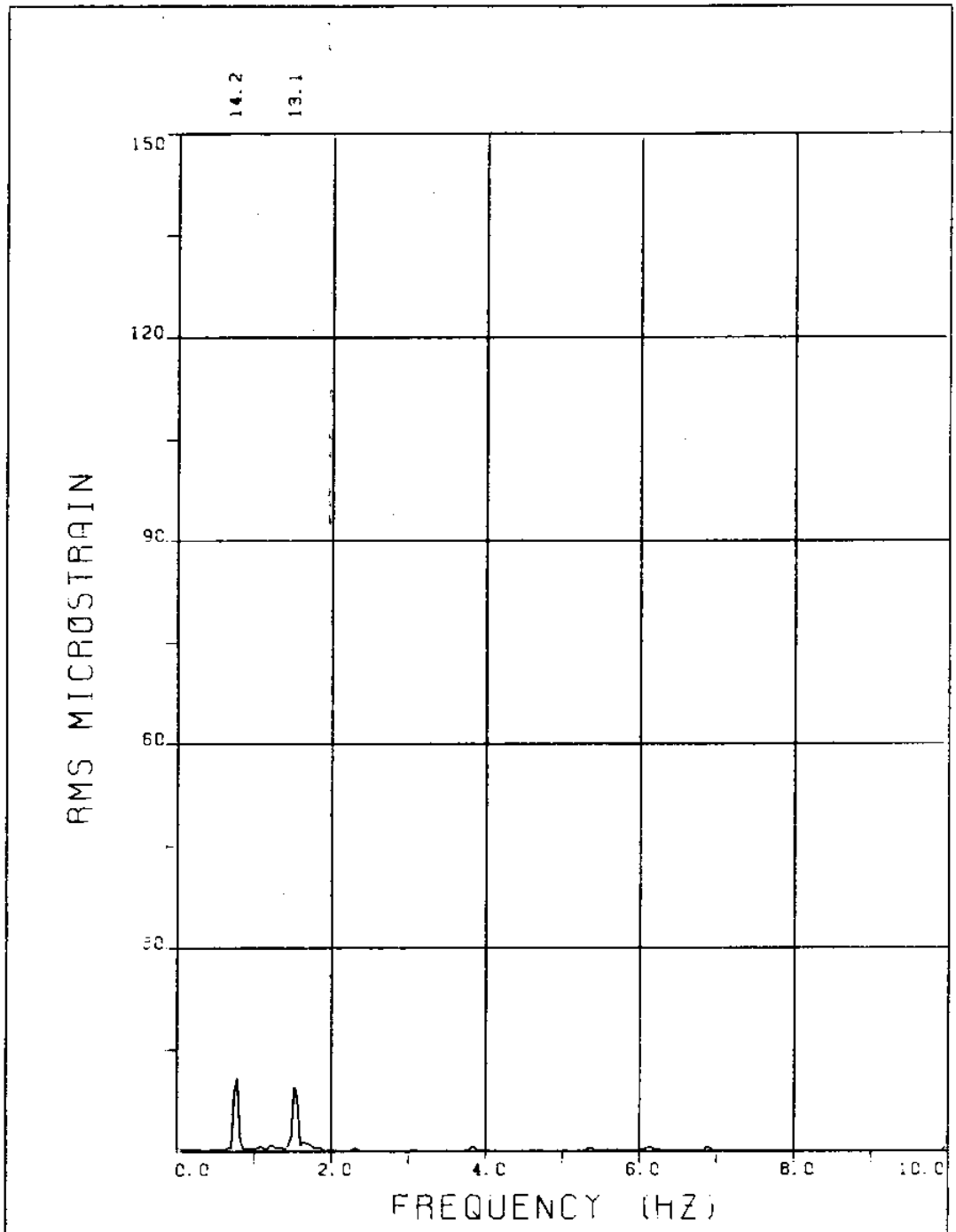

EXPERIMENT NUMBER 59

BRIDGE B3 ELEVATION=8L/11 BE=0.039

THETA=90 VC=120 FE=0.775 A/DE=1.90

MEASURED RESPONSE IN MICROSTRAIN

TOTAL DYNAMIC RMS=19.5

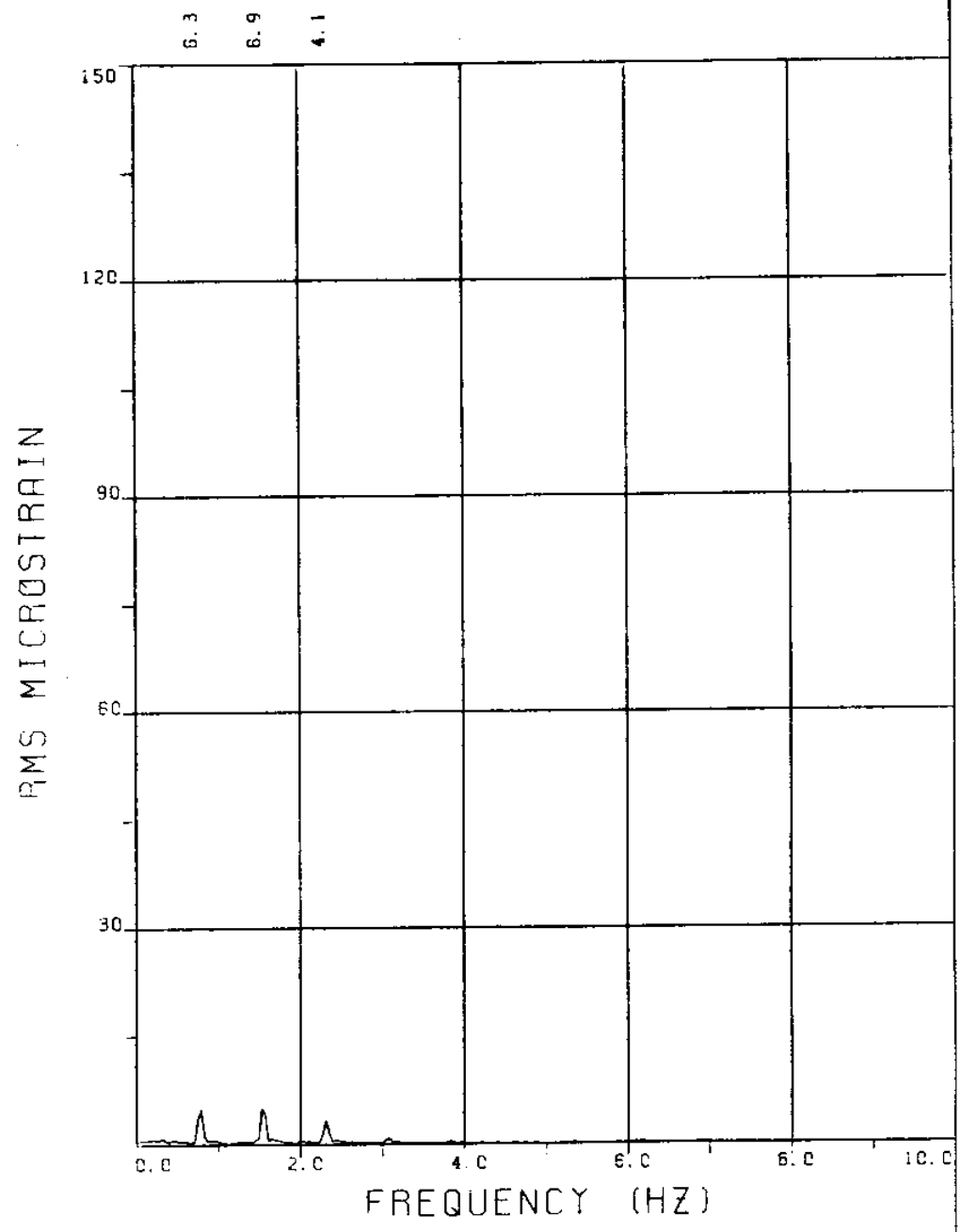

EXPERIMENT NUMBER 59

BRIDGE A8 ELEVATION=3L/11 BE=0.039

THETA=90 VC=120 FE=0.500 A/DE=1.90

MEASURED RESPONSE IN MICROSTRAIN

MEAN=27.5

TOTAL DYNAMIC RMS=10.6

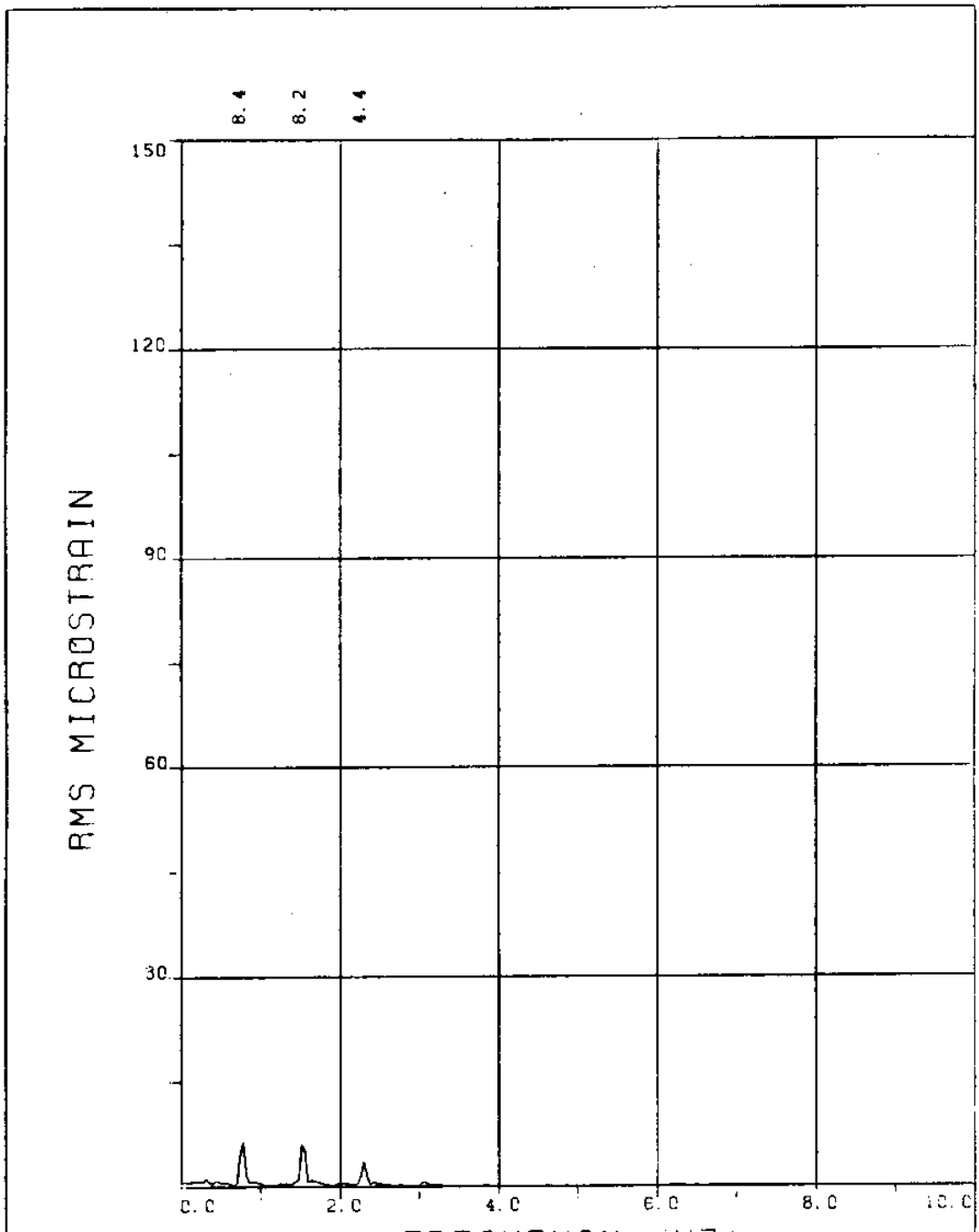

EXPERIMENT NUMBER 59

BRIDGE A6 ELEVATION=5L/11 BE=0.039

THETA=90 VC=120 FE=0.500 A/DE=1.90

MEASURED RESPONSE IN MICROSTRAIN

MEAN=33.0

TOTAL DYNAMIC RMS=12.8

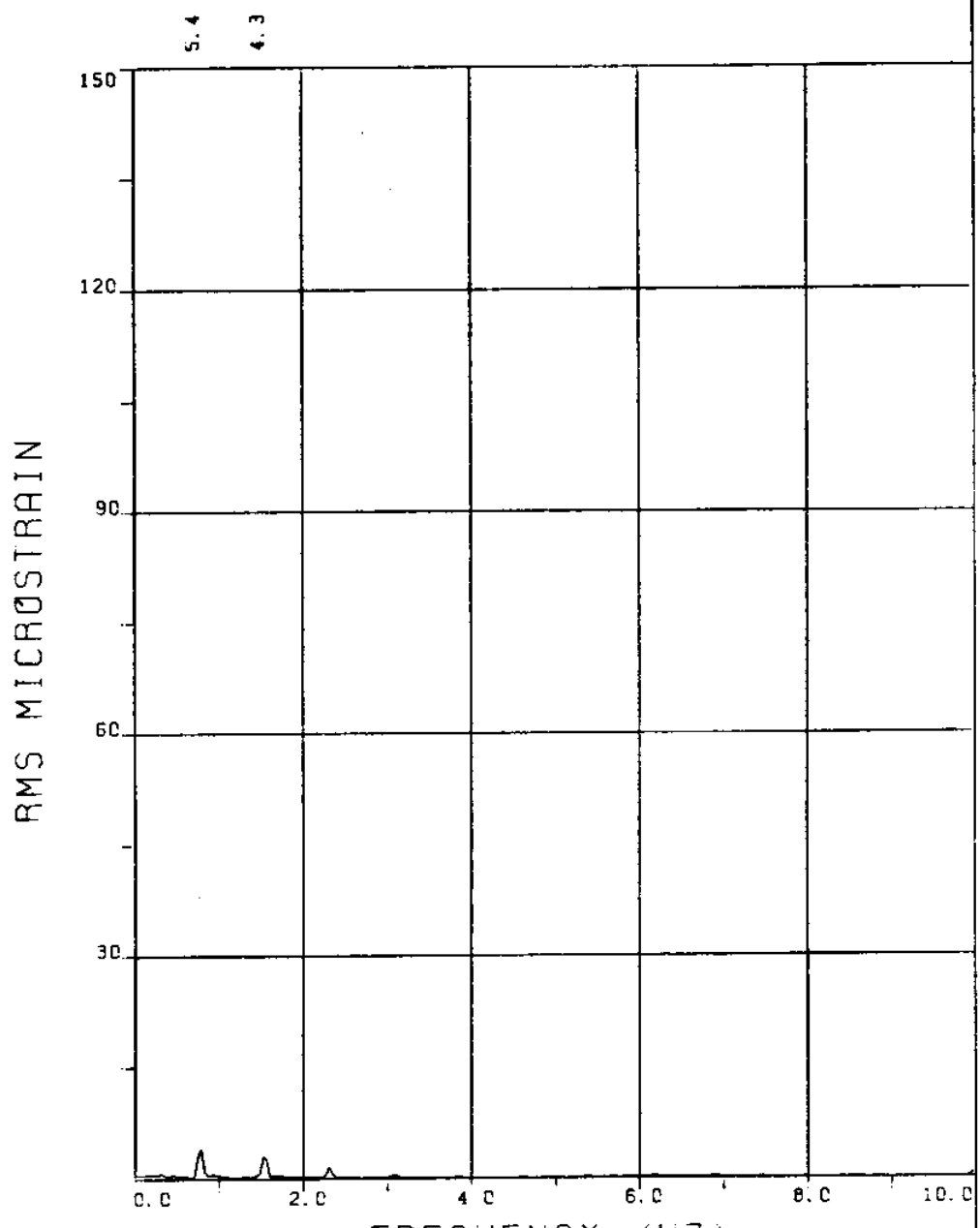

EXPERIMENT NUMBER 59

BRIDGE A3 ELEVATION=8L/11 BE=0.039

THETA=90 VC=120 FE=0.775 A/DE=1.90

MEASURED RESPONSE IN MICROSTRAIN

MEAN=29.1

TOTAL DYNAMIC RMS=7.5

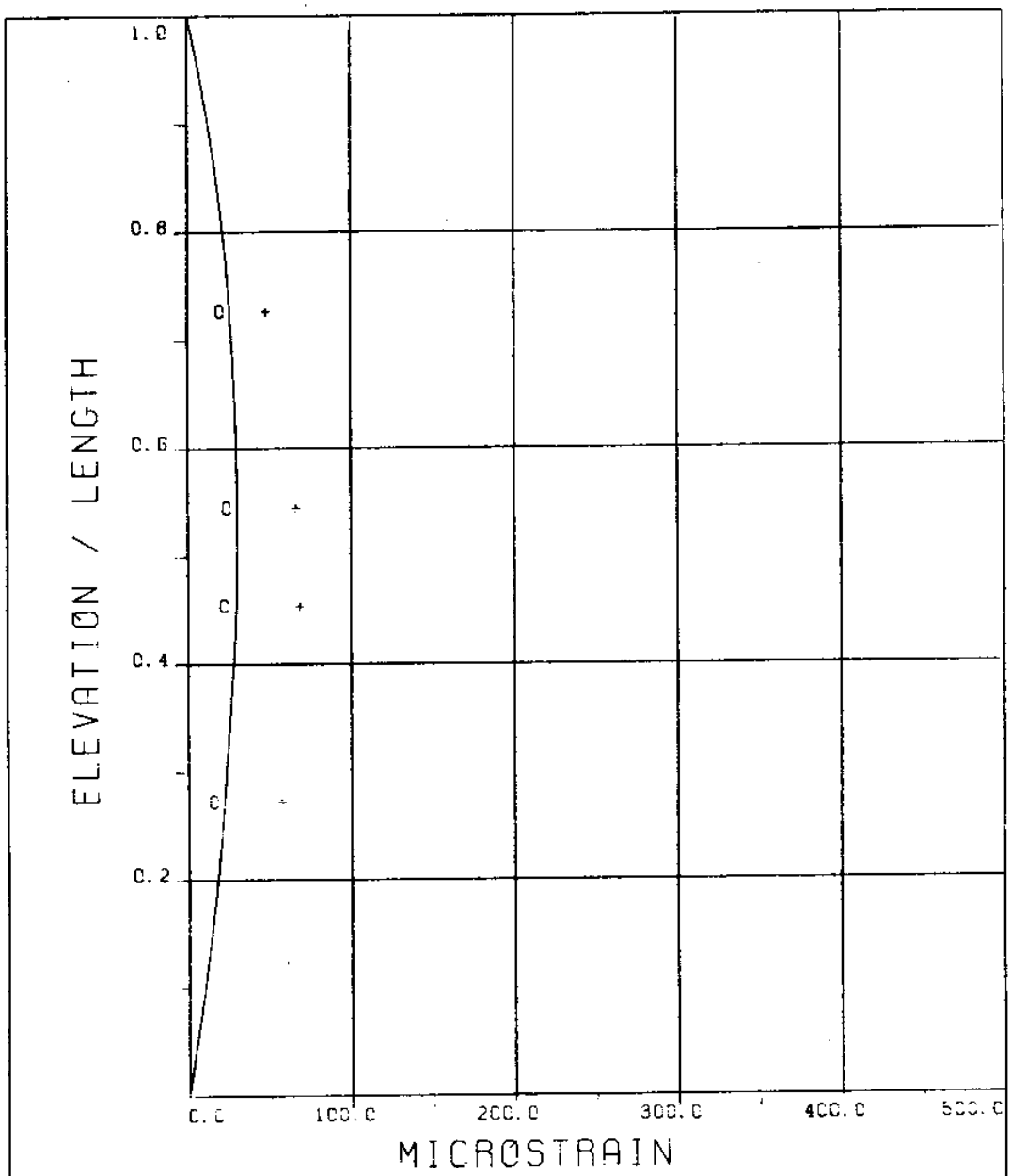

EXPERIMENT NUMBER 59

THETA=90 VC=120 FE=0.775 A/DE=1.90

DYNAMIC RESPONSE AT F=FE IN PLANE B

——— THEORY o o o EXPERIMENT

MAXIMUM DYNAMIC RESPONSE IN PLANE B

——— THEORY + + + EXPERIMENT

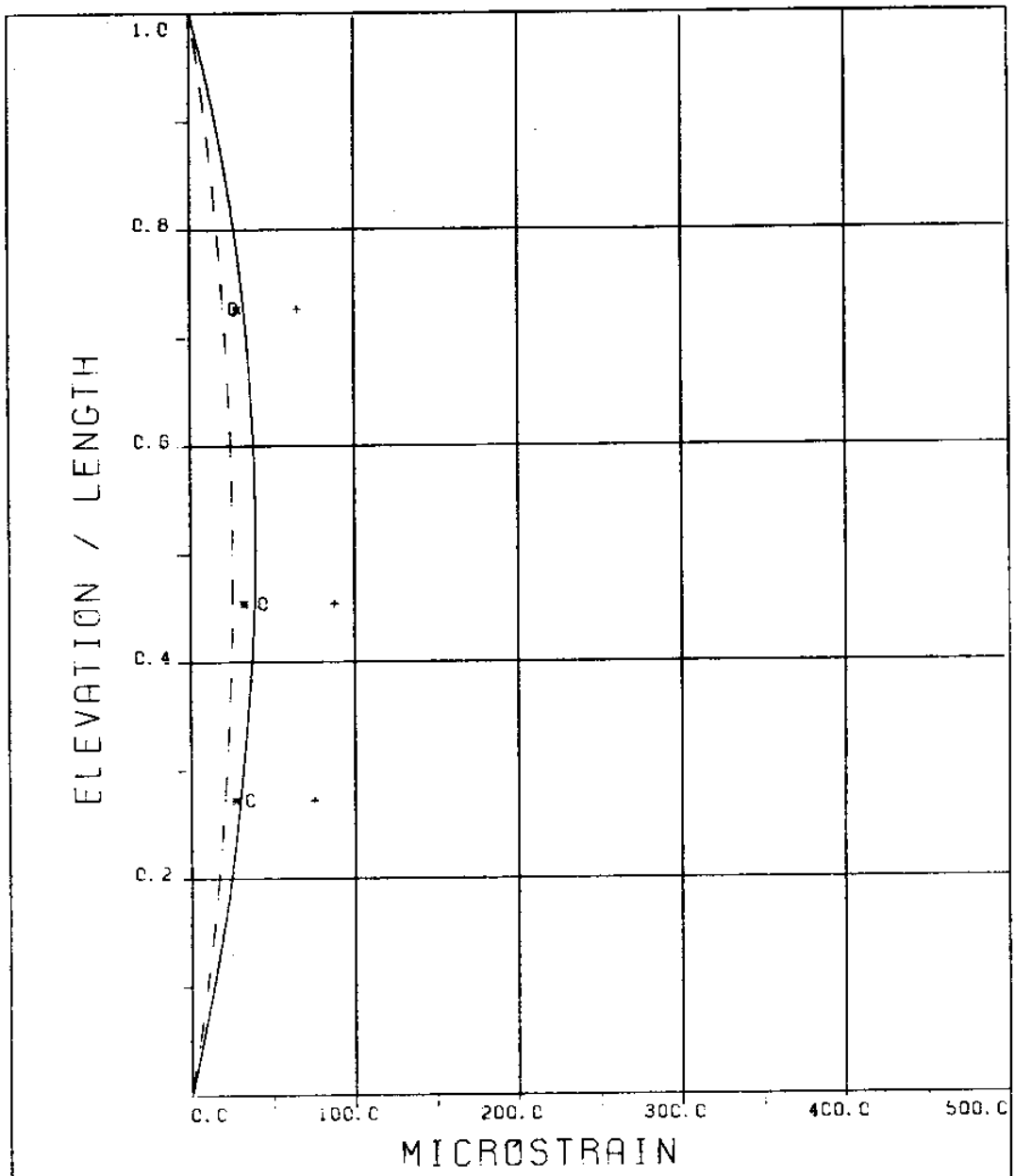

EXPERIMENT NUMBER 59

THETA=90 VC=120 FE=0.775 A/DE=1.90

STATIC RESPONSE IN PLANE A

----- THEORY * * * EXPERIMENT

MAXIMUM DYNAMIC RESPONSE IN PLANE A

o o o EXPERIMENT

MAXIMUM RESPONSE

_____ THEORY + + + EXPERIMENT

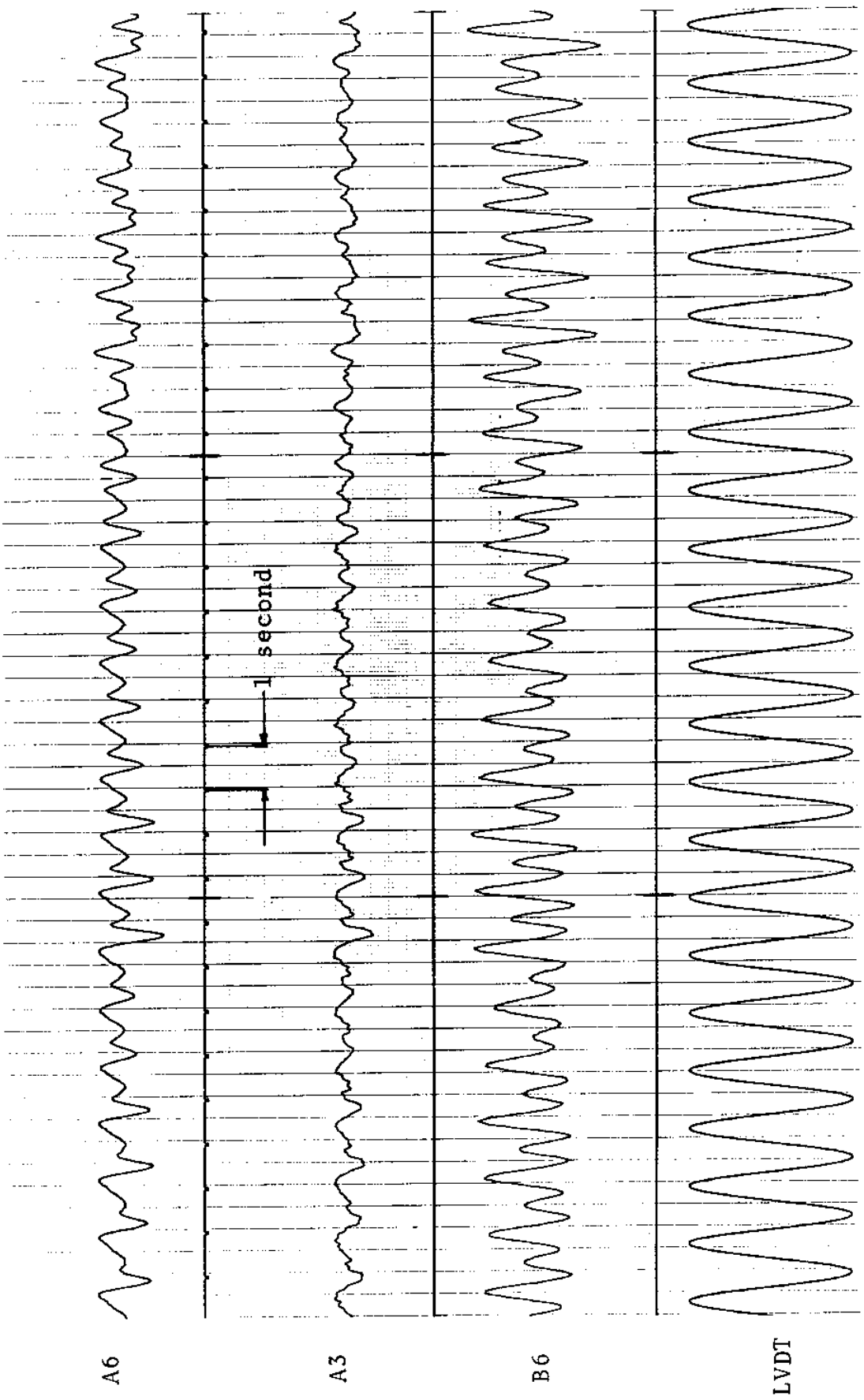

FIGURE 59Ta: LVDT: 0.087 D_e/DIVISION; STRAINS: 3.82 MICROSTRAIN/DIVISION

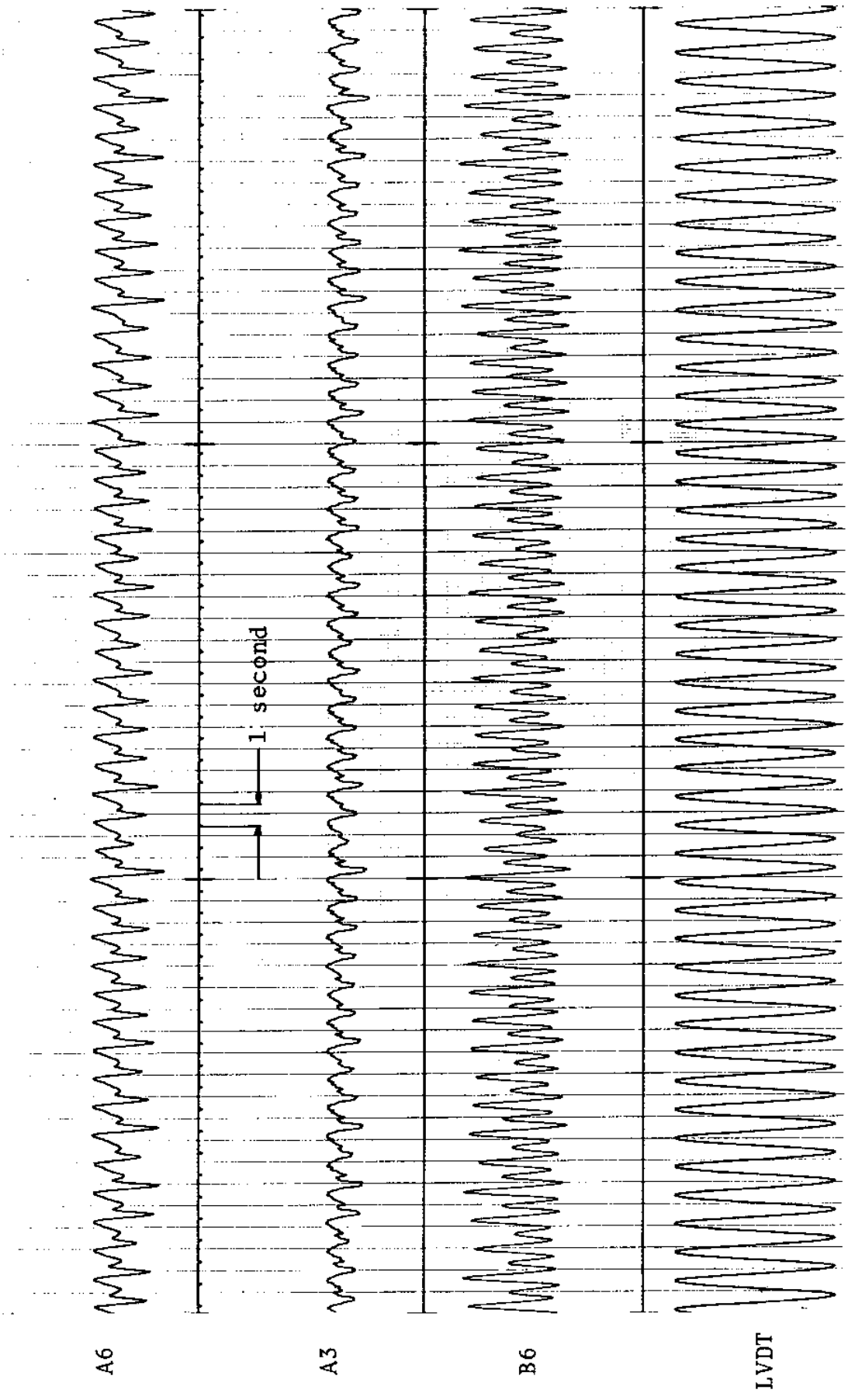

FIGURE 59Tb: LVDT: 0.087 D_e/DIVISION; STRAINS: 3.82 MICROSTRAIN/DIVISION

EXPERIMENT 71

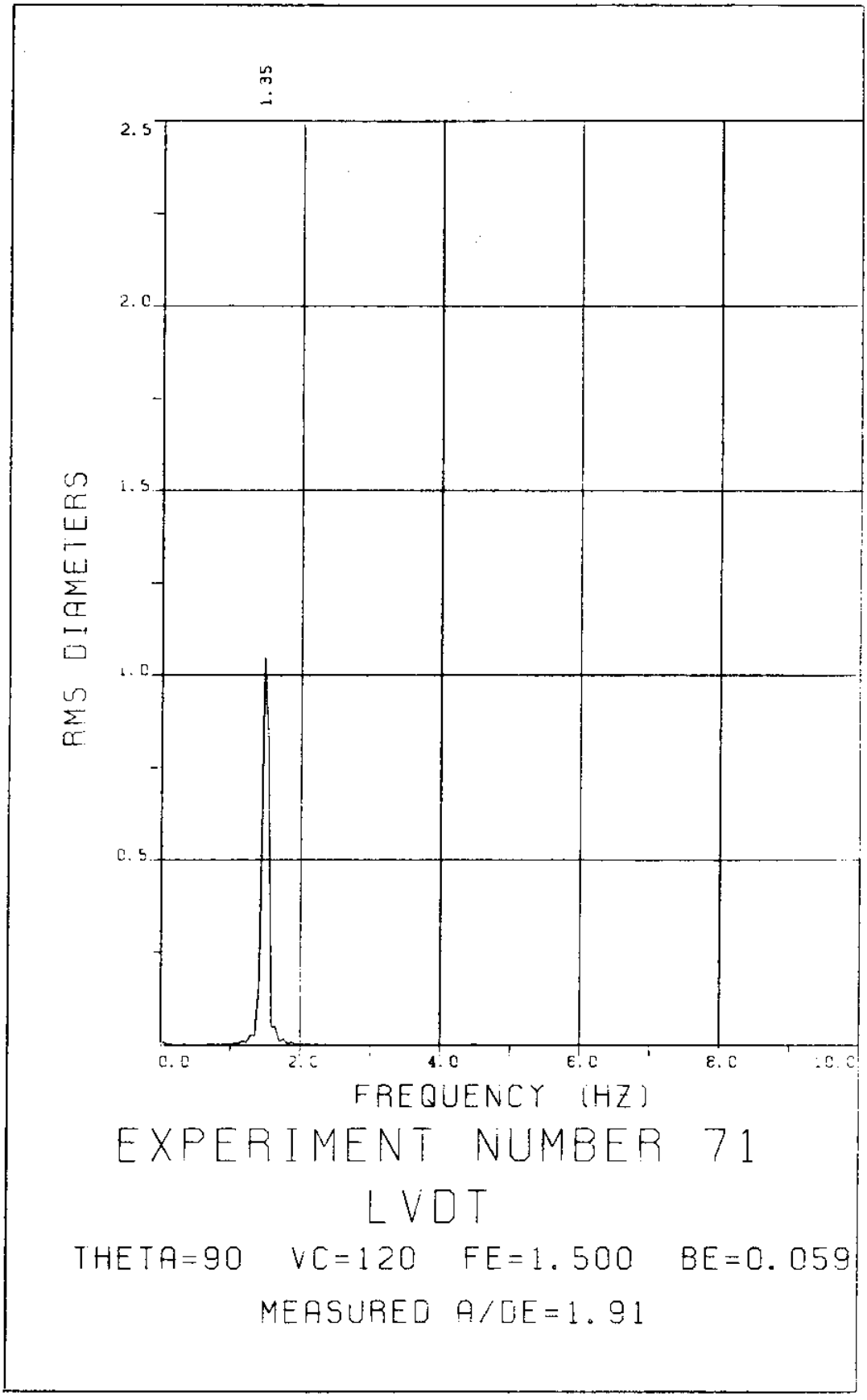
1.35
2.5
2.0
1.5
1.0
0.5
RMS DIAMETERS
0.0
2.0
4.0
6.0
8.0
10.0
FREQUENCY (HZ)
EXPERIMENT NUMBER 71
LVDT
THETA=90 VC=120 FE=1.500 BE=0.059
MEASURED A/DE=1.91

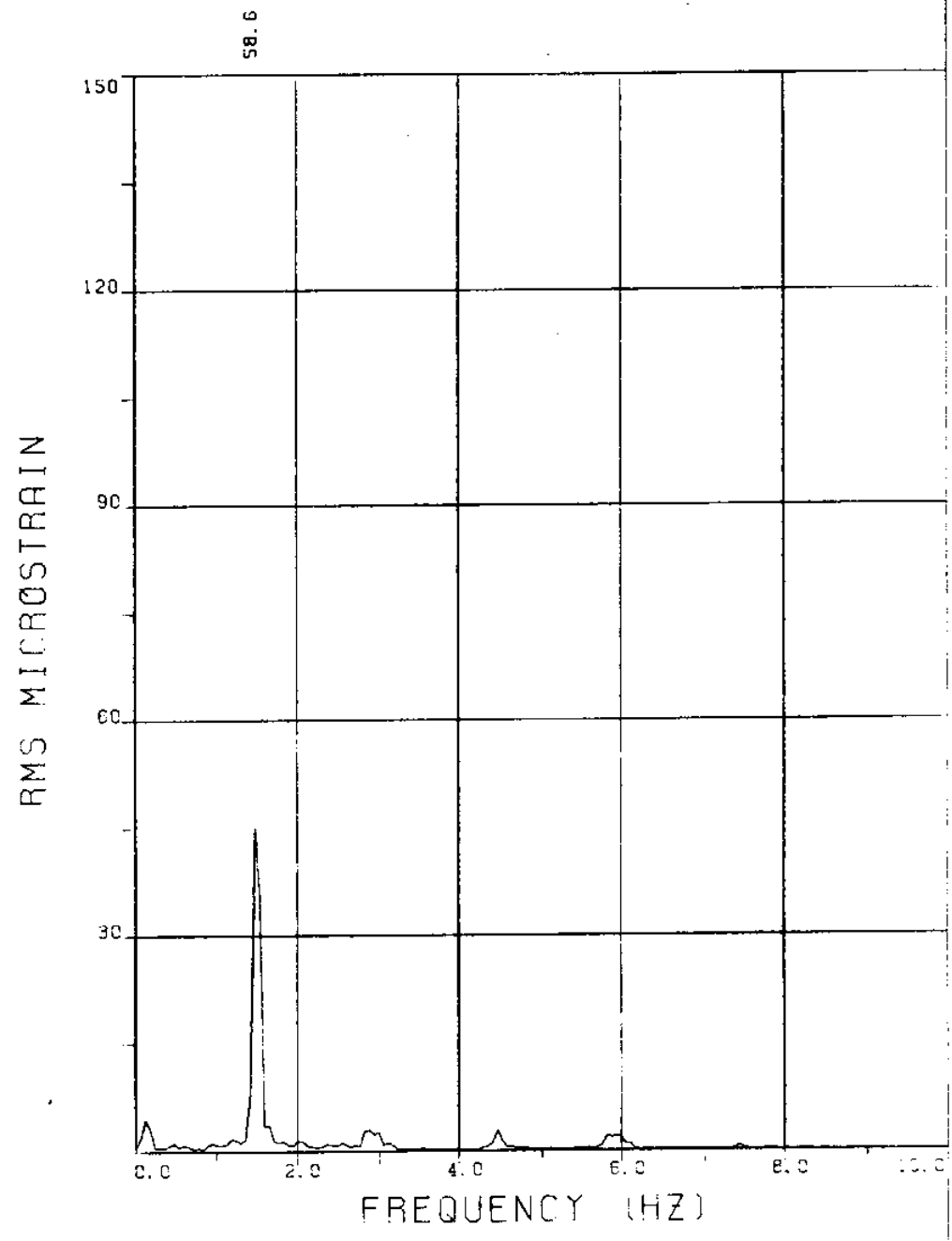

EXPERIMENT NUMBER 71

BRIDGE B8 ELEVATION=3L/11 BE=0.059

THETA=90 VC=120 FE=1.500 A/DE=1.91

MEASURED RESPONSE IN MICROSTRAIN

TOTAL DYNAMIC RMS=59.6

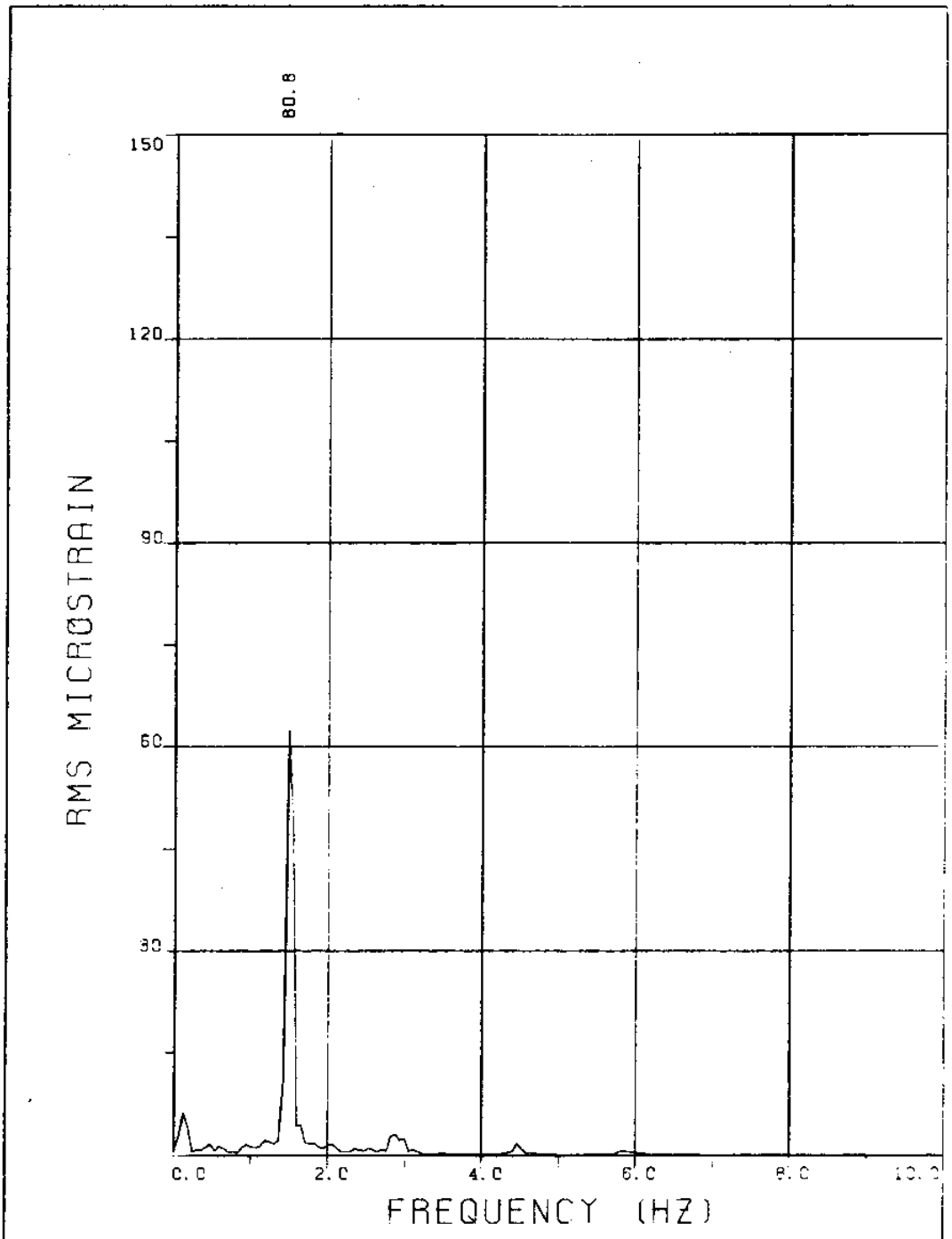

EXPERIMENT NUMBER 71

BRIDGE B6 ELEVATION=5L/11 BE=0.059

THETA=90 VC=120 FE=1.500 A/DE=1.91

MEASURED RESPONSE IN MICROSTRAIN

TOTAL DYNAMIC RMS=81.6

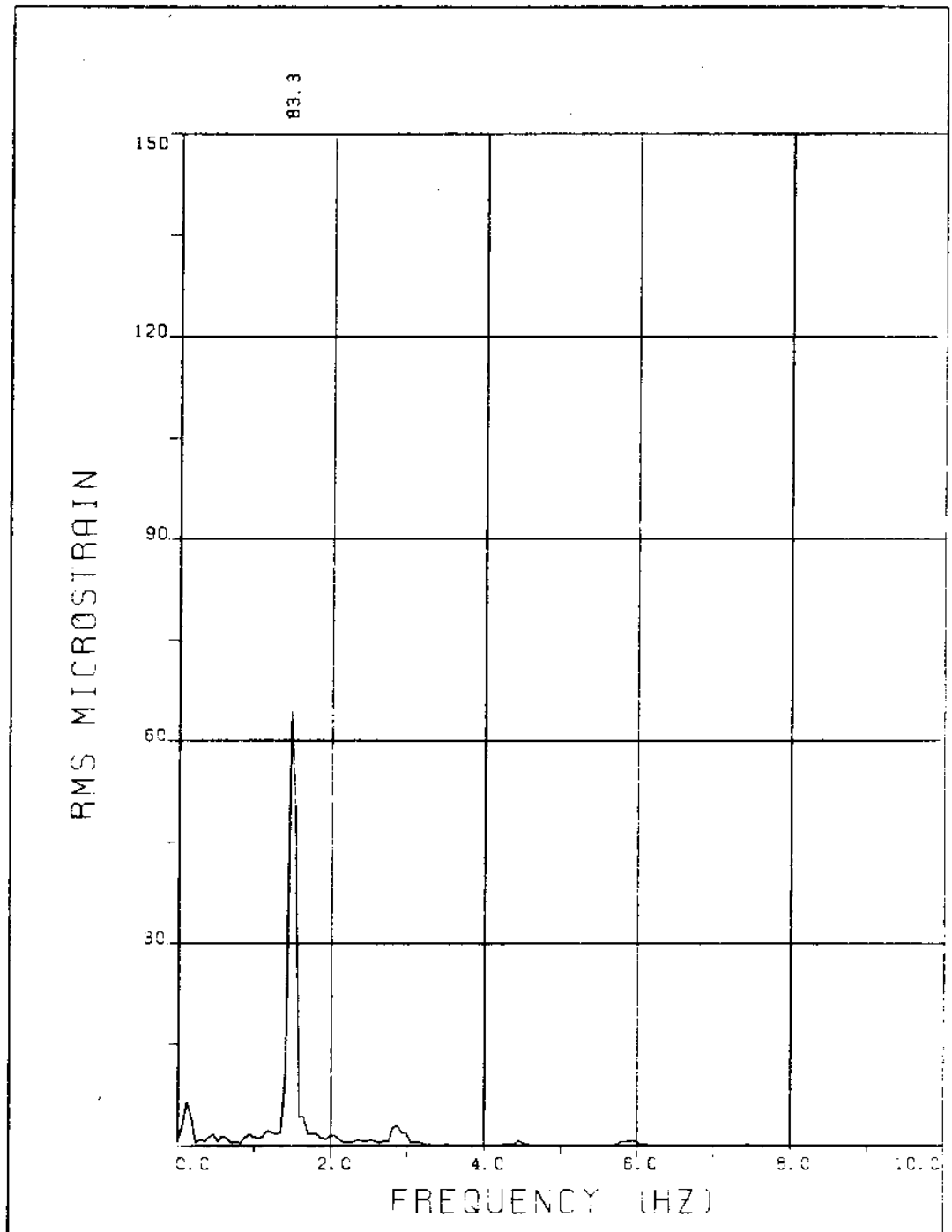

EXPERIMENT NUMBER 71

BRIDGE B5 ELEVATION=6L/11 BE=0.059

THETA=90 VC=120 FE=1.500 A/DE=1.91

MEASURED RESPONSE IN MICROSTRAIN

TOTAL DYNAMIC RMS=84.0

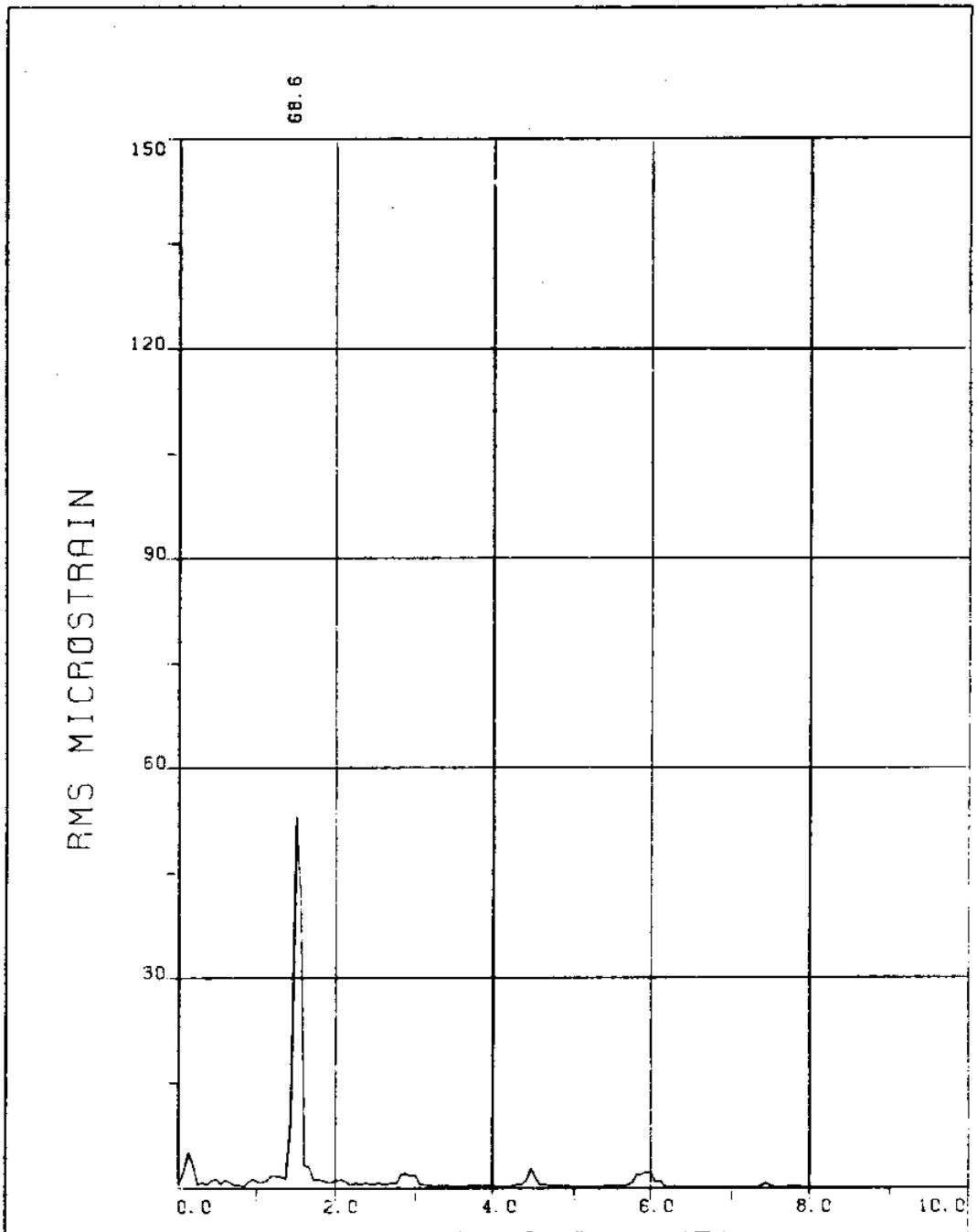

EXPERIMENT NUMBER 71

BRIDGE B3 ELEVATION=8L/11 BE=0.059

THETA=90 VC=120 FE=1.500 A/DE=1.91

MEASURED RESPONSE IN MICROSTRAIN

TOTAL DYNAMIC RMS=69.4

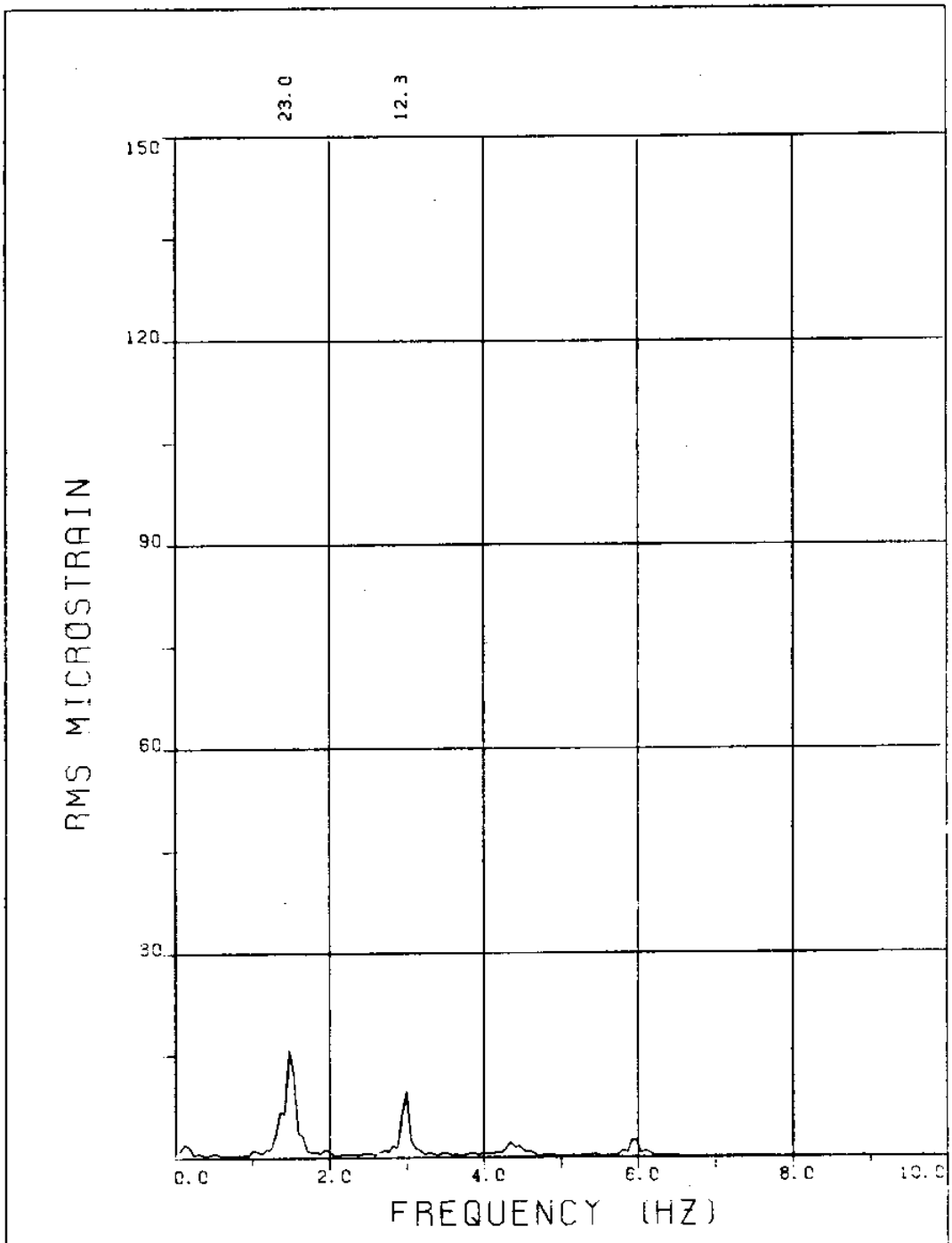

EXPERIMENT NUMBER 71

BRIDGE A8 ELEVATION=3L/11 BE=0.059

THETA=90 VC=120 FE=1.500 A/DE=1.91

MEASURED RESPONSE IN MICROSTRAIN

MEAN=45.6

TOTAL DYNAMIC RMS=27.0

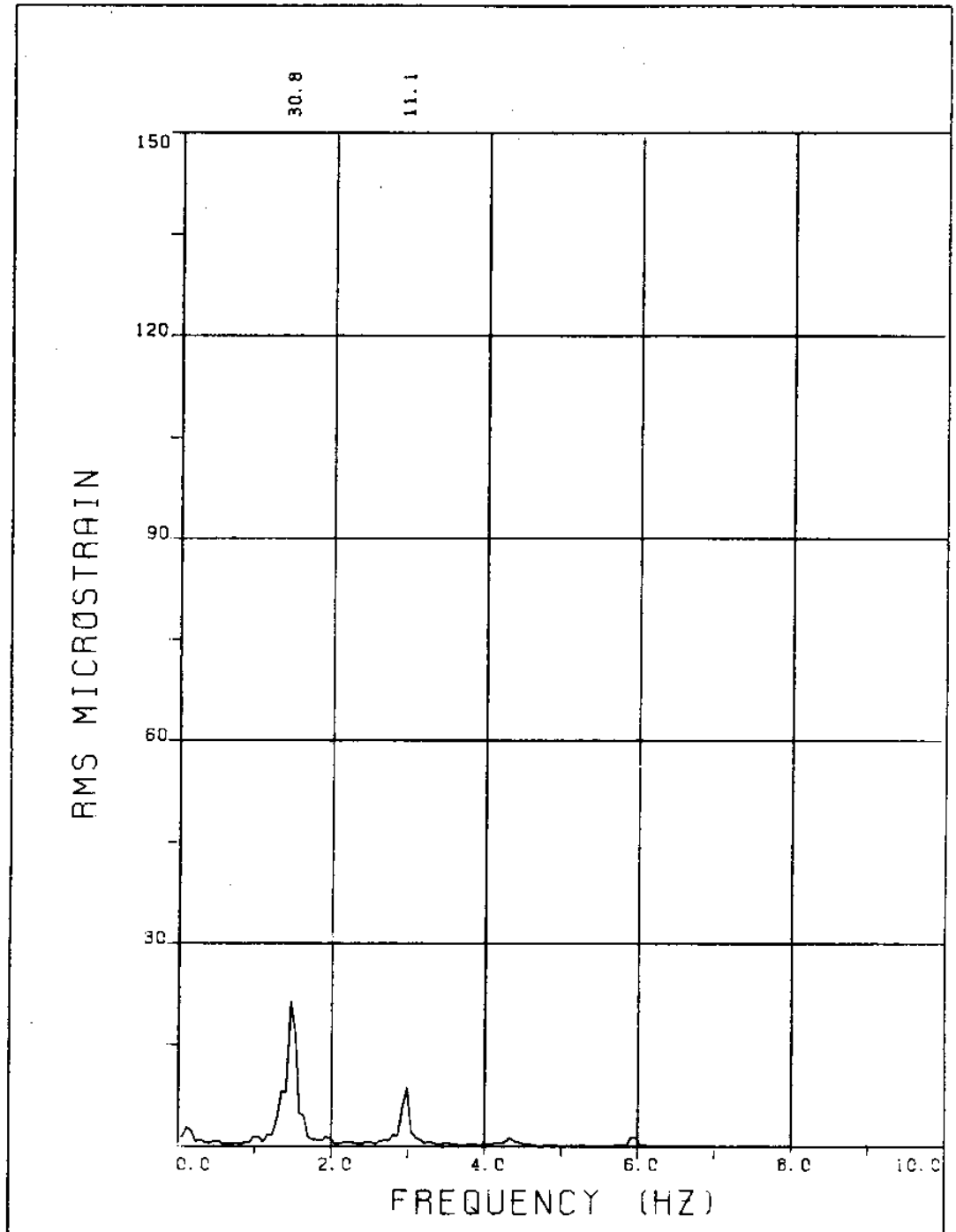

EXPERIMENT NUMBER 71

BRIDGE A6 ELEVATION=5L/11 BE=0.059

THETA=90 VC=120 FE=1.500 A/DE=1.91

MEASURED RESPONSE IN MICROSTRAIN

MEAN=52.3

TOTAL DYNAMIC RMS=33.4

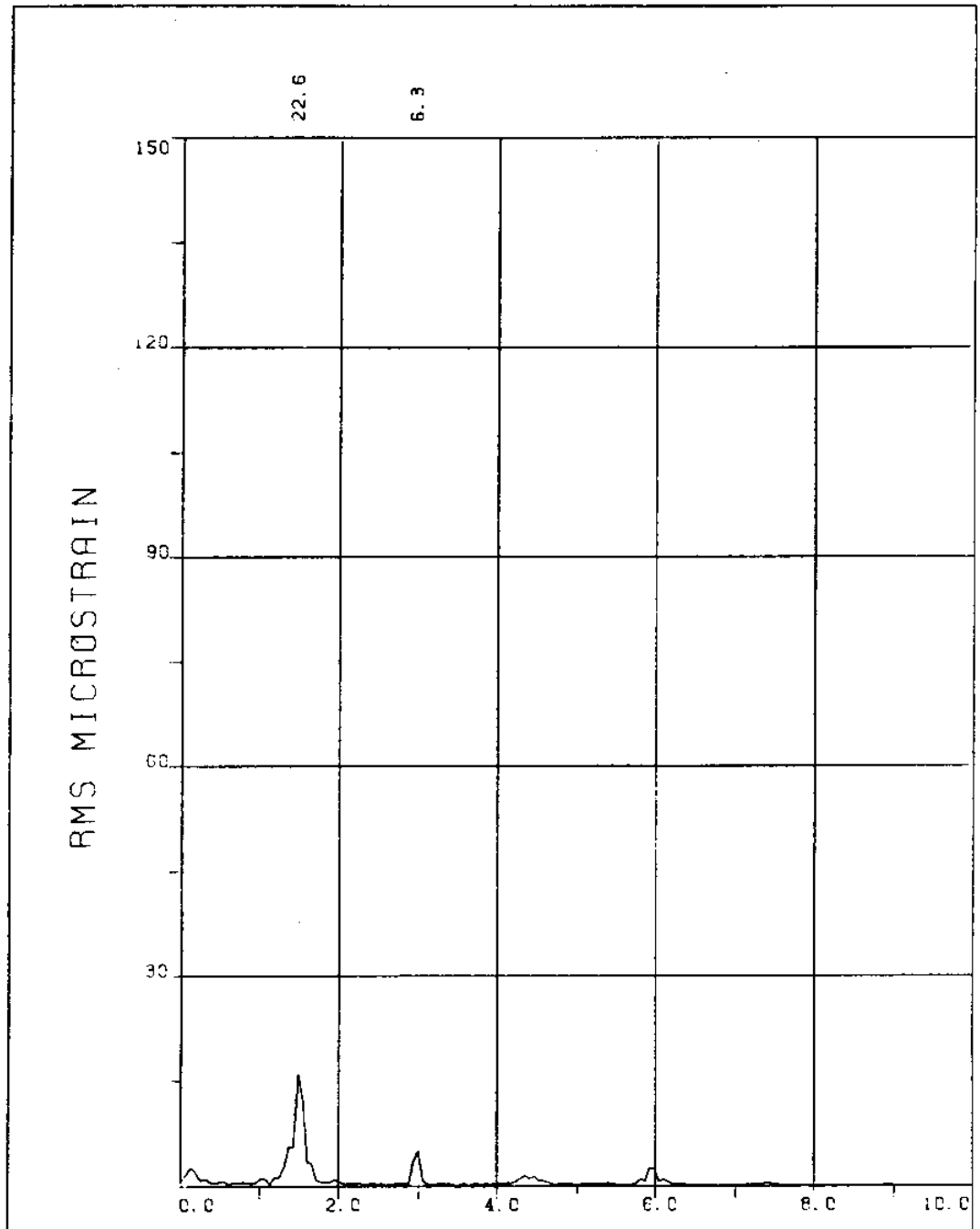

EXPERIMENT NUMBER 71

BRIDGE A3 ELEVATION=8L/11 BE=0.059

THETA=90 VC=120 FE=1.500 A/DE=1.91

MEASURED RESPONSE IN MICROSTRAIN

MEAN=50.6

TOTAL DYNAMIC RMS=24.6

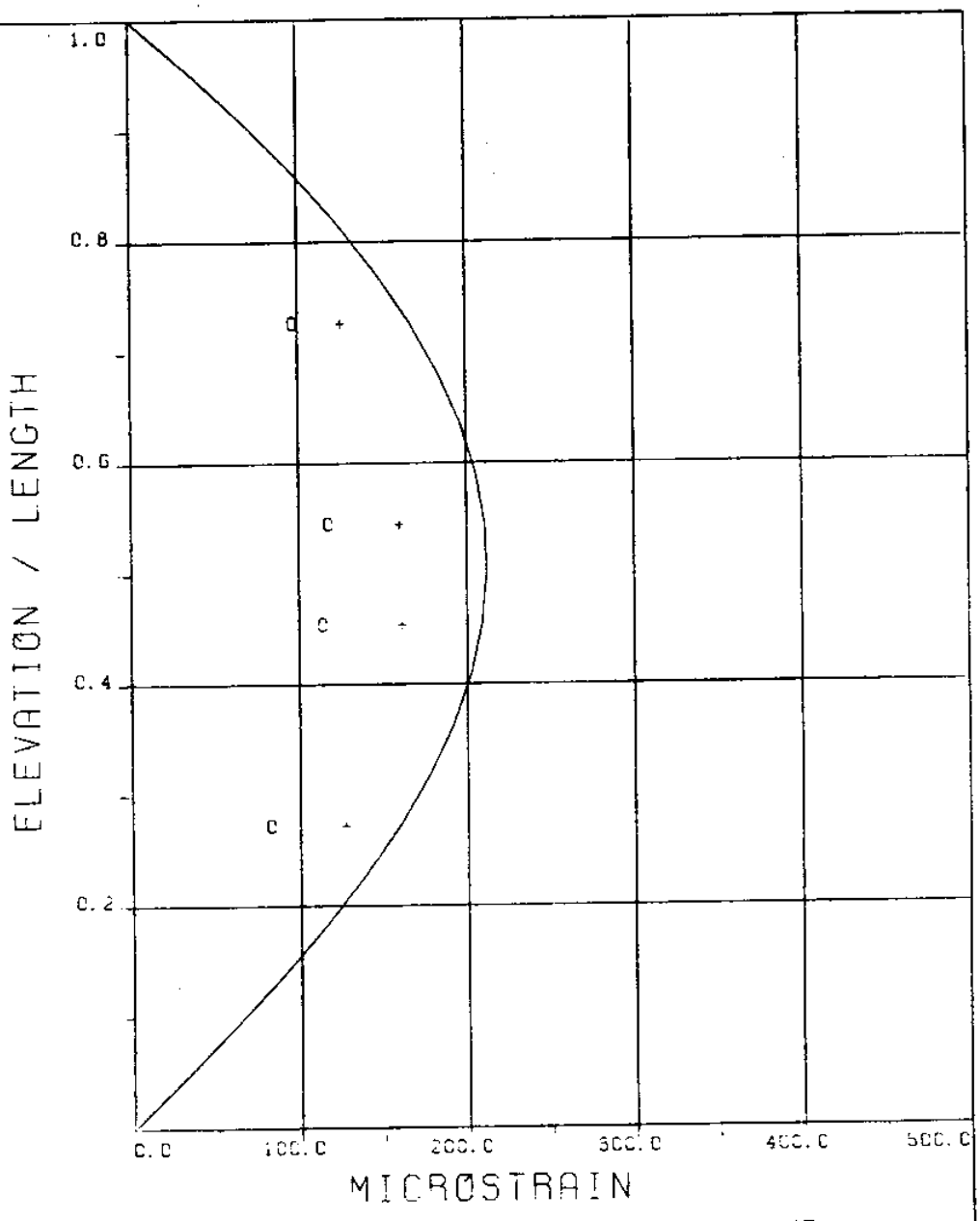

EXPERIMENT NUMBER 71

THETA=90 VC=120 FE=1.500 A/DE=1.91

DYNAMIC RESPONSE AT F=FE IN PLANE B
——— THEORY o o o EXPERIMENT

MAXIMUM DYNAMIC RESPONSE IN PLANE B
——— THEORY + + + EXPERIMENT

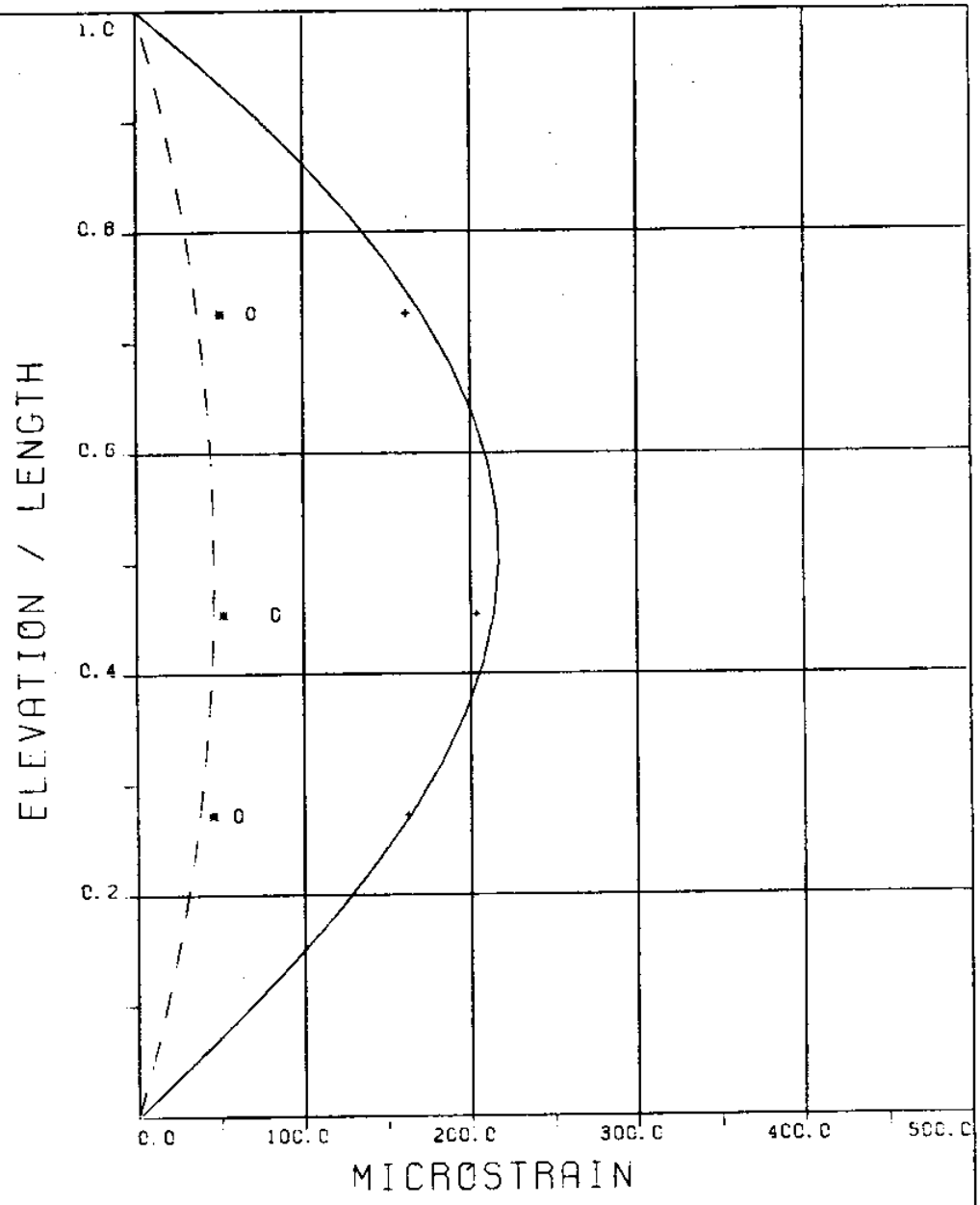

EXPERIMENT NUMBER 71

THETA=90 VC=120 FE=1.500 A/DE=1.91

STATIC RESPONSE IN PLANE A

----- THEORY * * * EXPERIMENT

MAXIMUM DYNAMIC RESPONSE IN PLANE A

o o o EXPERIMENT

MAXIMUM RESPONSE

_____ THEORY + + + EXPERIMENT

FIGURE 71a: LVDT: 0.087 D_e/DIVISION; STRAINS: 7.64 MICROSTRAIN/DIVISION

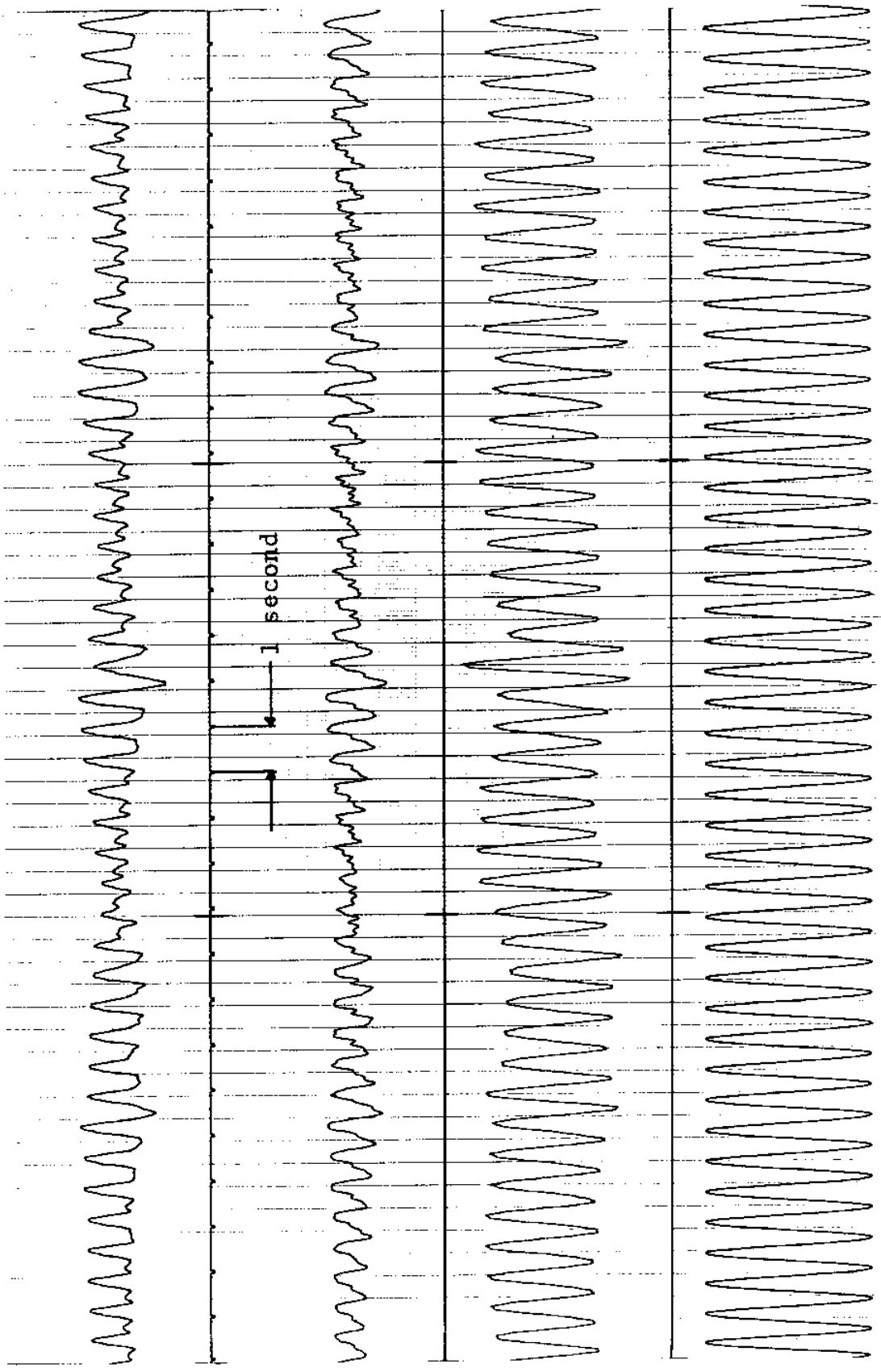

FIGURE 71b: LVDT: 0.087 D_e/DIVISION; STRAINS: 7.64 MICROSTRAIN/DIVISION

EXPERIMENT 80

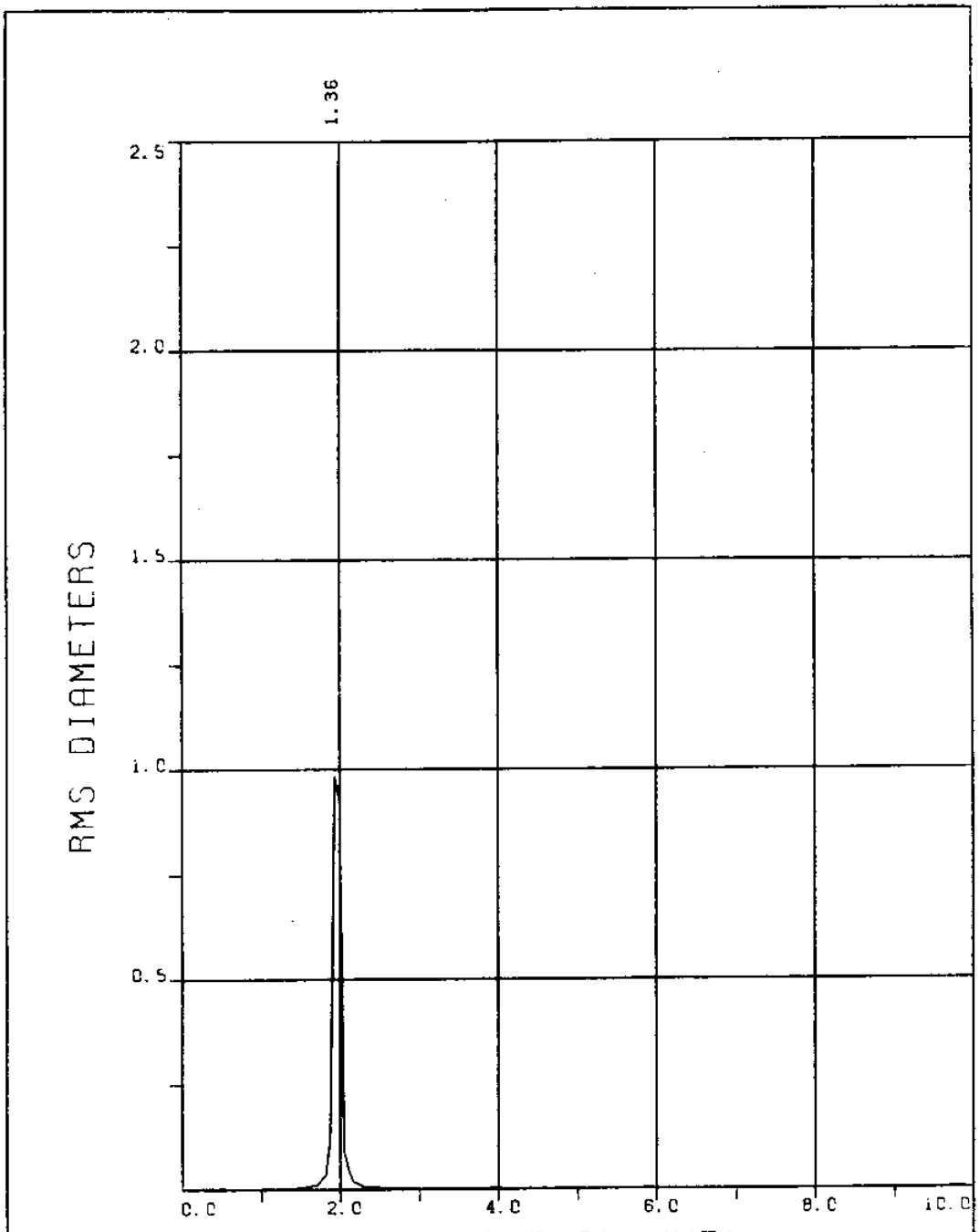

EXPERIMENT NUMBER 80

LVDT

THETA=90 VC=120 FE=1.950 BE=0.059

MEASURED A/DE=1.93

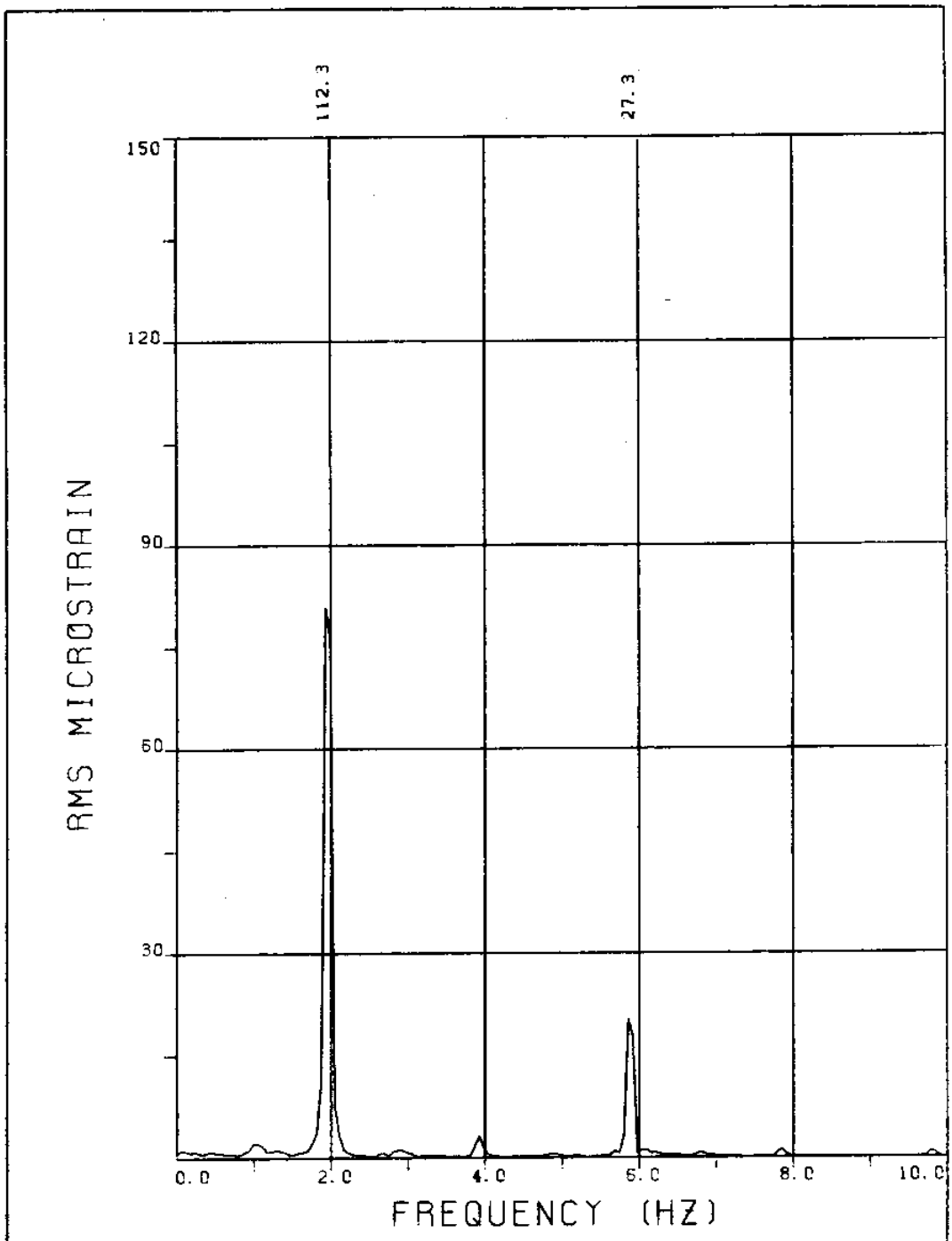

EXPERIMENT NUMBER 80

BRIDGE B8 ELEVATION=3L/11 BE=0.059

THETA=90 VC=120 FE=1.950 A/DE=1.93

MEASURED RESPONSE IN MICROSTRAIN

TOTAL DYNAMIC RMS=115.8

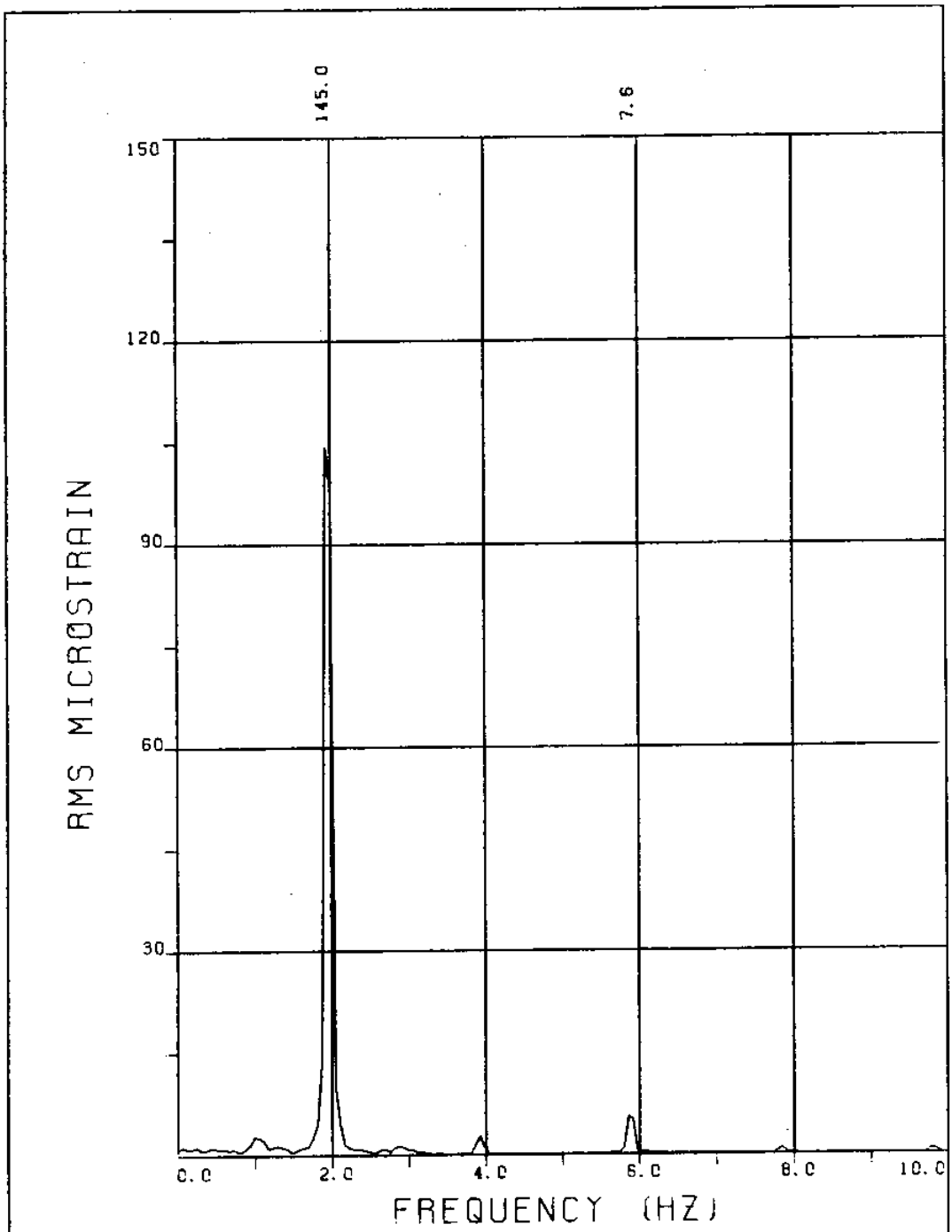

EXPERIMENT NUMBER 80

BRIDGE B6 ELEVATION=5L/11 BE=0.059

THETA=90 VC=120 FE=1.950 A/DE=1.93

MEASURED RESPONSE IN MICROSTRAIN

TOTAL DYNAMIC RMS=145.4

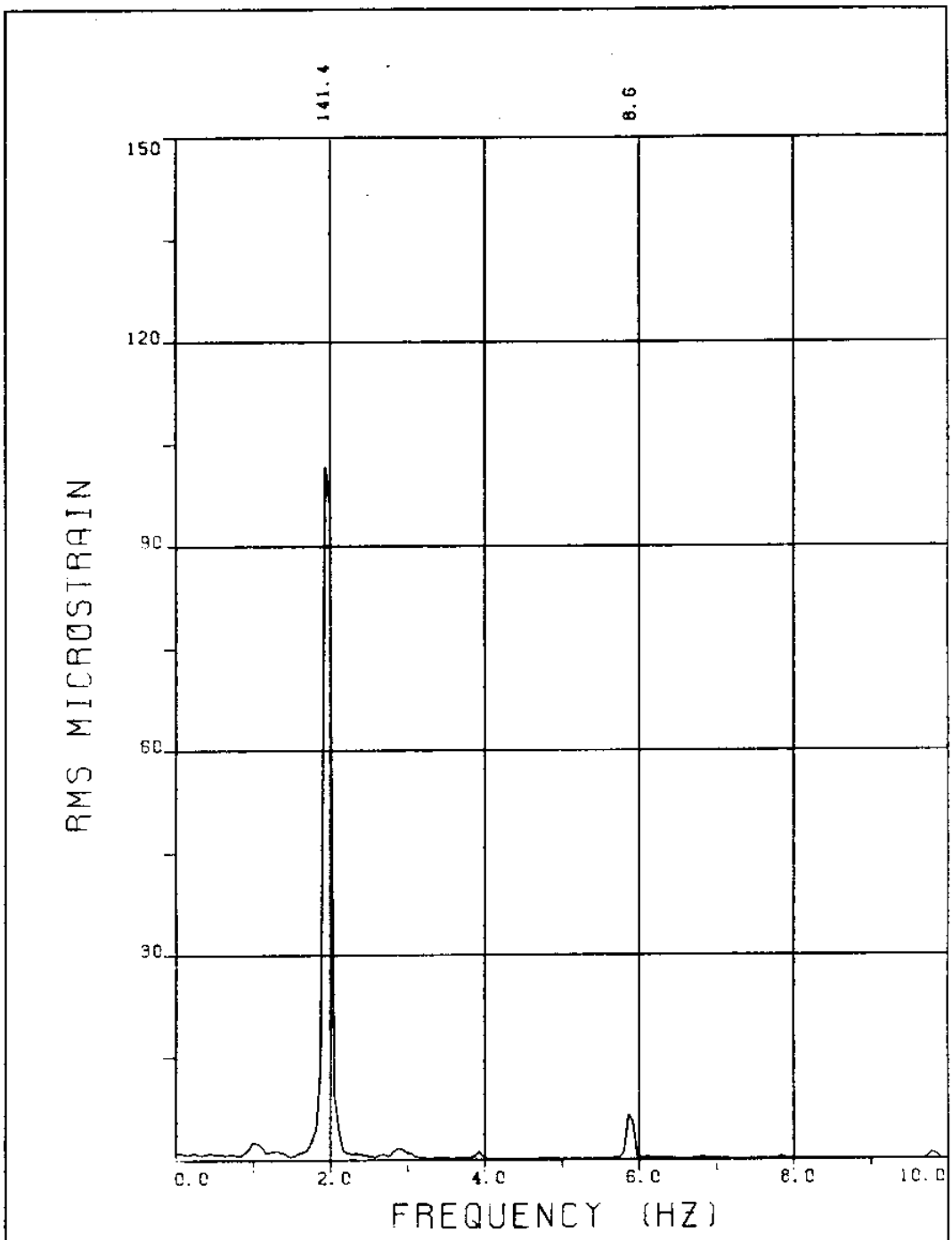

EXPERIMENT NUMBER 80

BRIDGE B5 ELEVATION=6L/11 BE=0.059

THETA=90 VC=120 FE=1.950 A/DE=1.93

MEASURED RESPONSE IN MICROSTRAIN

TOTAL DYNAMIC RMS=141.8

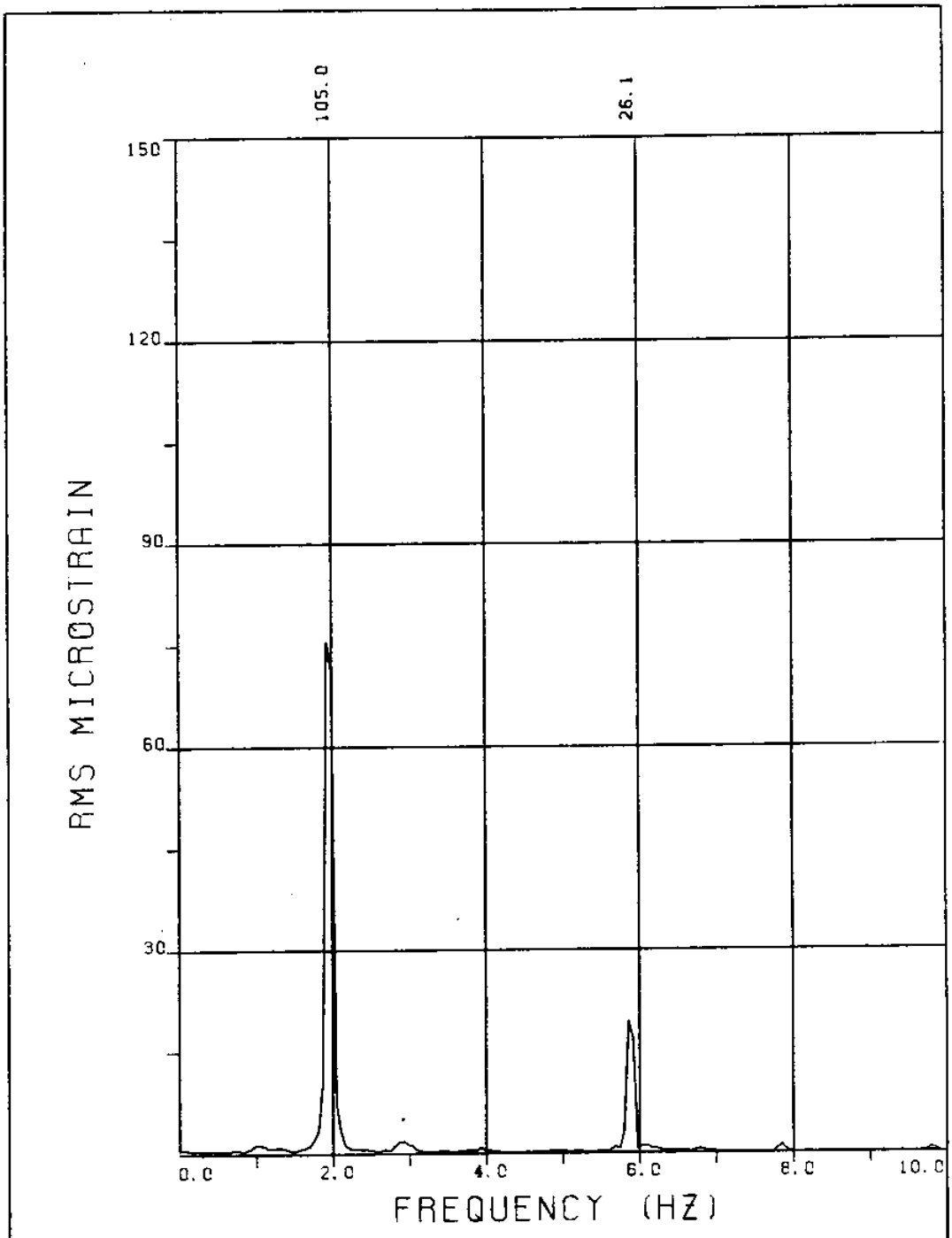

EXPERIMENT NUMBER 80

BRIDGE B3 ELEVATION=8L/11 BE=0.059

THETA=90 VC=120 FE=1.950 A/DE=1.93

MEASURED RESPONSE IN MICROSTRAIN

TOTAL DYNAMIC RMS=108.3

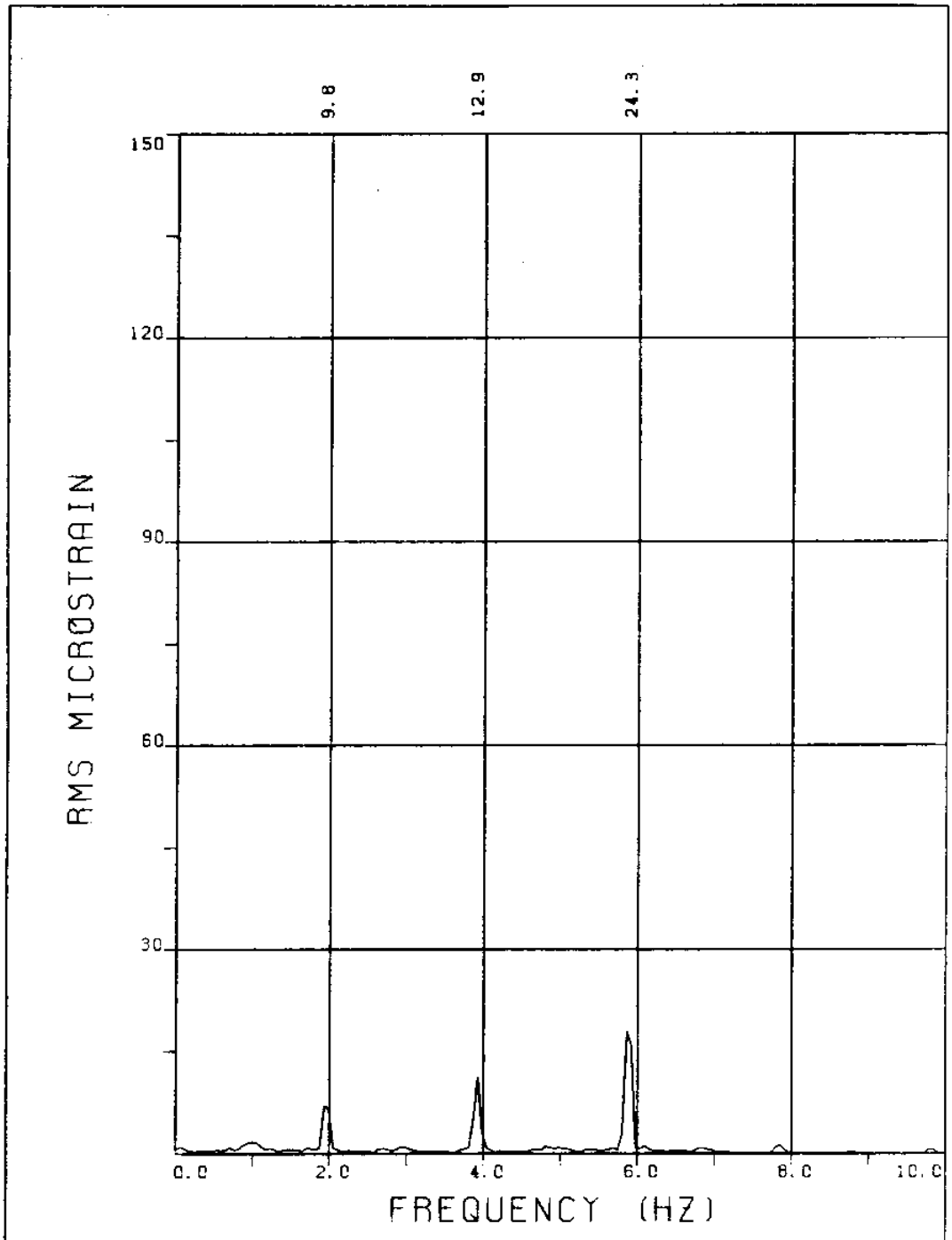

EXPERIMENT NUMBER 80

BRIDGE A8 ELEVATION=3L/11 BE=0.059

THETA=90 VC=120 FE=1.950 A/DE=1.93

MEASURED RESPONSE IN MICROSTRAIN

MEAN=42.7

TOTAL DYNAMIC RMS=29.8

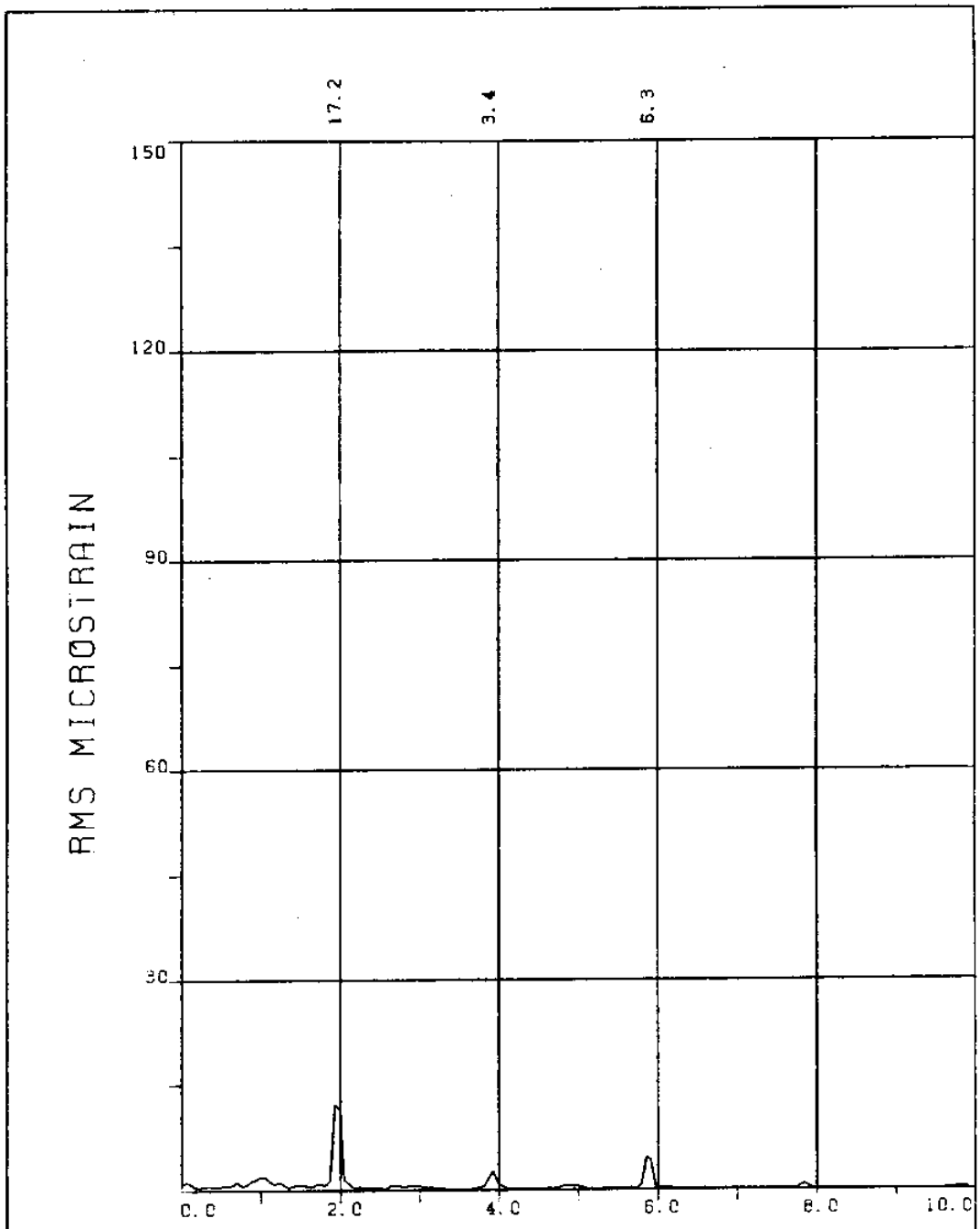

EXPERIMENT NUMBER 80

BRIDGE A6 ELEVATION=5L/11 BE=0.059

THETA=90 VC=120 FE=1.950 A/DE=1.93

MEASURED RESPONSE IN MICROSTRAIN

MEAN=45.4

TOTAL DYNAMIC RMS=19.4

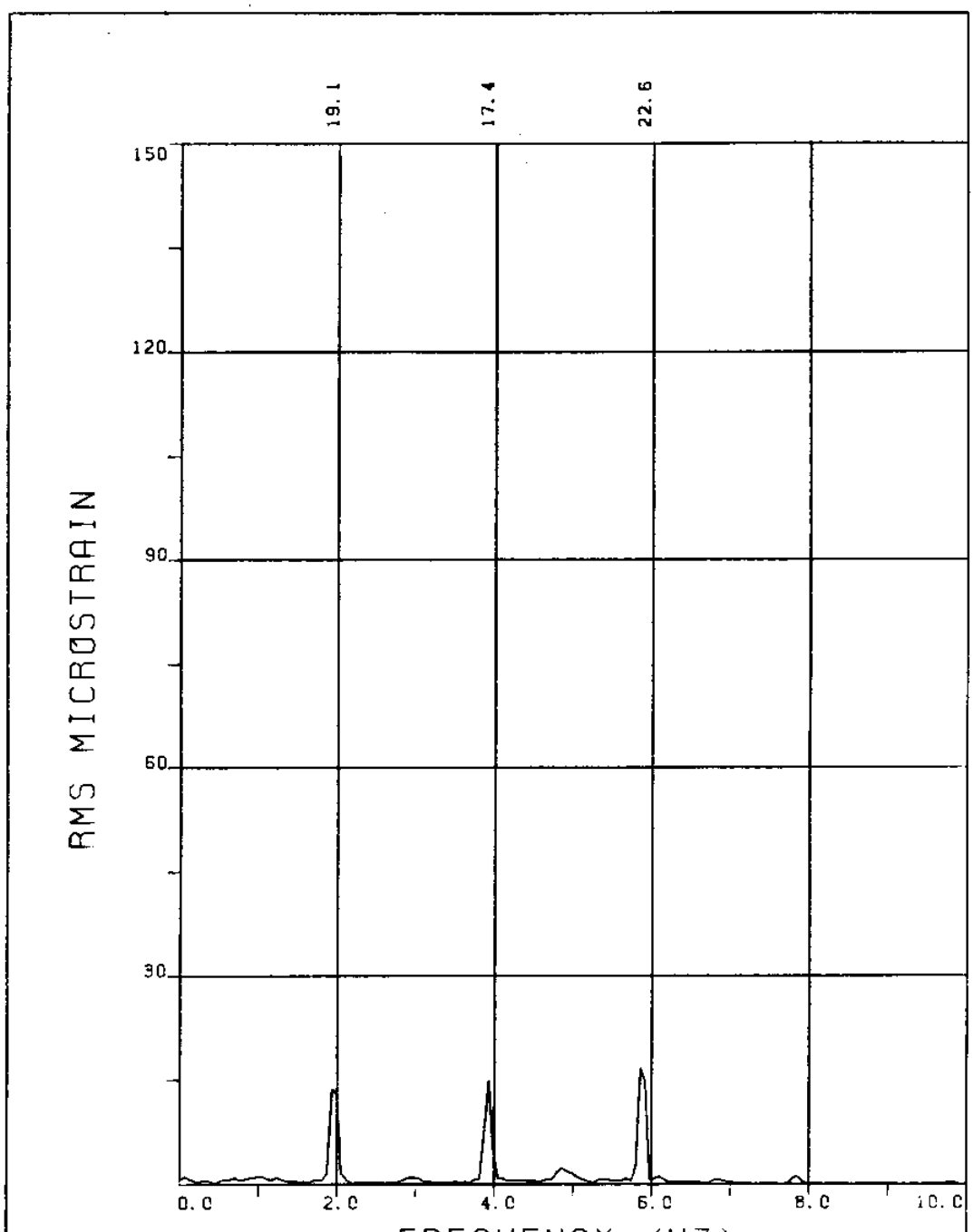

EXPERIMENT NUMBER 80

BRIDGE A3 ELEVATION=8L/11 BE=0.059

THETA=90 VC=120 FE=1.950 A/DE=1.93

MEASURED RESPONSE IN MICROSTRAIN

MEAN=42.8

TOTAL DYNAMIC RMS=35.0

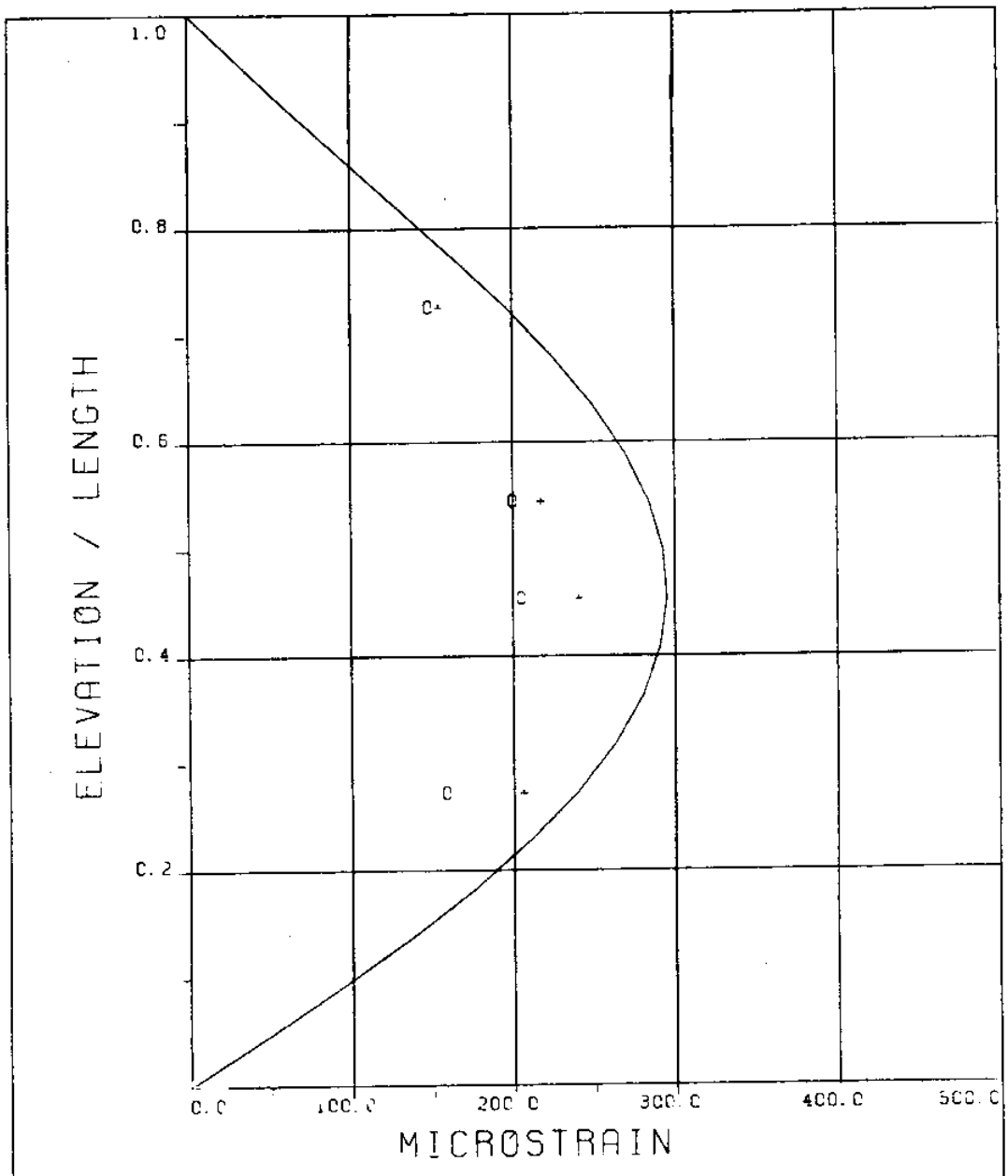

EXPERIMENT NUMBER 80

THETA=90 VC=120 FE=1.950 A/DE=1.93

DYNAMIC RESPONSE AT F=FE IN PLANE B

——— THEORY o o o EXPERIMENT

MAXIMUM DYNAMIC RESPONSE IN PLANE B

——— THEORY + + + EXPERIMENT

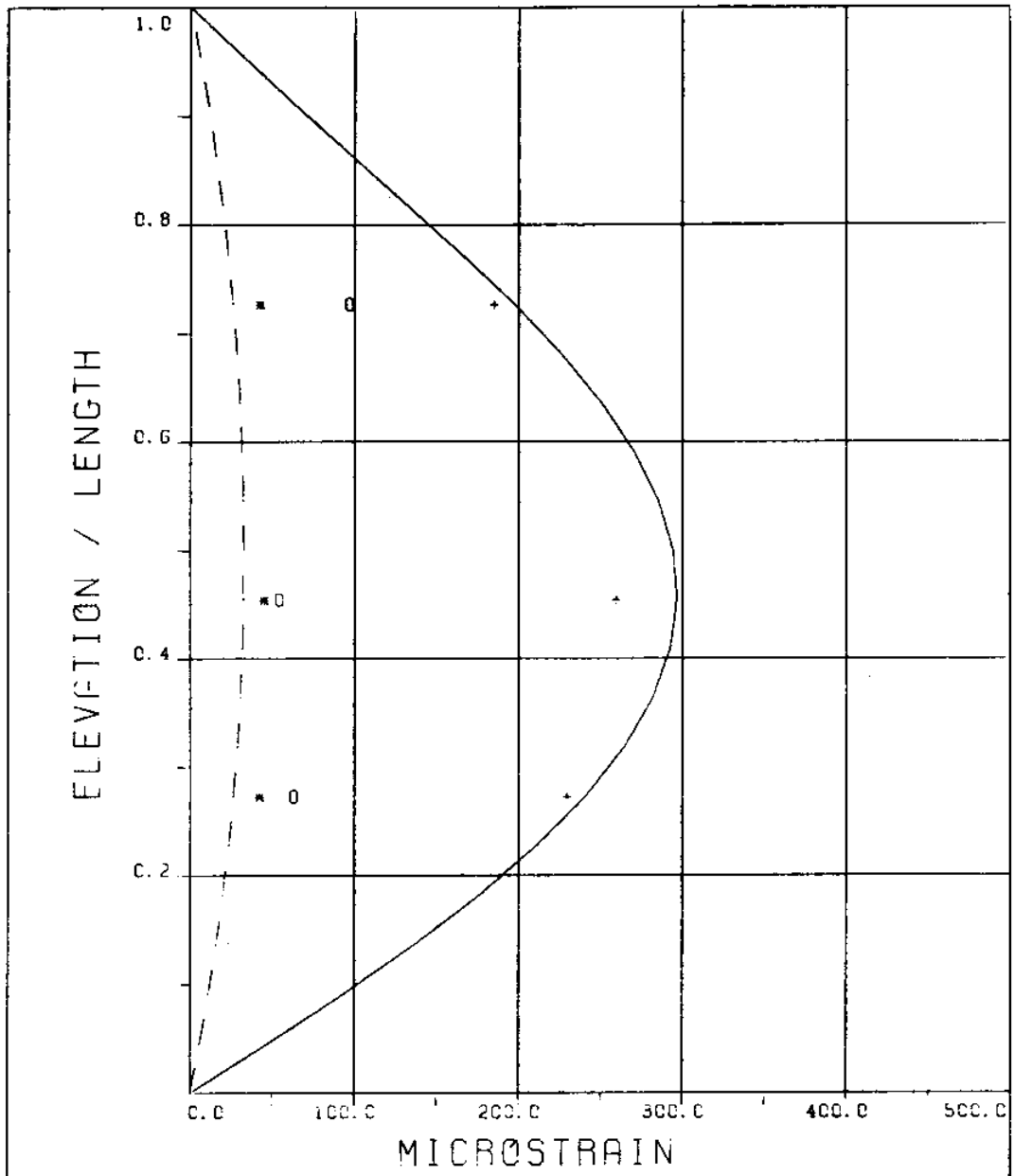

EXPERIMENT NUMBER 80

THETA=90 VC=120 FE=1.950 A/DE=1.93

STATIC RESPONSE IN PLANE A

----- THEORY * * * EXPERIMENT

MAXIMUM DYNAMIC RESPONSE IN PLANE A

o o o EXPERIMENT

MAXIMUM RESPONSE

_____ THEORY + + + EXPERIMENT

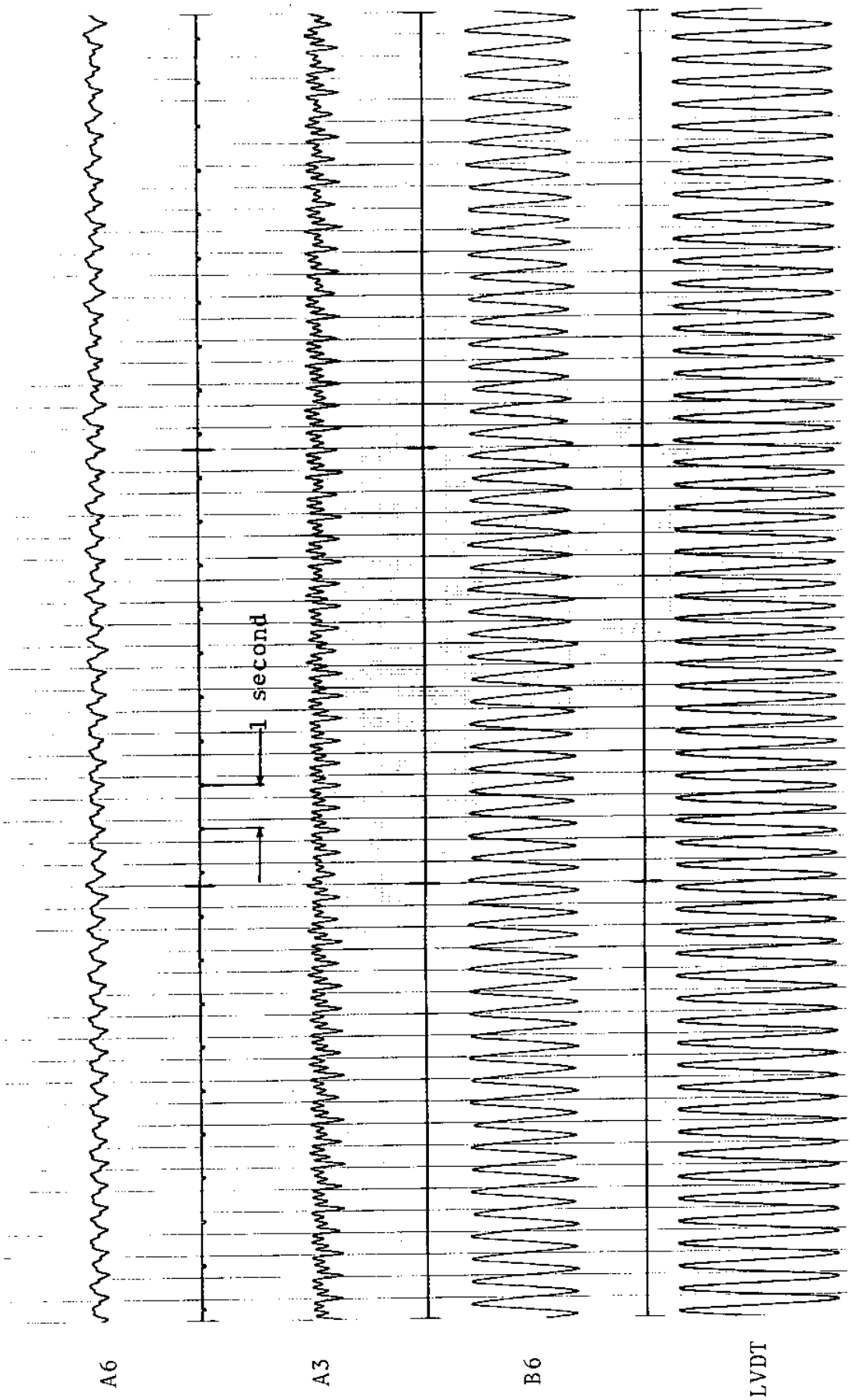

FIGURE 80Ta: LVDT: 0.087 D_e/DIVISION; STRAINS: 15.3 MICROSTRAIN/DIVISION

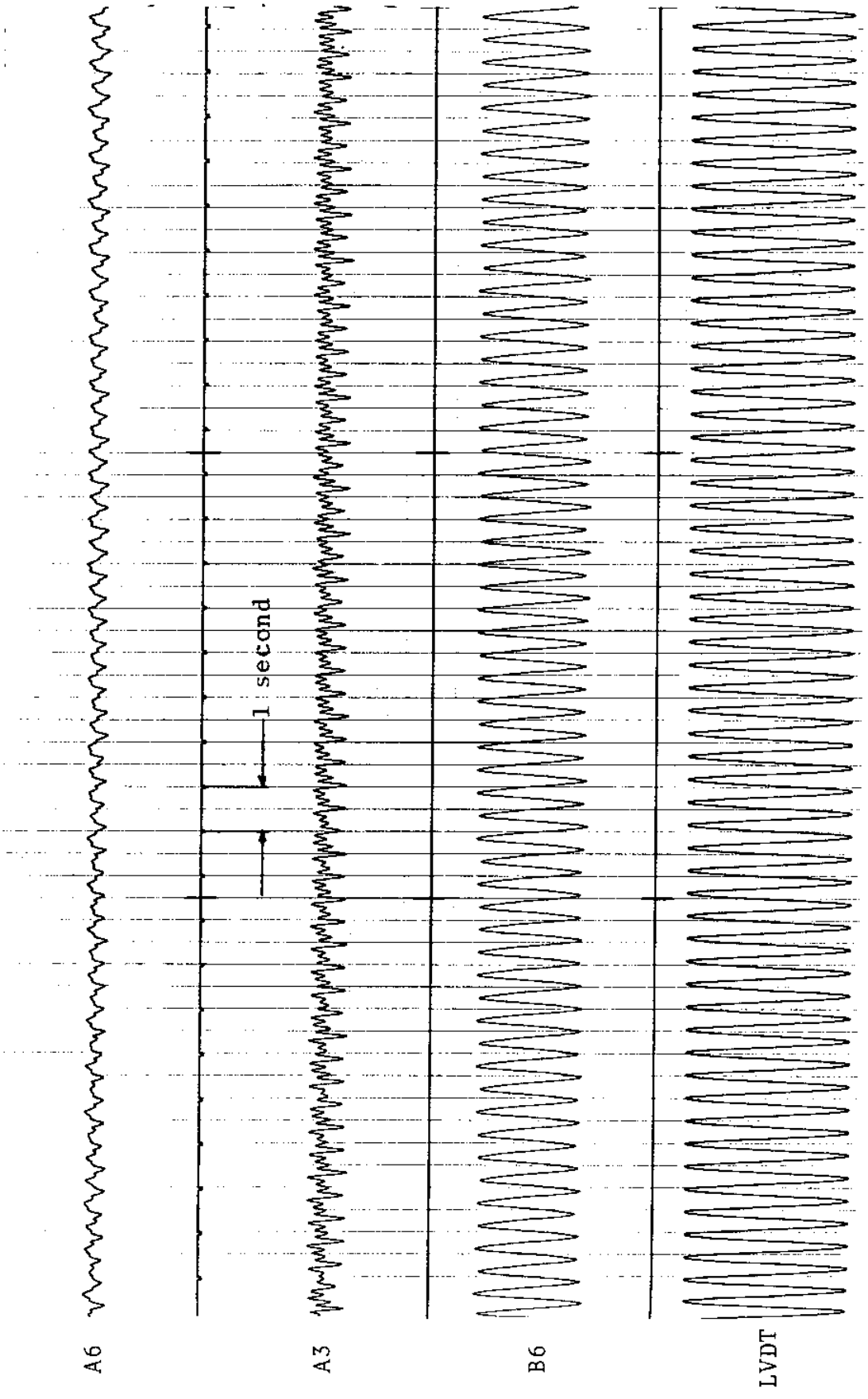

FIGURE 80Tb: LVDT: 0.087 D_e/DIVISION; STRAINS: 15.3 MICROSTRAIN/DIVISION

Experiment 89

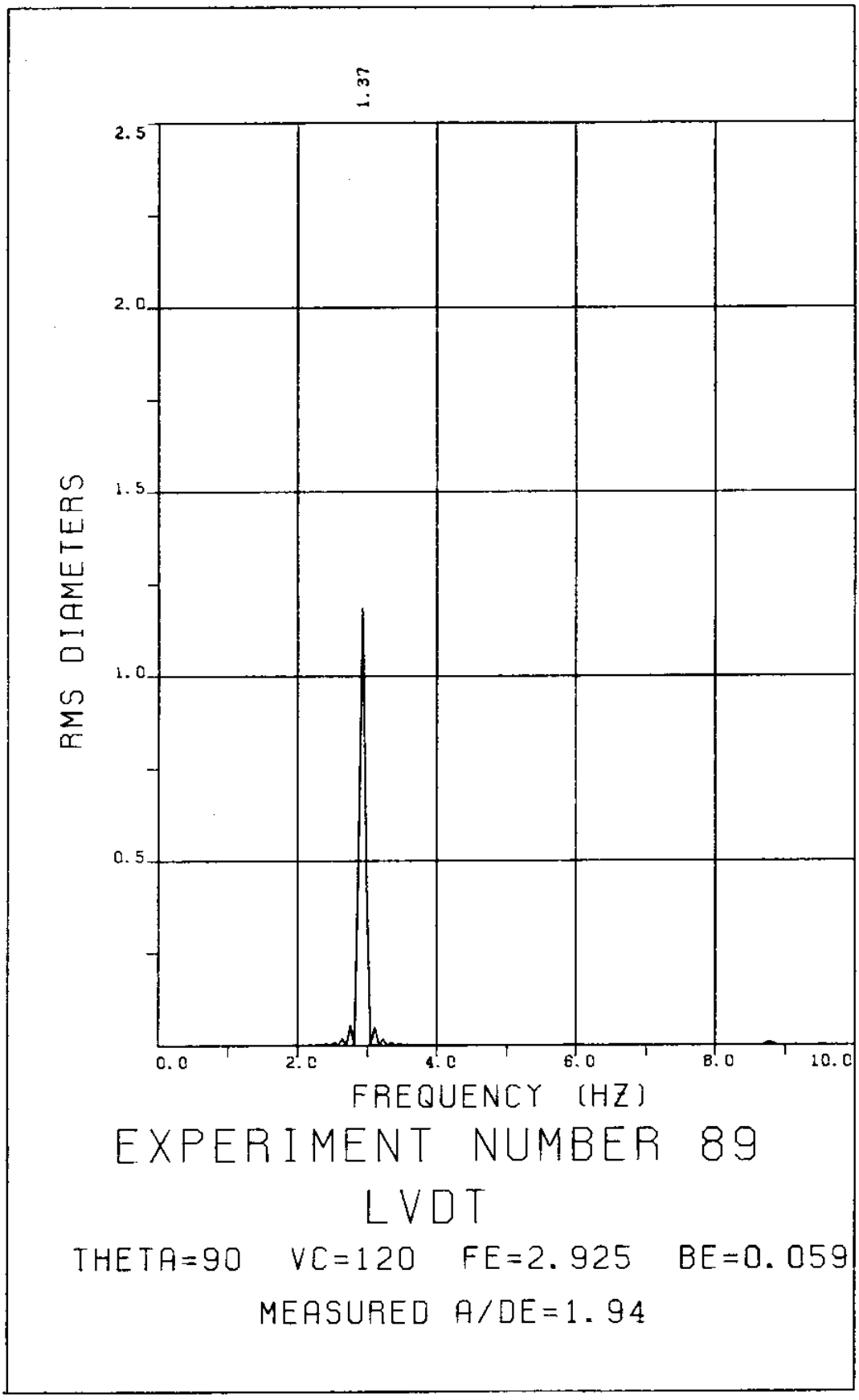
1.37
2.5
2.0
1.5
1.0
0.5
RMS DIAMETERS
0.0
2.0
4.0
6.0
8.0
10.0
FREQUENCY (HZ)
EXPERIMENT NUMBER 89
LVDT
THETA=90 VC=120 FE=2.925 BE=0.059
MEASURED A/DE=1.94

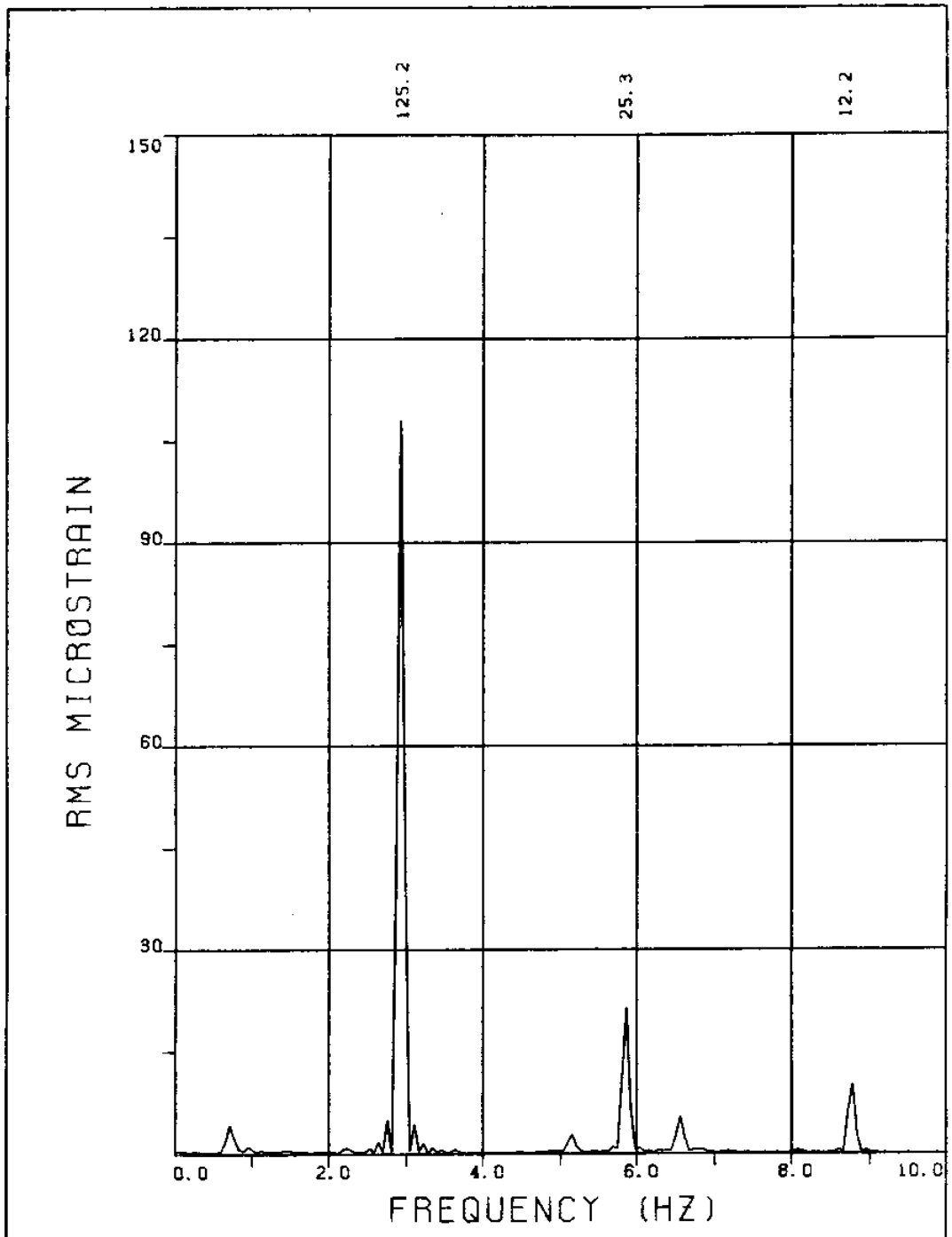

EXPERIMENT NUMBER 89

BRIDGE B8 ELEVATION=3L/11 BE=0.059

THETA=90 VC=120 FE=2.925 A/DE=1.94

MEASURED RESPONSE IN MICROSTRAIN

TOTAL DYNAMIC RMS=128.7

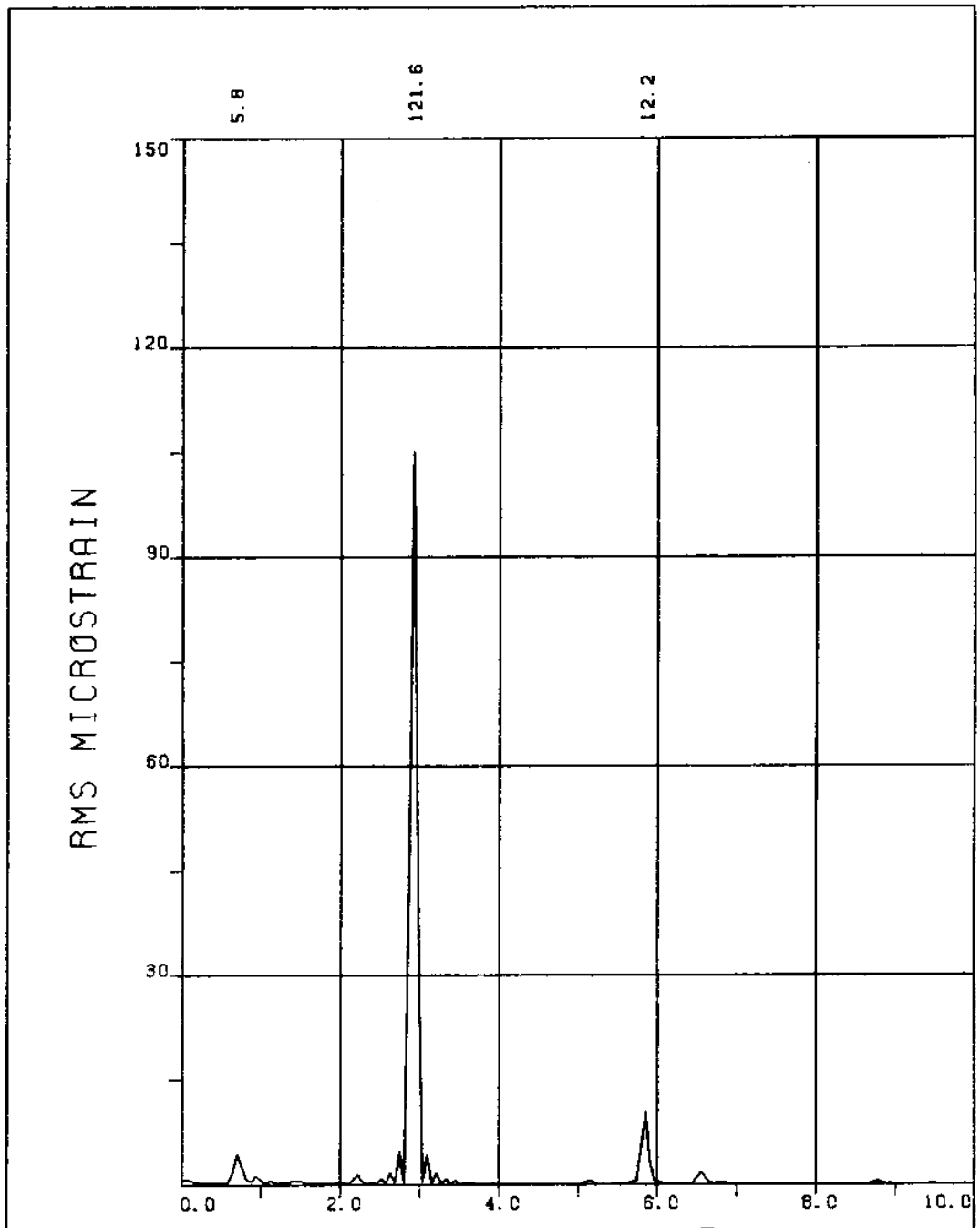

EXPERIMENT NUMBER 89

BRIDGE B6 ELEVATION=5L/11 BE=0.059

THETA=90 VC=120 FE=2.925 A/DE=1.94

MEASURED RESPONSE IN MICROSTRAIN

TOTAL DYNAMIC RMS=122.4

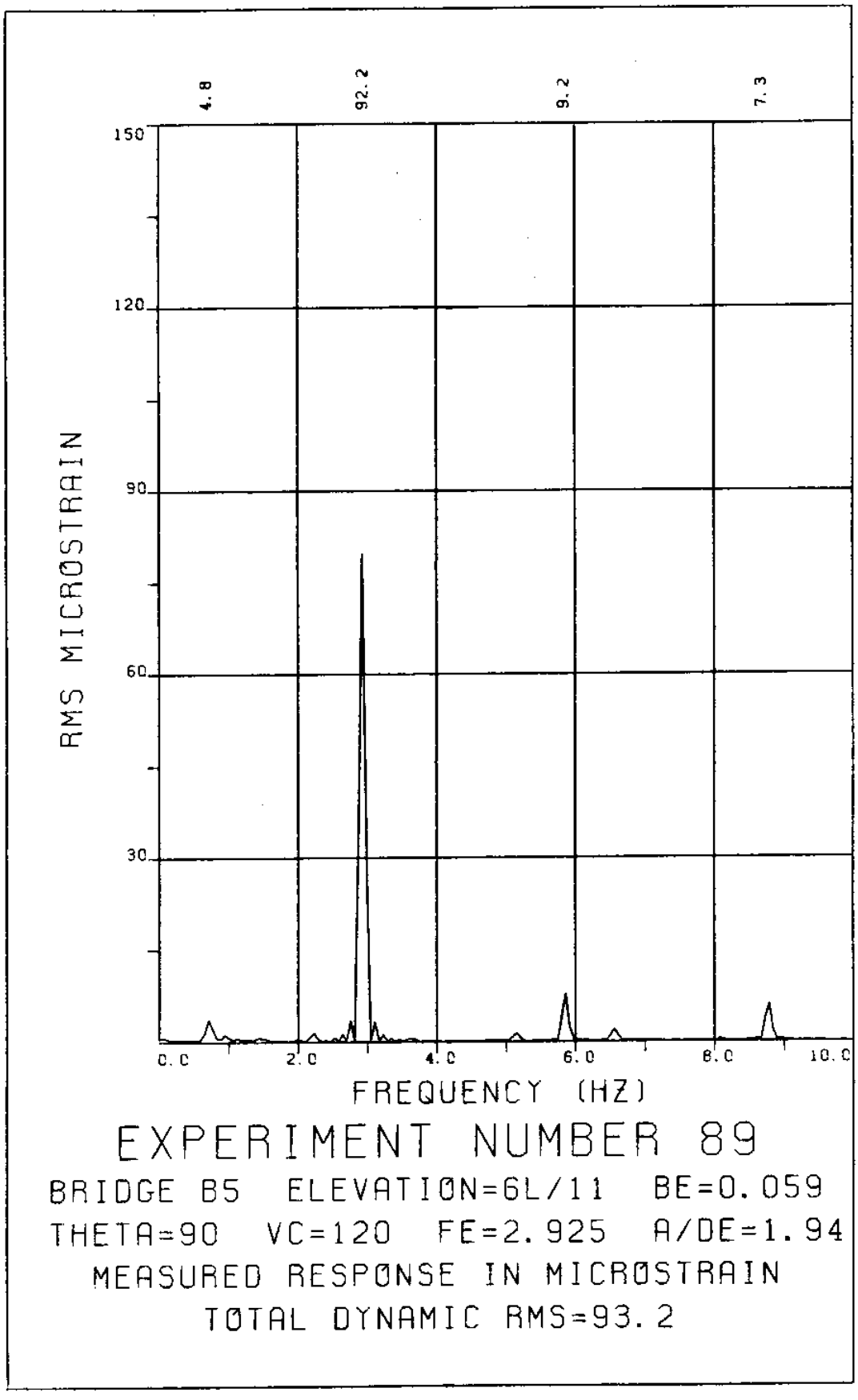
4.8
92.2
9.2
7.3
150
120
90
60
30
RMS MICROSTRAIN
0.0
2.0
4.0
6.0
8.0
10.0
FREQUENCY (HZ)
EXPERIMENT NUMBER 89
BRIDGE B5 ELEVATION=6L/11 BE=0.059
THETA=90 VC=120 FE=2.925 A/DE=1.94
MEASURED RESPONSE IN MICROSTRAIN
TOTAL DYNAMIC RMS=93.2

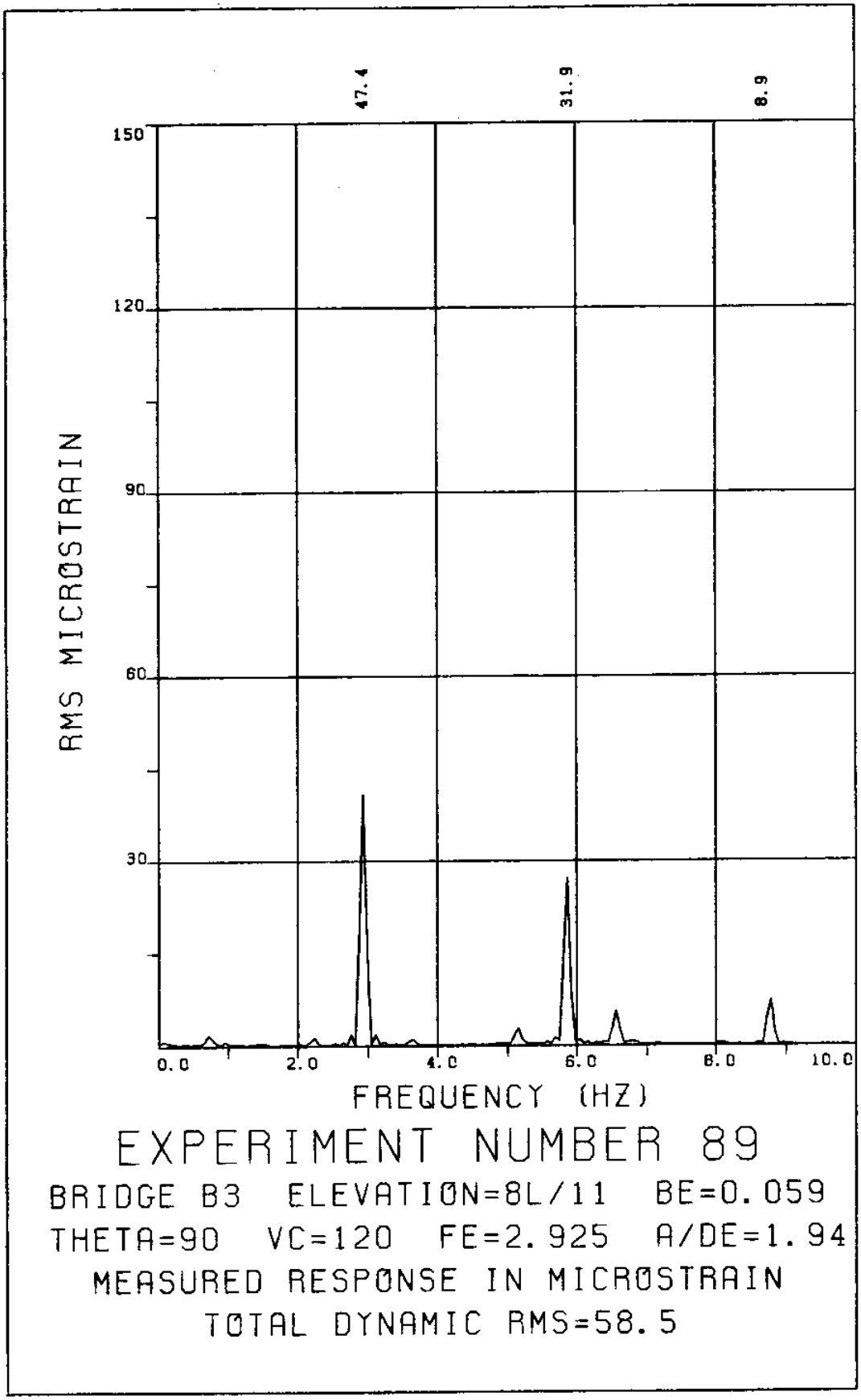
47.4
31.9
8.9
150
120
90
60
30
RMS MICROSTRAIN
0.0
2.0
4.0
6.0
8.0
10.0
FREQUENCY (HZ)
EXPERIMENT NUMBER 89
BRIDGE B3 ELEVATION=8L/11 BE=0.059
THETA=90 VC=120 FE=2.925 A/DE=1.94
MEASURED RESPONSE IN MICROSTRAIN
TOTAL DYNAMIC RMS=58.5

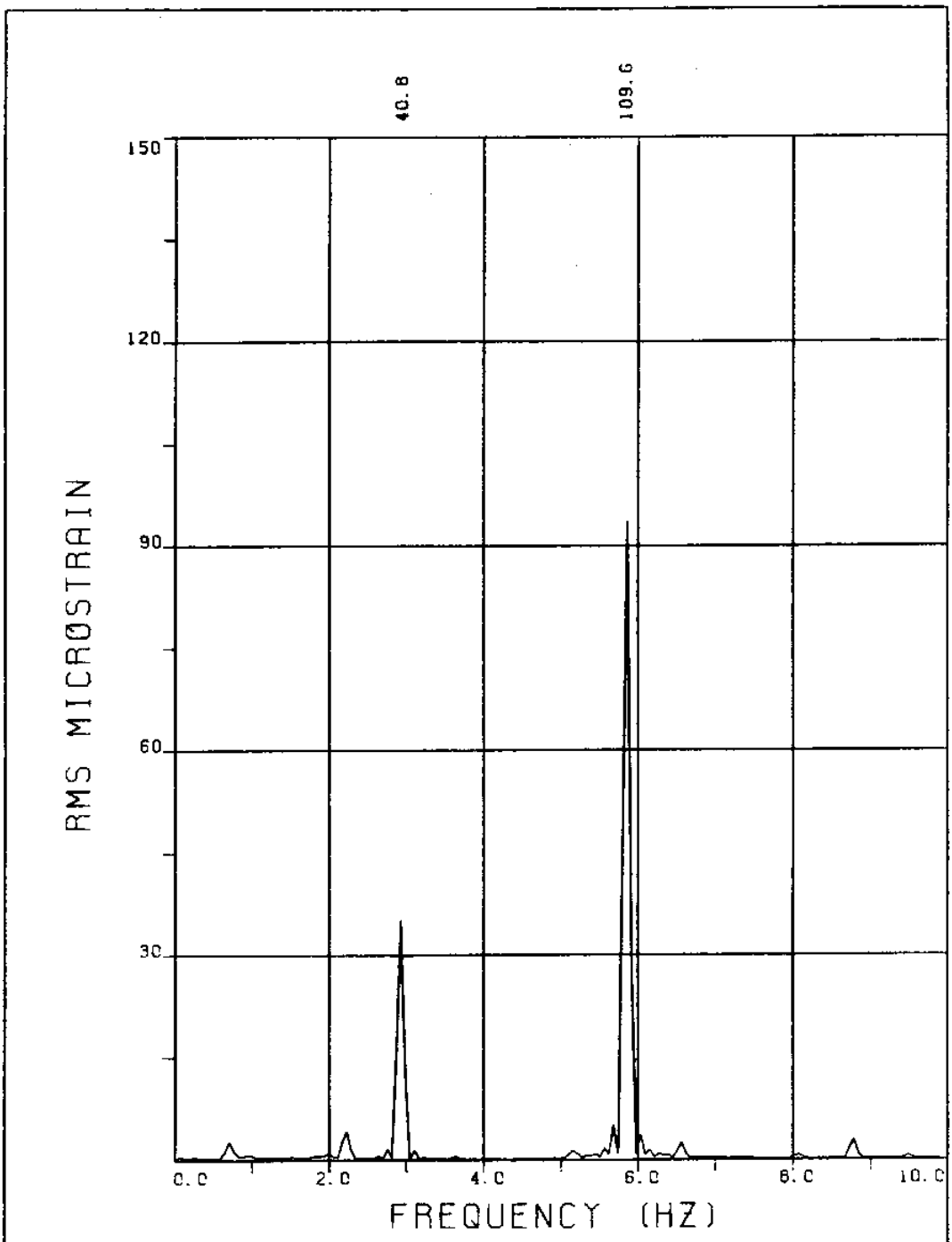

EXPERIMENT NUMBER 89

BRIDGE A8 ELEVATION=3L/11 BE=0.059

THETA=90 VC=120 FE=2.925 A/DE=1.94

MEASURED RESPONSE IN MICROSTRAIN

MEAN=50.3

TOTAL DYNAMIC RMS=117.3

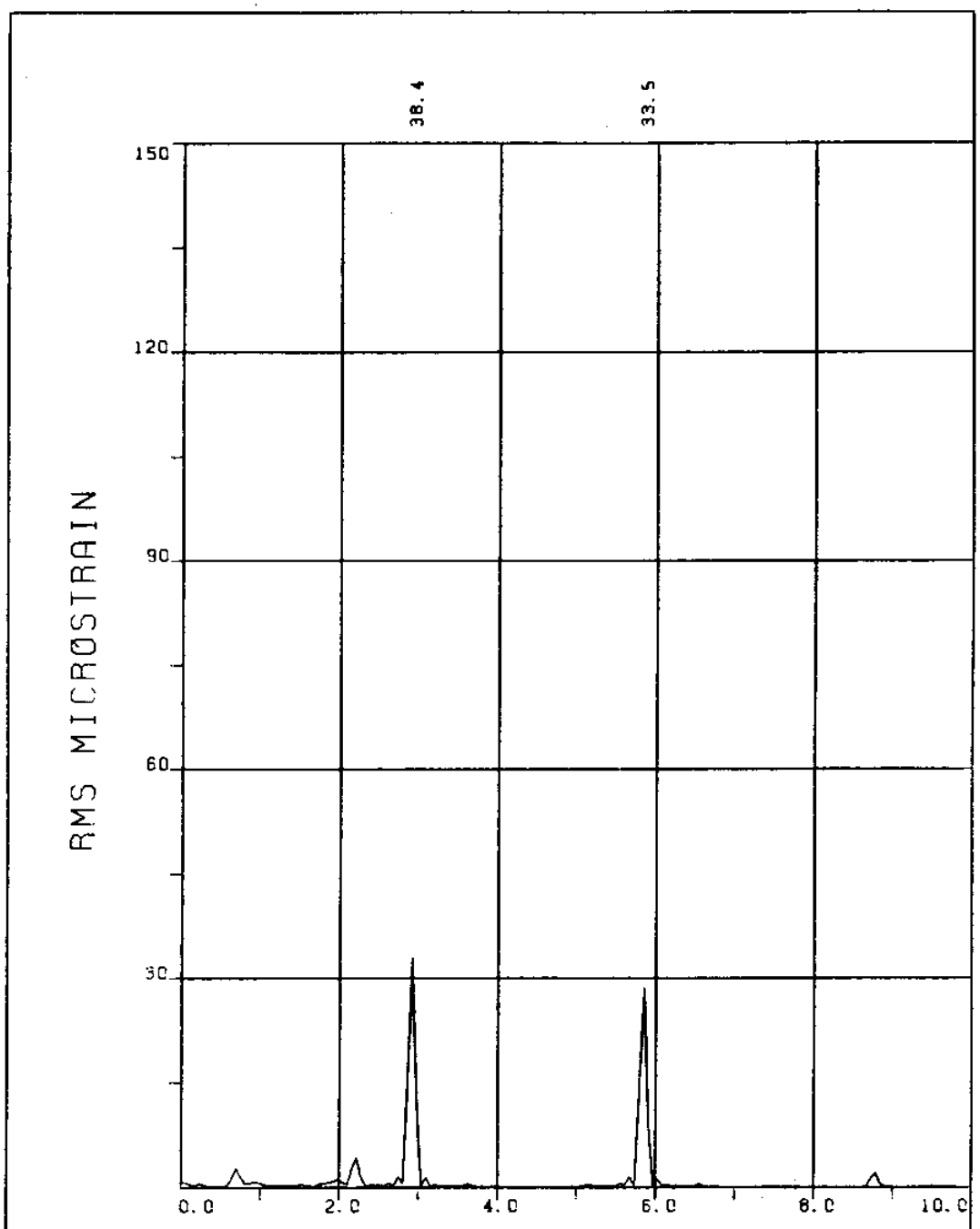

EXPERIMENT NUMBER 89

BRIDGE A6 ELEVATION=5L/11 BE=0.059

THETA=90 VC=120 FE=2.925 A/DE=1.94

MEASURED RESPONSE IN MICROSTRAIN

MEAN=49.2

TOTAL DYNAMIC RMS=51.6

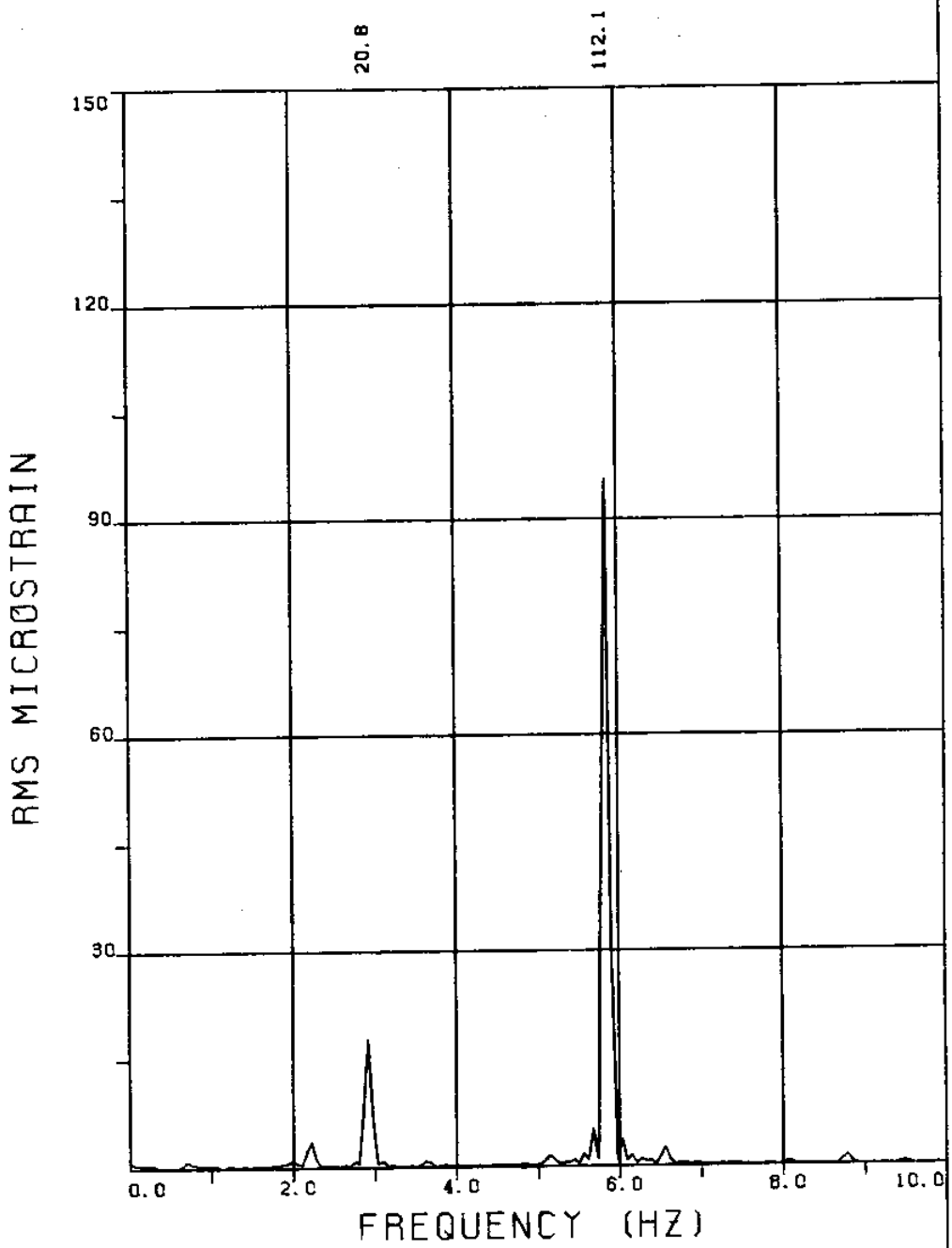

EXPERIMENT NUMBER 89

BRIDGE A3 ELEVATION=8L/11 BE=0.059

THETA=90 VC=120 FE=2.925 A/DE=1.94

MEASURED RESPONSE IN MICROSTRAIN

MEAN=46.6

TOTAL DYNAMIC RMS=114.2

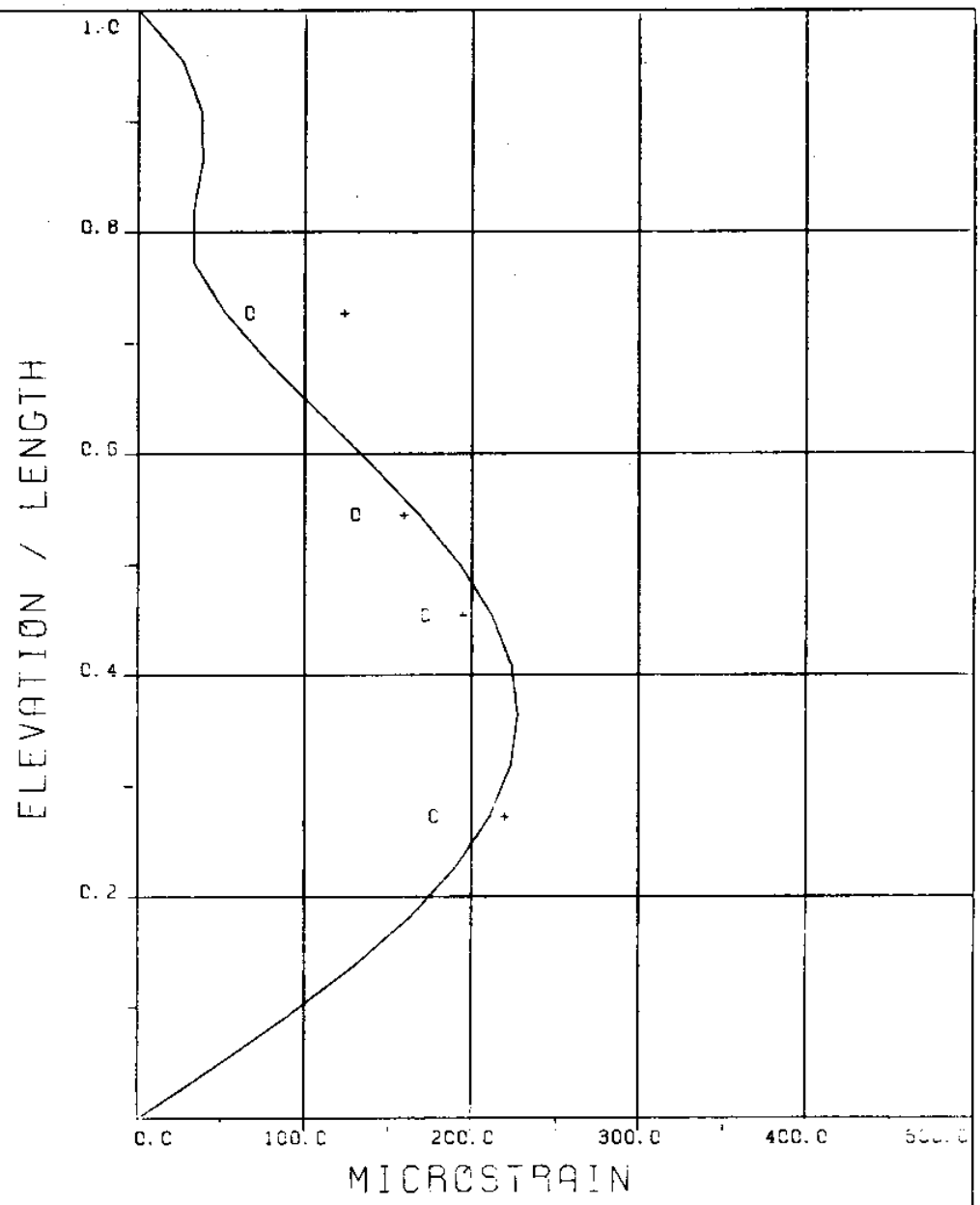

EXPERIMENT NUMBER 89

THETA=90 VC=120 FE=2.925 A/DE=1.94

DYNAMIC RESPONSE AT F=FE IN PLANE B

——— THEORY o o o EXPERIMENT

MAXIMUM DYNAMIC RESPONSE IN PLANE B

——— THEORY + + + EXPERIMENT

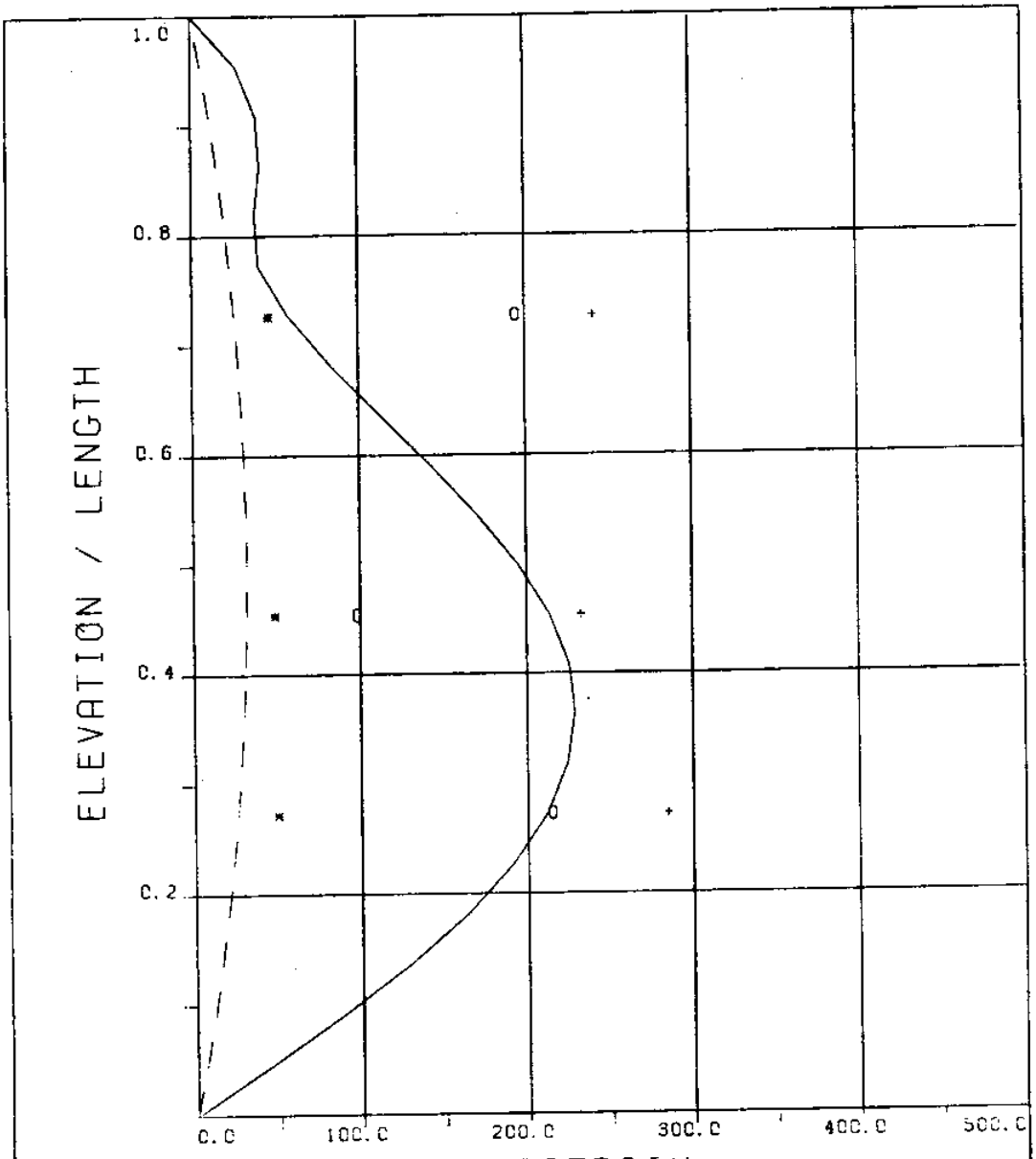

EXPERIMENT NUMBER 89

THETA=90 VC=120 FE=2.925 A/DE=1.94

STATIC RESPONSE IN PLANE A

----- THEORY * * * EXPERIMENT

MAXIMUM DYNAMIC RESPONSE IN PLANE A

o o o EXPERIMENT

MAXIMUM RESPONSE

_____ THEORY + + + EXPERIMENT

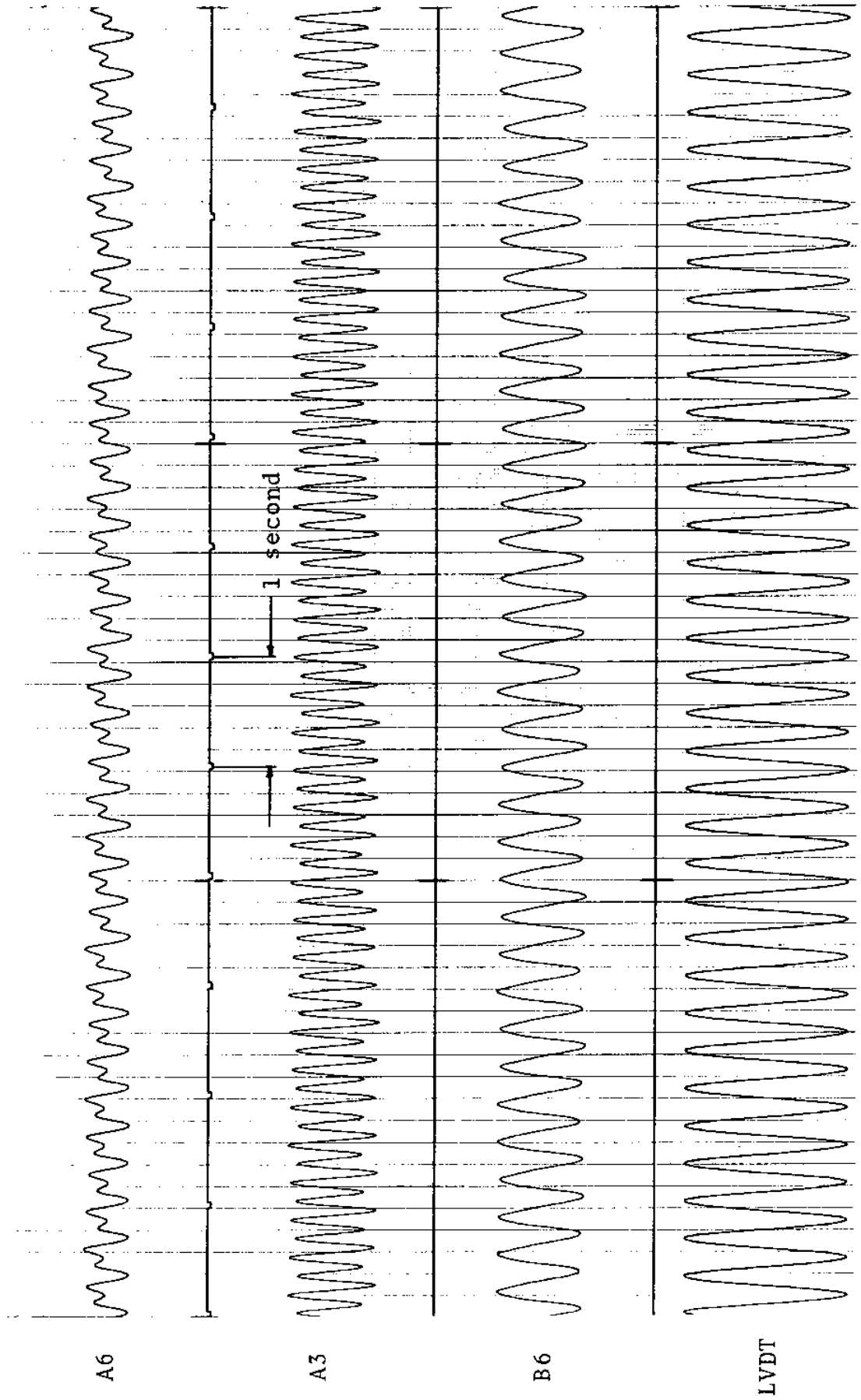

FIGURE 89T: LVDT: 0.087 D_e/DIVISION; STRAINS: 15.3 MICROSTRAIN/DIVISION

3. REFERENCES

1. Chryssostomidis, C. and Patrikalakis, N. M., 1982, "An Experimental Procedure for the Prediction of the Dynamic Behavior of Riser Type Systems," Proceedings, 3rd International Conference on the Behaviour of Offshore Structures, August 1982, 565-598, Hemisphere Publishing Co., New York.

2. Dean, R. B, Milligan, R. W. and Wootton, L. R., 1977, An Experimental Study of Flow Induced Vibration, Atkins Research and Development, Epsom, Surrey, England, Report December 1977/1.

3. International Mathematical and Statistical Library (IMSL), Reference Manual, 1981, Edition 8, IMSL, Inc.

4. Mercier, J. A., 1973, Large Amplitude Oscillation of a Circular Cylinder in a Low Speed Stream, Ph.D. Thesis, Stevens Institute of Technology, Department of Mechanical Engineering, Ann Arbor, MI: University Microfilms Order No. UM74-884.

5. Patrikalakis, N. M., 1983, Theoretical and Experimental Procedures for the Prediction of the Dynamic Behavior of Marine Risers," Ph.D. Thesis, MIT, Department of Ocean Engineering.

APPENDIX A

Figure A-1: Rigid Cylinder Results

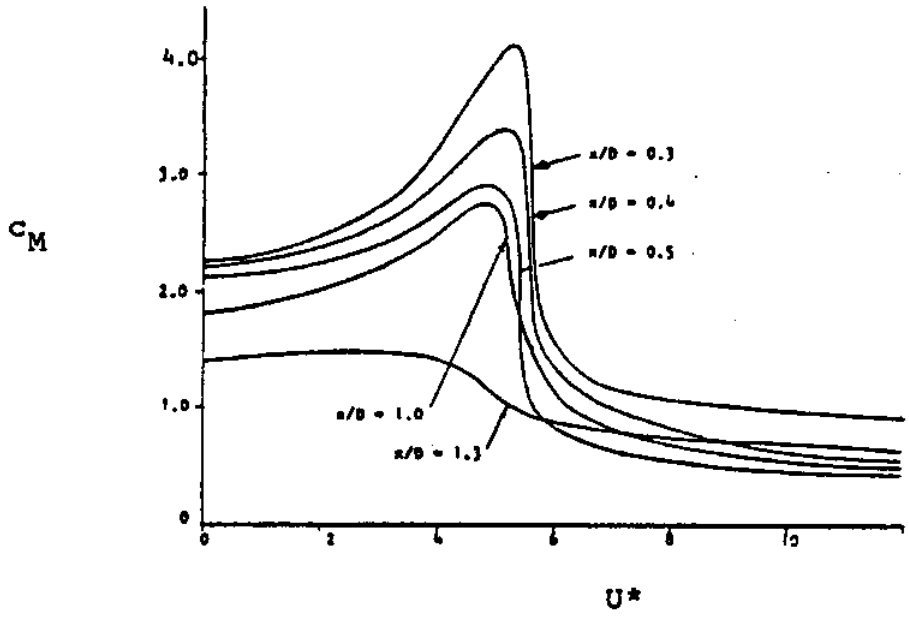

Inertia Coefficient c_M = Amplitude of Inertia Force Per Unit Length/$\rho A_o \omega^2 x+1$ as a Function of U* Parametrically with Respect to the Non-Dimensional Harmonic Oscillation Amplitude, x/D, Orthogonal to a Current, Mercier (1973).

Nomenclature:

ρ : Density of the fluid

$A_o = \pi D^2/4$

D : Cylinder Diameter

ω : Circular Frequency of Oscillation

x : Amplitude of Oscillation

Figure A-2: Rigid Cylinder Results

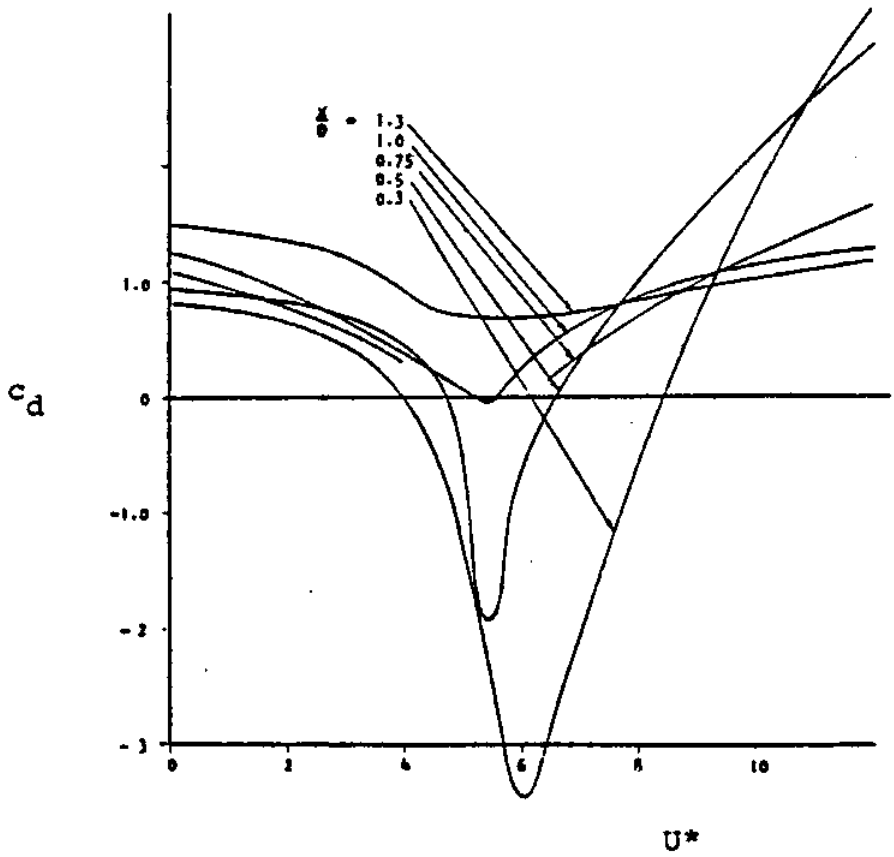

Drag Coefficient c_d = Amplitude of Drag Force Per Unit Length Parallel to the Oscillation/$0.5\rho D\omega^2 x^2$ as a Function of U* Parametrically with Respect to the Non-Dimensional Harmonic Oscillation Amplitude, x/D, Orthogonal to a Current, Mercier (1973)

Figure A-3: Rigid Cylinder Results

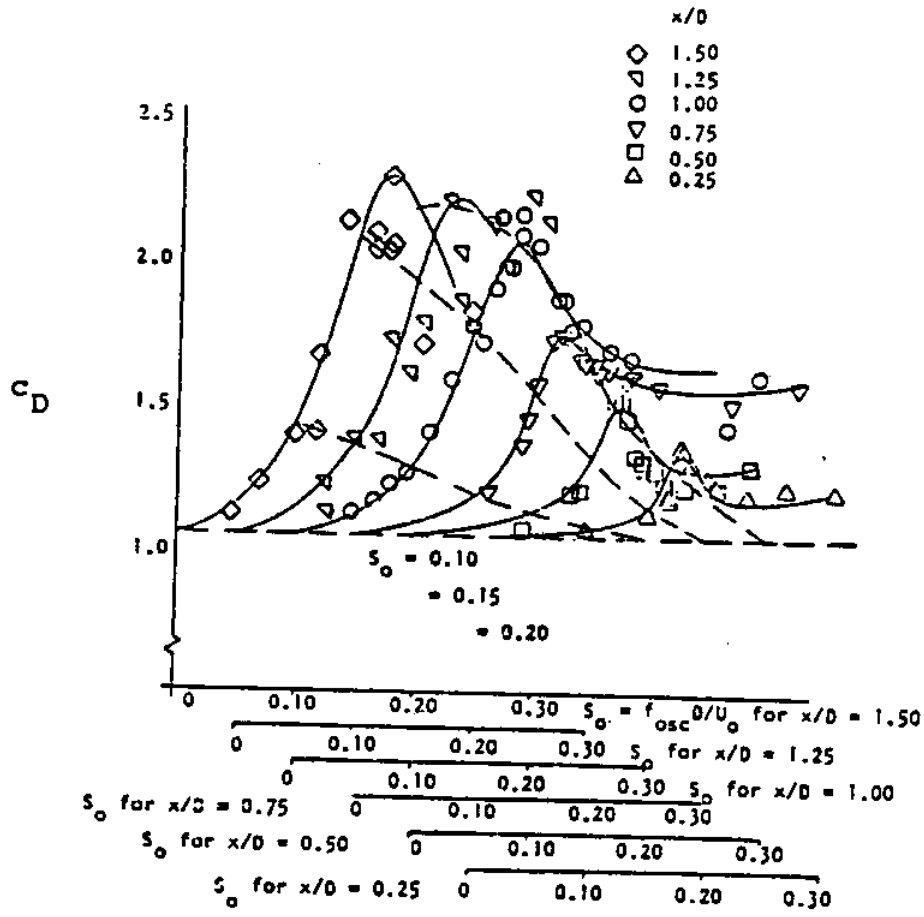

Average Drag Coefficient c_D = Average Drag Per Unit Length/ $0.5\rho DV_c^2$ as a Function of S_o = $1/U^*$ Parametrically with Respect to the Non-Dimensional Harmonic Oscillation Amplitude, x/D, Orthogonal to a Current, Mercier (1973).

Figure A-4: Spring Mounted Rigid Cylinder Results

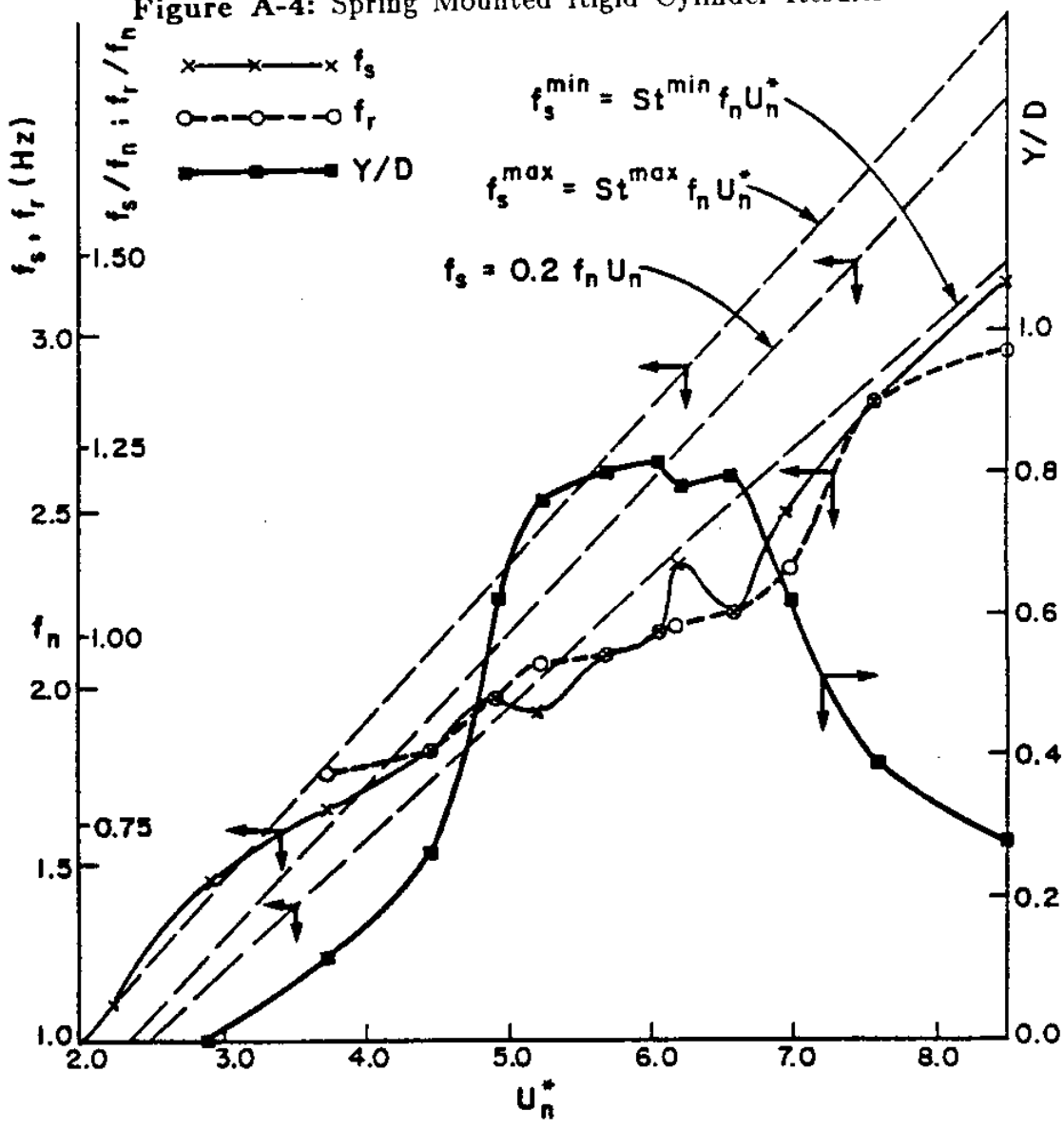

Plots of the Vortex Shedding Frequency, f_s, the Response Frequency f_r, and the Non-Dimensional Response Half Amplitude, Y/D, for a Smooth Spring Mounted Rigid Cylinder Oscillating Orthogonally to a Uniform Water Stream. Taken from Patrikalakis (1983) with data derived from Dean et al (1977). Model characteristics: f_n=2.15 Hz, D=25.4 mm, m=2.93, $\lambda \simeq 13$, δ=0.147, K_s=0.91, Re$\simeq$2680 to 10370.

Nomenclature for Figure A-4:

$U_n^* = V_c/f_nD$

$f_n = (K/M_e)^{1/2}/2\pi$

K = Spring constant

$M_e = M + M_a$

M = Mass of spring mounted cylinder

$M_a = A_o\rho L$

$m = M/A_o\rho L$

$\lambda = L/D$

L = Cylinder length

$K_s = 2\delta M_e/\rho D^2 L$

$\delta = \pi c/(KM_e)^{1/2}$

c = Dashpot coefficient

St^{max}, St^{min} : envelopes of Strouhal number

for a fixed rigid cylinder in a uniform stream,

derived from Figure 2 of Chapter IV of Patrikalakis (1983).